Identification and Mechanistic Study of Immunostimulatory Lipids in Juzen-Taiho-To

by

Anna Takaoka

A dissertation submitted to the Graduate Faculty in Biochemistry in partial fulfillment of the requirement for the degree of Doctor of Philosophy in the City University of New York

2012

This manuscript has been read and accepted for the Graduate Faculty in Biochemistry in satisfaction of the dissertation requirement for the degree of Doctor of Philosophy

Dr. Akira Kawamura

Date

Chair of Examining Committee

Dr. Edward J. Kennelly

Date

Executive Officer

Dr. Robert Bittman

Dr. David A. Foster

Dr. David R. Mootoo

Dr. Moriya Tsuji
Supervisory Committee

THE CITY UNIVERSITY OF NEW YORK

Abstract

Identification and Mechanistic Study of Immunostimulatory Lipids in Juzen-Taiho-To

by

Anna Takaoka

Advisor: Professor Akira Kawamura

Juzen-taiho-to (JTT) is an herbal medicine known to exhibit safe and effective immunostimulatory activity. It is clinically used to improve the immune functions of cancer patients undergoing chemotherapy and radiation therapy in Japan. The chemical constituents responsible for its therapeutic effects are poorly characterized due to the chemical complexity of this formulation and possible synergism. Identification of the active constituents would be the first step to systemically characterize the safety and efficacy of JTT and to understand the mechanism. The main objective of this thesis was the identification of macrophage (MΦ)-stimulating compound(s) in JTT by biomarker-guided screening, and the characterization of individual components to identify possible new biological effects of those compounds.

In this thesis, chapter 1 describes the establishment of the technique we used, biomarker-guided screening, to identify therapeutically relevant compounds from herbal medicines. The technique was established in our lab and refined using two different herbal medicines, namely Keishi-bukuryo-gan and Toki-shakuyaku-san. Chapter 2 describes the identification of common chemical components in MΦ-stimulating

fractions from two different batches of JTT. This is an important achievement because batch-to-batch variability is a major concern in the natural product research. Chapter 3 describes the characterization of individual compounds identified in MΦ-stimulating fractions, which led to the discovery of one system that exhibit significant synergistic MΦ-stimulating activity, i.e. β-Glucocerebroside (GlcCer) and C16:0-ceramide (Cer). This finding is important because it is a rare example of a structurally defined, small molecule mixture that exhibited synergistic MΦ-stimulating activity. In addition, the activity assay showed that MΦ-stimulating activity of GlcCer/Cer mixture was time-sensitive and diminished within 3 hr of sample reconstitution in DMSO. Further mechanistic study of GlcCer/Cer mixture using transmission electron microscope (TEM) and dynamic light scattering (DLS) revealed that GlcCer/Cer mixture forms nanoparticles in both DMSO and an aqueous environment, and the size of the nanoparticles correlated with the MΦ-stimulating activity. Our study provided a new basis of novel combinational therapy, and served as an important step to systemically characterize the safe and effective immunostimulatory herbal medicine, JTT.

Acknowledgement

I would like to take this opportunity to recognize many people who have supported and encouraged me throughout my graduate education at Hunter College and the Graduate Center of the City University of New York.

First and foremost, I would like to thank my mentor, Prof. Akira Kawamura for his guidance, support, encouragement and patience. He has taught me many things, not only about science, but also how to become a better scientist. His professional discipline and diligence have inspired me, and it was such a privilege and honor to have worked with him.

I would also like to thank all of my committee members for their support and help throughout the Ph.D. study, and for attending all of my committee meetings. Prof. Robert Bittman, for the valuable advise on lipids; Prof. David A. Foster, for letting me join his group for rotation; Prof. David R. Mootoo, for his guidance in organic synthesis; and Prof. Moriya Tsuji, for all the immunology work he has let me do in his lab.

I would like to take an opportunity to thank people who have helped me with experiments; Dr. Matthew Devany of NMR facility at Hunter College, for the NMR training and help with data collection/analyses; Dr. Cliff Soll, of Mass Spec facility at Hunter College and Dr. Yasuhiro Itagaki of Mass Spec facility at Columbia University, for the analyses of compounds in our fractions; Dr. Xiangming Li of Aaron Diamond AIDS Research Center, for FACS and many other immunological experiments; Dr. Jacopo Samson of the Nanoscale Analytics facility at Hunter College, for running TEM experiments; Ms. Parminder Kaur, for kindly providing me sodium phosphotungstate; Dr. Charles M. Drain and his lab members for the help with DLS experiments; Mr. Joon Kim

of qRT-PCR facility, for his help on qRT-PCR; Prof. Kleiman and their lab members for the assistance and letting me use their laboratory equipment; Dr. Stewart Bachan and Dr. Eddie Li for their assistance in organic synthesis. I would also like to thank Prof. Grohmann for giving me the opportunity to take his organic class and for introducing me to Akira when I was an undergraduate student.

I owe a lot to my colleagues who has supported and helped me throughout my Ph.D. study; Dr. Tal H. Hasson for teaching me all the experimental techniques from the time I joined the group; Dr. Maria Iacovidou and Dr. Doina Mihai for all of their help and support. We were like sisters and I miss spending time with them; Mr. Diego Montenegro, for helping me with DLS measurements; Ms. Olga Aminova for the assistance in many qRT-PCR experiments. AK lab members got along well, and I would like to thank everybody for making the lab environment very enjoyable. I would also like to thank my classmates, Sandy, Jason and Artem, for their help throughout the graduate study. Study groups and review sessions were very helpful, and I really wish all the best in the future.

I owe my deepest gratitude to my family, especially my parents, for their support throughout my stay in the US. It was their hard work, which made it possible for me to come here. I cannot thank enough for their unconditional love and encouragement.

Last but not least, I would like to thank my husband, David, for always being there for me. He was very supportive, being patient when I was staying late in the lab, and always encouraged me when I was going through a tough time. I love you, and I am very excited to build a new chapter of our life together.

Table of Contents

List of Figures

List of Tables of Schemes

List of Abbreviations

AFM	atomic force microscopy
AI	acetone insoluble
AS	acetone soluble
ATP	adenosine triphosphate
BSA	bovine serum albumin
BSSG	β-sitosterol-D-glucoside
BSS	β-sitosterol
CD14	cluster of differentiation 14
CD1d	cluster of differentiation 1d
cDNA	complementary DNA
C_T	cycle threshold
COSY	correlation spectroscopy
COX	cyclooxygenase
cRNA	complementary RNA
DC	dendritic cells
DLS	dynamic light scattering
$\Delta\Delta C_T$	delta delta C_T
dsDNA	double-stranded DNA
ELISA	enzyme-linked immunosorbent assay
ELSD	evaporative light scattering detector
ERT	enzyme replacement therapy
ESI-MS	electrospray ionization mass spectrometry
FACS	fluorescence-activated cell sorting
FBS	fetal bovine serum
FAM	6-carboxyfluorescein
GalCer	galactosylceramide
GlcCer	glucosylceramide
GM-CSF	granulocyte macrophage colony stimulating factor
HIV	human immunodeficiency virus

HMOX-1	heme oxygenase 1
HMBC	heteronuclear multiple bond correlation
HPLC	high performance liquid chromatography
hr	hour
HRMS	high-resolution mass spectrometry
HSC	hematopoietic stem cells
HSQC	heteronuclear multiple quantum correlation
HUVEC	human umbilical vein endothelial cells
ICAM-1	intercellular adhesion molecule 1
ICP-MS	inductively coupled plasma mass spectrometer
iNOS	inducible isoform of nitric oxide synthase
IL	interleukin
JTT	Juzen-taiho-to
KBG	Keishi-bukuryo-gan
LAL	limulus amebocyte lysate
LC/MS	liquid chromatography/mass spectroscopy
LPS	lipopolysaccharide
M^+	molecular ion
MARCO	macrophage receptor with collagenous structure
MFI	mean fluorescence intensity
MIP-1	macrophage inflammatory protein
MTS	3-(4,5-dimethylthiazol-2-yl)-5-(3-carboxymethoxyphenyl)-2-(4-sulfophenyl)-2H-tetrazolium
MΦ	macrophage
mRNA	messenger RNA
MS	mass spectroscopy
NF-κB	nuclear factor kappa-light-chain-enhancer of activated B cells
NMR	nuclear magnetic resonance
NK	natural killer
NKT	natural killer T cells
NSAID	nonsteroidal anti-inflammatory drug

PAMP	pathogen associated molecular patterns
PBMC	peripheral blood mononuclear cell
PCR	polymerase chain reaction
PRR	pathogen recognition receptors
qRT-PCR	quantitative reverse-transcription polymerase chain reaction
RASGRP	RAS guanyl nucleotide-releasing protein
SPE	solid phase extraction
SR	scavenger receptor
SR-PSOX	scavenger receptor that binds phosphatidylserine and oxidized lipoprotein
TCM	traditional Chinese medicine
TDEYA	(6E,12E)-tetradecadiene-8,10-diyne-1,3-diol diacetate
TEM	transmission electron microscopy
Th	T-helper cell
TLR	toll like receptor
TNF-α	tumor necrosis factor alpha
TREM2	triggering receptor expressed on myeloid cells 2
TSS	Toki-shakuyaku-san
UV/VIS	ultraviolet-visible

Chapter I: Identification of hidden potential in herbal medicine using biomarker-guided screening

Chapter I

I.1: Herbal medicine

Nature is full of biologically useful molecules. Plants are especially rich in many therapeutically important compounds. From early human history, people have learned to use plants to treat various conditions and diseases, such as insomnia, anxiety, obesity, asthma, infection, eczema, etc.[1,2] The use of plants for therapeutic applications is called "herbal medicine" and could be a single plant, a plant mixture, an extract of a plant, or a decoction of multiple herbs.

Herbal medicine, in a form of "Kampo medicine," plays an important role in medical treatment in Japan. Kampo medicine was established in Japan, after being introduced from China in the 7th century. It is a group of herbal formulations in a specific ratio, which was refined over thousands of years, and used to treat various diseases that often arise from the imbalance of the whole body, such as menopausal disorders, autonomic imbalance, asthma, dermatitis, etc.[2] More than 80% of the practicing physicians in Japan have used of Kampo medicine.[2] Having been optimized through the long history of patient treatments, Kampo is considered to be one of the safest and most effective traditional medicines with few adverse side effects.

Herbal medicine, including Kampo medicine, holds great therapeutic potential, and many researchers have attempted to isolate and identify the active constituents. Many of the active constituents, however, are still unknown because of the heterogeneity of the herbal formulations. Many of therapeutically important compounds are hidden within

complex chemical mixtures.[3] Thus, appropriate bioassays are required to identify therapeutically relevant chemical constituents from herbal medicines.

In order to identify therapeutically relevant compounds, reproducible, cell-based assay is necessary. Cytotoxicity assays are frequently used to identify anti-cancer compounds, but it would not be useful for the identification of therapeutically important compounds in many Kampo formulations because Kampo medicines do not exhibit toxicity at therapeutic dosage. Assays based on animal models, on the other hand, would be too costly because fractionation of chemically complex herbal medicines yields large numbers of fractions. Thus, screening of herbal medicine calls for a new strategy to identify suitable cell-based assays relevant to the therapeutic effects of herbal medicine. To address this issue, we turned to the emerging tools in genomics.[3]

I.2: Biomarker-guided screening

In order to facilitate the identification of bioactive compounds in herbal medicine, our group has established a simple protocol called biomarker-guided screening. In this screening, powerful genomic tools, such as DNA arrays, are used to identify genes associated with the therapeutic effects of herbal medicine (i.e., "biomarkers" of therapeutic effects).[3–5] DNA array is a comprehensive and unbiased way to examine the effects of herbal medicine on cellular transcriptome. It is capable of quantifying over 47,000 transcripts simultaneously.[6–8] By comparing the transcriptome profiles of cells treated with herbal medicine and vehicle control, we can identify genes (biomarker) associated with the known therapeutic effect of that particular herbal medicine (Figure I.1). Once the biomarkers of the herbal medicine of interest are identified, the quantitative

reverse transcription-polymerase chain reaction (qRT-PCR) is used to guide the fractionation of herbal medicine.[3–5]

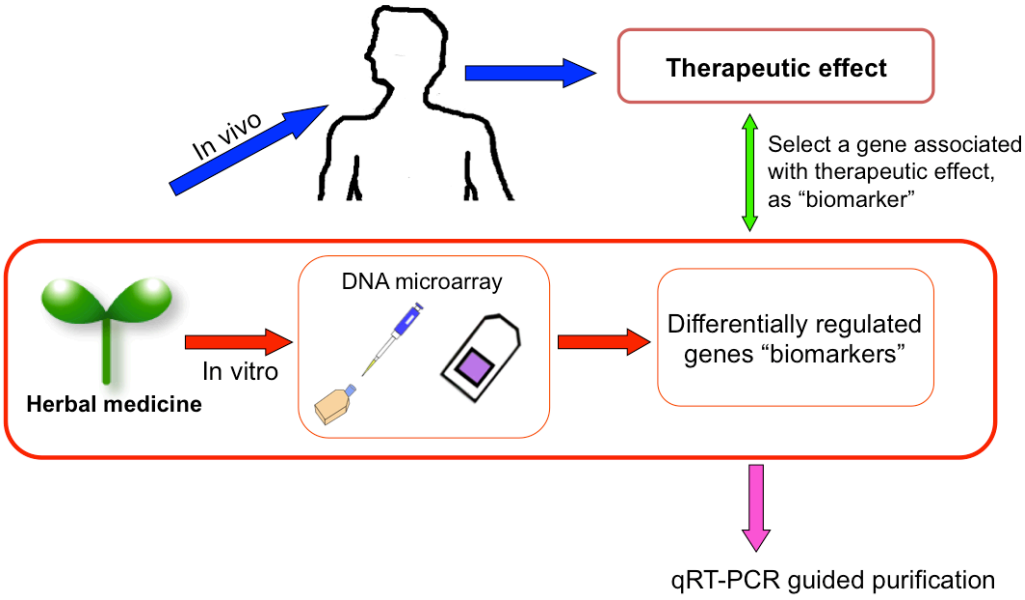

Figure I.1: Overview of biomarker-guided screening. DNA microarray is used to identify biomarkers associated with the therapeutic effect of the herbal medicine of interest. The purification of active compounds is then guided by qRT-PCR.

I.3: Proof-of-concept – identification of hidden potential in Keishi-bukuryo-gan (KBG)

First biomarker-guided screening was conducted with an herbal medicine called Keishi-bukuryo-gan (KBG).[4] KBG is used to treat various disorders, such as atherosclerosis, brain ischemia, rheumatoid arthritis, and ameliorate menopausal symptoms such as hot flashes.[3,4,9] KBG is known as a "blood cleansing" formula, and its therapeutic effect is associated with blood circulation.[3] Therefore, primary human umbilical vein endothelial cells (HUVEC) were selected to conduct biomarker-guided screening. HUVEC was treated with KBG, and transcriptome profiling revealed several

genes that were differentially regulated by KBG. Due to the vasoprotective characteristics of heme oxygenase 1 (HMOX-1), HMOX-1 was selected as a gene that is linked to the therapeutic effect of KBG.[10,11] HMOX-1 guided fractionation of KBG formula led to the identification of linoleic acid as an HMOX-1- regulating agent (Figure I.2, top).[3,4] This work served as an important proof-of-concept study to establish the protocol of our biomarker-guided screening.

One technical issue identified in this study was the gene expression profiling, which was carried out with spotted oligonucleotide arrays on glass slides. It turned out that the glass slide arrays were susceptible to many experimental errors, which limited our ability to identify the biomarkers of KBG. To address this problem, a more reliable tool (Affymetic GeneChip®) was employed in the subsequent studies.

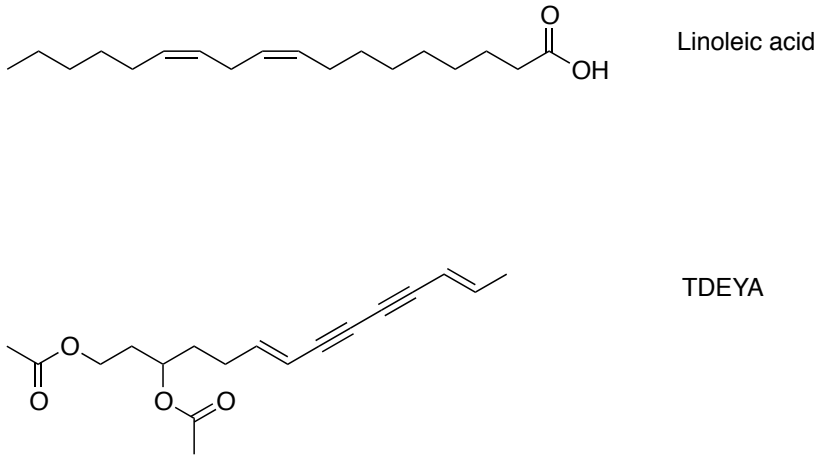

Figure I.2: Structures of linoleic acid ((9*Z*, 12*Z*)-octadecadienoic acid) and (6*E*,12*E*)-tetradecadiene-8,10- diyne-1,3-diol diacetate (TDEYA)

I.4: Refinement of experimental protocol using Toki-shakuyaku-san (TSS)

Further refinement of the protocol was conducted using Toki-shakuyaku-san (TSS). TSS consists of six different herbs, namely Hoelin, Cnidium rhizome, Angelica

sinensis, Peony root, Atractylodes rhizome, and Alisma rhizome. TSS is used to treat gynecological and obstetric disorders.[3,5] TSS is also known to ameliorate conditions caused by the poor blood circulation. Gene expression profiling of TSS was carried out with the Affymetrix GeneChip.® The profiling revealed a series of differentially regulated genes, including those that are linked to thrombosis, namely serpin peptidase inhibitor, clade B member 2 (SerpinB2), and cyclooxygenase-2 (COX-2).[12] The serpinB2 level in pregnant women is a biomarker for placental function and intrauterine growth. Low levels of SerpinB2 indicate decreased placental function and intrauterine growth retardation.[12] COX-2 inhibition is known to be associated with an increased risk of thrombotic cardiovascular events.[13] SerpinB2 was used for qRT-PCR guided screening of TSS, which revealed that (6*E*,12*E*)-tetradecadiene-8,10-diyne-1,3-diol diacetate (TDEYA) was responsible for the induction of SerpinB2 (Figure I.2, bottom).[5]

I.5: Applying biomarker-guided screening in identification of macrophage-stimulants in Juzen-taiho-to (JTT).

Juzen-taiho-to (JTT) is an immunostimulatory herbal formulation composed of 10 different herbs (Figure I.3). The Japanese Ministry of Health and Welfare approved the clinical use of JTT in 1980's.[2] Since then, JTT has often been prescribed to cancer patients recovering from surgery, chemotherapy, and radiation therapies.[2,14] JTT is known to reduce the adverse reactions of cancer treatments, such as anemia, leukopenia, and systemic weariness.

Figure I.3: Herbal components of JTT

JTT is also known as "immune booster." A number of studies have demonstrated its preventative effects of cancer progression and metastasis. JTT, instead of directly acting on cancer cells, activates macrophages (MΦ) to prevent metastasis (Figure I.4).[2,14,15] Thus, JTT is a source of MΦ stimulating compounds, although many of them are still undefined due to the enormous chemical heterogeneity of this herbal formulation. In addition, it is believed that synergism of active constituents could make it even more difficult to identify bioactive compounds in JTT.

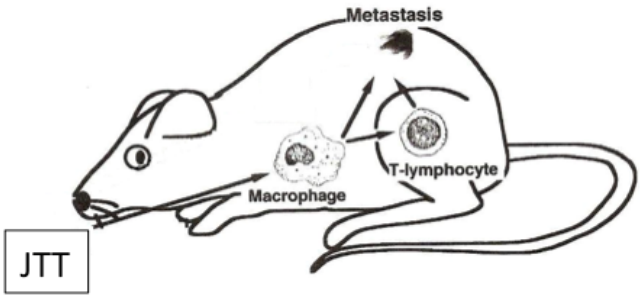

Figure I.4: Mechanism of preventative cancer progression and metastasis through activation of macrophages.[2,14,15]

Identification of MΦ stimulants in JTT is an important first step to understand the safety and efficacy of this herbal formulation. Mechanistic studies on JTT have been hampered by the fact that many bioactive constituents, including MΦ stimulants, have not been identified. In addition, identification of MΦ stimulants would permit the analysis of synergism, which has been suspected to play important roles in herbal medicine.

The screening of JTT was initiated in our group in 2003.[16,17] The biomarker-guided screening, which had been established and refined through the studies of KBG and TSS,[4,5] was employed for the identification of MΦ stimulatory compounds from JTT.[16] For the screening of JTT, we employed THP-1 cells (a human acute monocytic leukemia cell line) because it was impractical to use primary monocytes/macrophages for this screening. GeneChip profiling of JTT-treated THP-1 cells revealed up-regulation of many genes that can be used as biomarkers of immunostimulation.[16] Many of those genes are known to be regulated by the NF-κB pathway, i.e. ICAM-1, IL-1B, IL-8, TNF, and RASGRP (Table I.1).[18–21] The DNA array results were verified by real-time PCR. Since ICAM-1, a prototypical biomarker for inflammation, showed the most reproducible results, it was chosen for the subsequent screening of JTT.[16] The purification scheme was established to reproducibly enrich the MΦ stimulatory activity.

Table I.1: Genes most distinctively regulated by JTT in THP-1 cells

UniGene	Genes	Fold Change	Log Ratio[a]	Change p-value[b]
Hs.75703	Chemokine (C-C motif) ligand 4 (CCL4)	88.95	6.5	0.00006
Hs.437322	Tumor necrosis factor, alpha-induced protein 6 (TNFAIP6)	74.8	6.2	0.00002
Hs.632586	Chemokine (C-X-C motif) ligand 10 (CXCL10)	54.76	5.8	0.00002
Hs.450230	Insulin-like growth factor binding protein 3 (IGFBP3)	26.91	4.8	0.0004
Hs.574492	Nucleoporin 62kDa (NUP62)	26	4.7	0.00017
Hs.137459	Shroom family member 3 (SHROOM3)	23.4	4.55	0.00075
Hs.31210	B-cell CLL/lymphoma 3 (BCL3)	17.8	4.15	0.00009
Hs.514107	Chemokine (C-C motif) ligand 3 (CCL3)	17.4	4.13	0.00003
Hs.126256	Interleukin 1, beta (IL1B)	16	4	0.00035
Hs.624	Interleukin 8 (IL8)	14.9	3.9	0.00003
Hs.632592	Chemokine (C-X-C motif) ligand 11 (CXCL11)	14.2	3.83	0.0007
Hs.241570	Tumor necrosis factor (TNF superfamily, member 2) (TNF)	13.5	3.75	0.00007
Hs.643447	Intercellular adhesion molecule 1 (CD54), human rhinovirus receptor (ICAM1)	11.9	3.58	0.00033
Hs.591338	Tumor necrosis factor, alpha-induced protein 3 (TNFAIP3)	11.5	3.53	0.00002
Hs.319171	Nuclear factor of kappa light polypeptide gene enhancer in B-cells inhibitor, zeta (NFKBIZ)	10	3.33	0.00002
Hs.591286	Pentraxin-related gene, rapidly induced by IL-1 beta (PTX3)	9.4	3.23	0.00002
Hs.484703	CD83 molecule (CD83)	8.1	3.03	0.00002

a. **Log Ratio**: Log_2(ratio of average signals). Genes with |Log ratio| of 3 or higher are listed on this table. None of the down-regulated genes had |Log ratio| of 3 or higher (i.e., Log ratio -3 or lower). b. **Change p-value**: Change p-values are calculated using the Wilcoxon signed rank test and Tukey Biweight on the Affymetrix GeneChip® Operating Software. The software calls a gene down-regulated if its p-value is between 1 and 0.997, whereas a gene is considered up-regulated if its p-value is between 0 and 0.003. In our analysis, the following criteria were used to select the genes for further analysis: Change p-values of 0.001 or lower for the up-regulated genes and Change p-values of 0.999 or higher for the down-regulated genes. See Experimental Procedure section for more details (page 41-42).

I.6: Objective, central hypothesis, and significance

The main objective of the study was to identify MΦ-stimulatory compound(s) in JTT using biomarker-guided screening. In addition, the individual characterization of identified compounds was one of the important aspects of the study. Characterization of individual components would enable us to identify possible new biological effects of the individual compounds. This study would serve as the first step to systemically characterize the safe and effective immunostimulatory herbal medicine, JTT.

As described in later chapters, we have overcome the technical difficulties to sort out numerous chemical constituents by biomarker-guided screening. Concerns on the reproducibility, which is a major issue in the studies of herbal medicine, were addressed by examining two different batches of JTT. This was an important achievement since chemical constituents of different batches of herbal medicine could be slightly different due to genetic factors, climate difference, soil quality, and other external factors that affect the plants in the herbal medicine.

Identification of MΦ-stimulatory factors in JTT opened an opportunity to study the mixture effects, which led us to the discovery of a synergistic interaction among the identified compounds. Further mechanistic studies of the synergistic mixture revealed the formation of nanoparticles that are important for the observed MΦ-stimulatory activity.

I.7: References

1. Sumner, J. *The Natural History of Medicinal Plants*. (Timber Press: 2000).

2. Yamada, H. & Saiki, I. *Juzen-taiho-to (Shi-Quan-Da-Bu-Tang): Scientific Evaluation and Clinical Applications*. (CRC Press: 2005).

3. Kawamura, A. Uncovering the therapeutic potential of natural products with biomarker-guided screening. *IDrugs* **13**, 321–324 (2010).

4. Kawamura, A., Brekman, A., Grigoryev, Y., Hasson, T. H., Takaoka, A., Wolfe, S. & Soll, C. E. Rediscovery of natural products using genomic tools. *Bioorg. Med. Chem. Lett* **16**, 2846–2849 (2006).

5. Kawamura, A., Iacovidou, M., Takaoka, A., Soll, C. E. & Blumenstein, M. A polyacetylene compound from herbal medicine regulates genes associated with thrombosis in endothelial cells. *Bioorg. Med. Chem. Lett.* **17**, 6879–6882 (2007).

6. Brown, P. O. & Botstein, D. Exploring the new world of the genome with DNA microarrays. *Nat. Genet.* **21**, 33–37 (1999).

7. Cousins, R. J., Blanchard, R. K., Popp, M. P., Liu, L., Cao, J., Moore, J. B. & Green, C. L. A global view of the selectivity of zinc deprivation and excess on genes expressed in human THP-1 mononuclear cells. *Proc. Natl. Acad. Sci. USA* **100**, 6952–6957 (2003).

8. Lipshutz, R. J., Fodor, S. P., Gingeras, T. R. & Lockhart, D. J. High density synthetic oligonucleotide arrays. *Nat. Genet.* **21**, 20–24 (1999).

9. Goto, H., Shimada, Y., Sekiya, N., Yang, Q., Kogure, T., Mntani, N., Hikiami, H., Shibahara, N. & Terasawa, K. Effects of Keishi-bukuryo-gan on vascular function and hemorheological factors in spontaneously diabetic (WBN/kob) rats. *Phytomedicine* **11**, 188–195 (2004).

10. Fujita, T., Toda, K., Karimova, A., Yan, S. F., Naka, Y., Yet, S. F. & Pinsky, D. J. Paradoxical rescue from ischemic lung injury by inhaled carbon monoxide driven by derepression of fibrinolysis. *Nat. Med.* **7**, 598–604 (2001).

11. Yachie, A., Niida, Y., Wada, T., Igarashi, N., Kaneda, H., Toma, T., Ohta, K., Kasahara, Y. & Koizumi, S. Oxidative stress causes enhanced endothelial cell injury in human heme oxygenase-1 deficiency. *J. Clin. Invest.* **103**, 129–135 (1999).

12. Medcalf, R. L. & Stasinopoulos, S. J. The undecided serpin. The ins and outs of plasminogen activator inhibitor type 2. *FEBS J.* **272**, 4858–4867 (2005).

13. Yu, Y., Ricciotti, E., Scalia, R., Tang, S.Y., Grant, G., Yu, E., Landesberg, G., Crichton, I., Wu, W., Pure, E., Funk, C.D. & FitzGerald, G.A. Vascular COX-2 modulates blood pressure and thrombosis in mice. *Sci. Transl. Med.* **4**, 132-54 (2012).

14. Saiki, I. A Kampo medicine 'Juzen-taiho-to'--prevention of malignant progression and metastasis of tumor cells and the mechanism of action. *Biol. Pharm. Bull* **23**, 677–688 (2000).

15. Ohnishi, Y., Fujii, H., Hayakawa, Y., Sakukawa, R., Yamaura, T., Sakamoto, T., Tsukuda, K., Fujimaki, M., Nunome, S., Komatsu, Y. & Saiki, I. Oral Administration of a Kampo (Japanese Herbal) Medicine Juzen-taiho-to inhibits liver metastasis of colon 26-L5 carcinoma cells. *Cancer Science* **89**, 206–213 (1998).

16. Hasson, T. H. *Isolation and Characterization of Immunomodulatory Compounds from Juzen-Taiho-To: Novel Understanding of Phytosteryl Glucosides Nano-Aggregates and Synergism.* (The Graduate Center of CUNY: New York, 2009).

17. Iacovidou, M. *Uncovering hidden potential of natural products*. (The Graduate Center of CUNY: New York, 2010).

18. Kunsch, C. & Rosen, C. A. NF-kappa B subunit-specific regulation of the interleukin-8 promoter. *Mol. Cell. Biol* **13**, 6137–6146 (1993).

19. Pahl, H. L. Activators and target genes of Rel/NF-kappaB transcription factors. *Oncogene* **18**, 6853–6866 (1999).

20. Van De Stolpe, A., Caldenhovenm E., Stade, B. G., Koenderman, L., Raaijmakers, J. A., Johnson, J. P. & Van Der Saag, P. T. 12-O-Tetradecanoylphorbol-13-acetate- and tumor necrosis factor alpha-mediated induction of intercellular adhesion molecule-1 is inhibited by dexamethasone. Functional analysis of the human intercellular adhesion molecular-1 promoter. *J. Biol. Chem.* **269**, 6185–6192 (1994).

21. Shakhov, A. N., Collart, M. A., Vassalli, P., Nedospasov, S. A. & Jongeneel, C. V. Kappa B-type enhancers are involved in lipopolysaccharide-mediated transcriptional activation of the tumor necrosis factor alpha gene in primary macrophages. *J. Exp. Med.* **171**, 35 –47 (1990).

Chapter II: Identification of MΦ-stimulatory factors in JTT

Chapter II

II.1: Introduction

Natural products have been a great source of biologically important compounds.[1,2] More than 60% of the small-molecule drugs are either natural products or derived from compounds isolated from the natural sources.[2,3] Numerous drugs have been developed using natural compounds for the treatment or prevention of cancer, heart disease, diabetes, HIV, bacterial, and fungal infection.[2,4] The primary focus of natural product discovery has been on the cytotoxic and antibiotic properties of natural compounds.[5] The advent of new biological assays, however, has enabled the discovery of natural products with novel biological activities, which could not be detected by traditional cytotoxicity assays.[6–9]

One such class of compounds is immunomodulatory natural products. Over the past fifty years several natural products with potent immunomodulatory activity were identified.[2,4,5] There are, for example, natural products that induce cell-mediated immune response, such as saponins. Saponins are triterpenoid glycosides, and many researchers have studied their immunostimulatory properties. For example, QS21, an immunostimulatory saponin mixture isolated from Soap Bark tree,[8,10] is under various clinical trials as a vaccine adjuvant (Figure II.1). Another well-known natural product with immunostimulatory activity is agelasphin. Agelasphin is a glycolipid that was isolated from an Okinawan marine sponge.[11] Intensive structure-activity studies revealed that a synthetic analog of agelasphin, namely, KRN7000, has shown potent anti-tumor activity by stimulating immune cells (Figure II.1).[12–14] KRN7000 stimulates Natural Killer T (NKT) cells by binding to the CD1d receptor on dendritic cells (DC). The

conventional cytotoxic assay would have not revealed the immune-stimulating properties of these compounds. This example highlights the fact that nature is still a rich source of unnoticed therapeutically useful compounds, including immunomodulatory compounds.

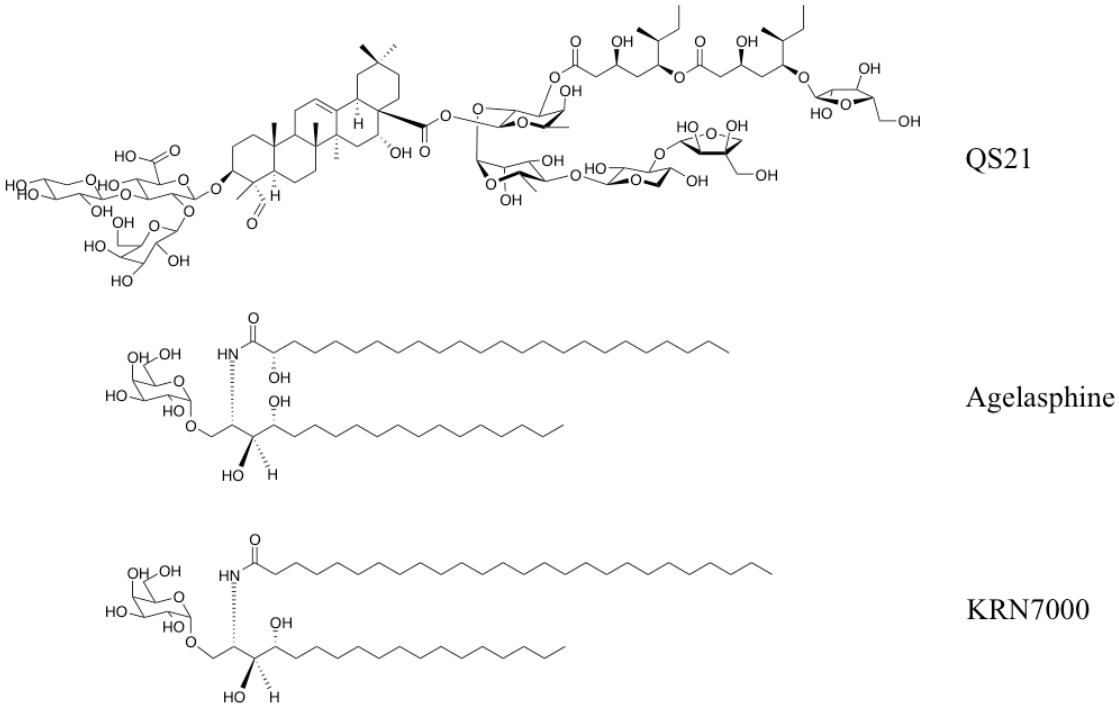

Figure II.1: Structures of QS21, Agelasphine and KRN7000

Natural compounds that stimulate monocytes/MΦ hold a potent therapeutic promise in the treatments of various diseases. Compounds that control monocytes/MΦ with small molecules could be beneficial to our health. Monocytes and MΦ are involved in both innate and adaptive immunities to fight against microbial pathogens such as bacteria, viruses, and fungi (Figure II.2).[15–17]

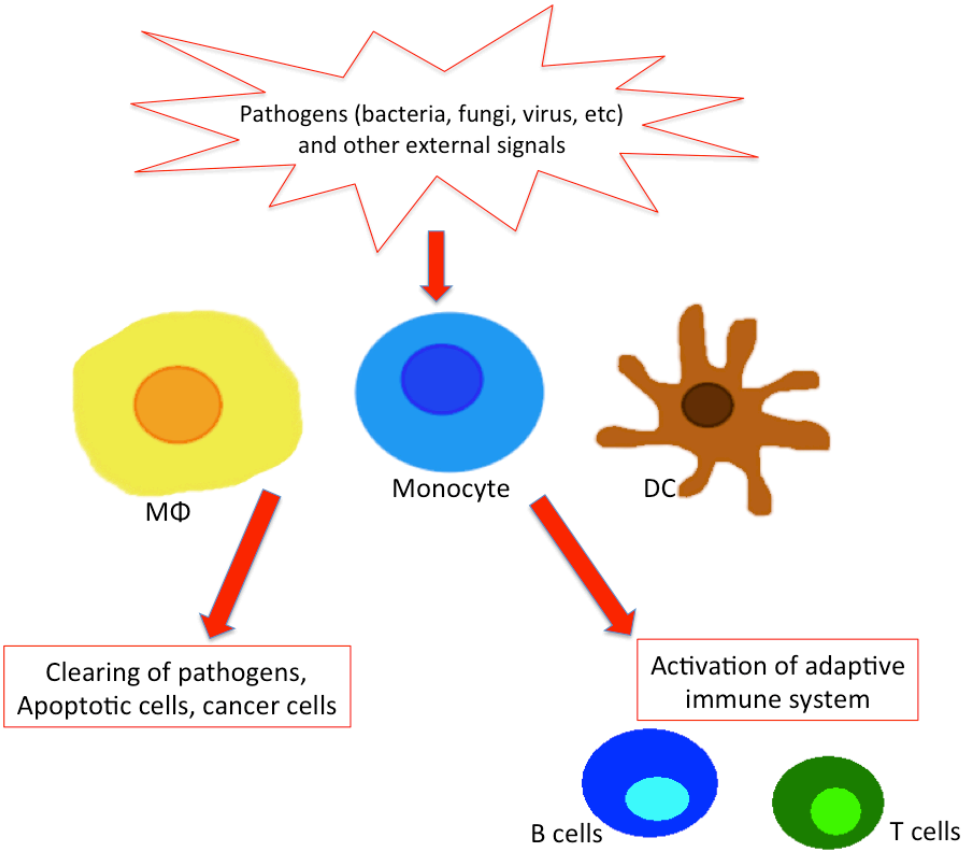

Figure II.2: Biology of macrophages (MΦ)/monocytes/dendritic cells (DC)

In addition, MΦ are involved in clearing out apoptotic cells, virus-infected cells of the host organisms, and cancer cells. Monocytes and MΦ are crucial first defense against threats to our body.[16,17] MΦ sense any danger to the host organisms by recognizing the molecule secreted by the microbial pathogens or molecules presented by those pathogens (PAMPs: pathogen-associated molecular patters).[17] Recognition is mediated through pathogen recognition receptors (PRRs), and the recognition of PAMPs leads to the activation of MΦ, resulting in activation of certain transcription factors for the secretion of cytokines, interleukins, and maturation of MΦ, inducing the immune

response (Figure II.3).[15,16] Therefore, molecules that safely control monocytes/MΦ are of great interest in biomedical research.

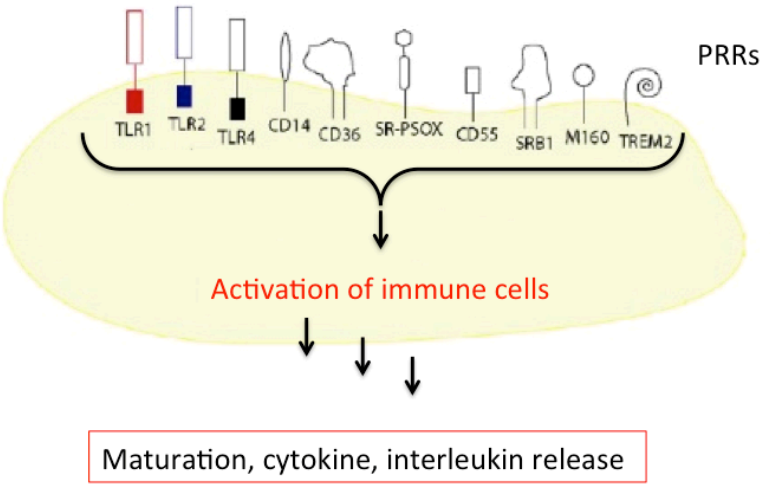

Figure II.3: PRRs expressed on MΦ: Abbreviations: TLR, tool-like receptor; CD14, cluster of differentiation 14; CD36, cluster of differentiation 36 (Scavenger receptor class B); SR-PSOX, scavenger receptor for phosphatidylserine and oxidized low-density lipoprotein; CD55, Complement decay-accelerating factor; SRB1, Scavenger receptor class B1; M160, scavenger receptor CD163; TREM2, triggering receptor expressed on myeloid cells 2.

It is, however, not a trivial task to identify molecules that can safely activate monocytes/MΦ. Although many compounds are known to stimulate MΦ, their uses in clinical setting are questionable. For example, the bacterial lipopolysaccharide (LPS) is a well-known potent immunostimulant, but the obvious concern of the use of LPS is an uncontrolled stimulation of immune cells, which leads to septic shock.[18] Other PRR ligands are also considered as potential MΦ stimulants, although many of them are of

bacteria origin and the safety concern remains (Table II.1). Granulocyte macrophage colony stimulating factor (GM-CSF) is another example of MΦ stimulants.[19] Although GM-CSF has been used to develop a FDA-approved drug, Leukine, to accelerate white blood cell recovery for patients who received a bone marrow transplant, the safety of GM-CSF is a potential problem because it is known to mediate the inflammation in rheumatoid arthritis.[20] The controversy of effectiveness and safety of GM-CSF still remains. Then, where can one find safe and effective MΦ stimulants?

Table II.1: Summery of PRRs, their ligands and origins of those ligands.

PRR	Ligand	Origin	Ref.
TLR1	Triacyl lipopolypeptides	Mycobacteria	[21]
TLR2	Peptidoglycan, LTA	Gram+ bacteria	[16]
TLR4	LPS	Gram – bacteria	[22]
CD14	LPS (in the presence of LBP)	Gram – bacteria	[23]
CD36	Diacylated lipopeptide	Gram + bacteria	[24]
SR-PSOX	Phosphatidylserine	Apoptotic cells	[25]
CD55	LPS	Gram – bacteria	[26]
SR-B1	LPS	Gram – bacteria	[27]
M160	Intact bacteria	Gram+ and – bacteria	[28]
TREM2	Anionic carbohydrates	Gram+ and – bacteria	[29]

One potential source of safe and effective MΦ stimulants is JTT. As mentioned in Chapter 1, JTT is a safe and effective immunostimulatory herbal medicine. JTT is known to stimulate a wide variety of cells in the immune system including monocytes, MΦ, and DC.[30–34] So far, the majority of immuostimulants found in JTT are carbohydrates.[35] On the other hand, hydrophobic compounds have not been extensively studied. Screening of the hydrophobic constituents in JTT, therefore, could reveal new classes of MΦ stimulants that could provide new mechanistic insights into the safe and effective immunostimulation by JTT.

The search for MΦ stimulants in complex herbal mixtures, such as JTT, could be complicated due to following reasons: 1. limited suitable screening methods available; 2. endotoxin contamination; and 3. batch-to-batch variability of herbal components. First, there are only limited suitable screening methods available to efficiently isolate and identify active ingredients from a complex herbal mixture. Activity-guided screening of complex herbal formulations like JTT requires an inexpensive and reliable biological assay because a large number of fractions have to be screened by the assay over a period of months or even years. Second, the identification of immunostimulants from natural sources could be deceived by the presence of endotoxin contamination. Endotoxin contamination is always one of the most common problems in purification of immunostimulatory compounds from natural sources.[36] As mentioned previously, endotoxin, such as LPS of bacteria, is a potent immunostimulatory agent, and even a minute quantity as a contamination from air, glassware, container, or solvents, can cause immune response. Residual endotoxin contamination has been the cause of immunostimulatory response in plant extracts. Therefore, it is necessary to ensure that the activity of our immunostimulatory fraction does not come from the endotoxin contamination. Finally, batch-to-batch variability of herbal chemical constituents causes reproducibility issues.[37] Genetic factors, climate, soil quality, and other external factors could greatly affect the chemical constituents of herbs, thereby varying the chemical constituents between the batches.[37] Isolation and identification from one batch of herbal medicine do not necessarily ensure the presence of those compounds in other batch. In order to gain confidence in our purification from the first batch, another purification from a different batch using a different purification scheme is required.

Some of the issues above have been resolved previously in our group. First, the assay problem has been resolved by using biomarker-guided screening as described in Chapter 1. This screening method allowed us to enrich MΦ stimulants, and subsequent spectroscopic analyses led to the identification of several chemical components from the first batch. Second, an issue with endotoxin contamination has been also resolved. The active fractions were submitted for an endotoxin test, known as Limulus amebocyte lysate (LAL) endotoxin test (Lonza). The test showed that the endotoxin levels in the active fractions of JTT were under the detection limit.[38] Endotoxin, even if it existed, could not account for the observed immunostimulatory activity of those fractions.

The major focus of this chapter is the identification of MΦ stimulants that are reproducibly observed in different batches of JTT. We established protocols to reproducibly enrich MΦ stimulants from JTT, in which MΦ stimulatory activity is followed by an assay using THP-1 cells. Using these protocols, we successfully enriched MΦ-stimulatory activity from two different batches of JTT. The analyses of the enriched samples revealed a series of plant lipids that are consistently seen in these two preparations of MΦ-stimulatory activity.

Another focus of this chapter is the characterization of the enriched fraction using primary MΦ and DC. This is necessary because THP-1 was used in the screening. The biological assessment of identified monocyte-stimulants using human monocytes/MΦ is also an important issue that needs to be addressed in identifying MΦ-stimulants. The MΦ-stimulant rich fractions were identified using biomarker-guided screening, which utilizes human monocytic leukemia cell line, THP-1. THP-1 is a cancer cell line, and it is easy to culture and very useful in our screening, but it may lack important biological

activity of monocyte/MΦ. In order to find out whether our purified fractions can also stimulate primary lymphocytes, it is necessary to examine the effect of the active fraction on human CD14+ cells (monocytes/MΦ) and DCs isolated from peripheral blood mononuclear cells (PBMC).

II.2: Identification of MΦ stimulants reproducibly observed in two different batches of JTT

II.2.1: Chemical constituents in the JTT fraction enriched with MΦ-stimulatory activity (the first batch)

Biomarker-guided screening has been employed in our group to establish the purification scheme to enrich MΦ stimulatory activity from JTT.[38,39] Briefly, gene expression profiling study revealed a series of genes that are differentially expressed in THP-1 upon JTT treatment (Table I.1). Among them are the genes associated with MΦ stimulation, such as TNF, IL-8, and ICAM-1.[38] For our screening of JTT, we chose ICAM-1 because (1) it is highly induced by JTT, (2) it is a well-known marker of MΦ stimulation,[40] and (3) the ICAM1 protein level can be easily analyzed by FACS. Thus, fractionation of JTT was guided by the qRT-PCR of ICAM1 in THP-1 cells.

The activity-guided fractionation of JTT (the first batch) led to the purification scheme as shown in Scheme II.1.[38] The initial extraction of JTT was conducted by a modified Folch method, which is known to enrich hydrophobic compounds, such as lipids.[41] Accordingly, JTT was extracted with 2:1 $CHCl_3$/MeOH, which enriched hydrophobic compounds with MΦ stimulatory activity. The extract was then partitioned

between 1-butanol and water. The MΦ stimulatory activity remained in the butanol layer. The butanol layer was separated into four fractions by silica gel column chromatography (gradient elution using CH_2Cl_2/MeOH). The fraction that was eluted with 20% MeOH in CH_2Cl_2 (R_f = 0.5-0.85) retained the highest activity. Mass spectrometric analyses of this fraction suggested that it was a very crude mixture. Therefore, it was further fractionated using solid-phase extraction (SPE C8 column), which gave three fractions, namely, 50%$MeOH_{aq}$, 75%$MeOH_{aq}$, and 100%MeOH. The MΦ-stimulatory activity was retained in the 100% MeOH fraction. Fractionation up to this solid-phase extraction was repeated many times, which confirmed the reproducibility of this fractionation scheme.

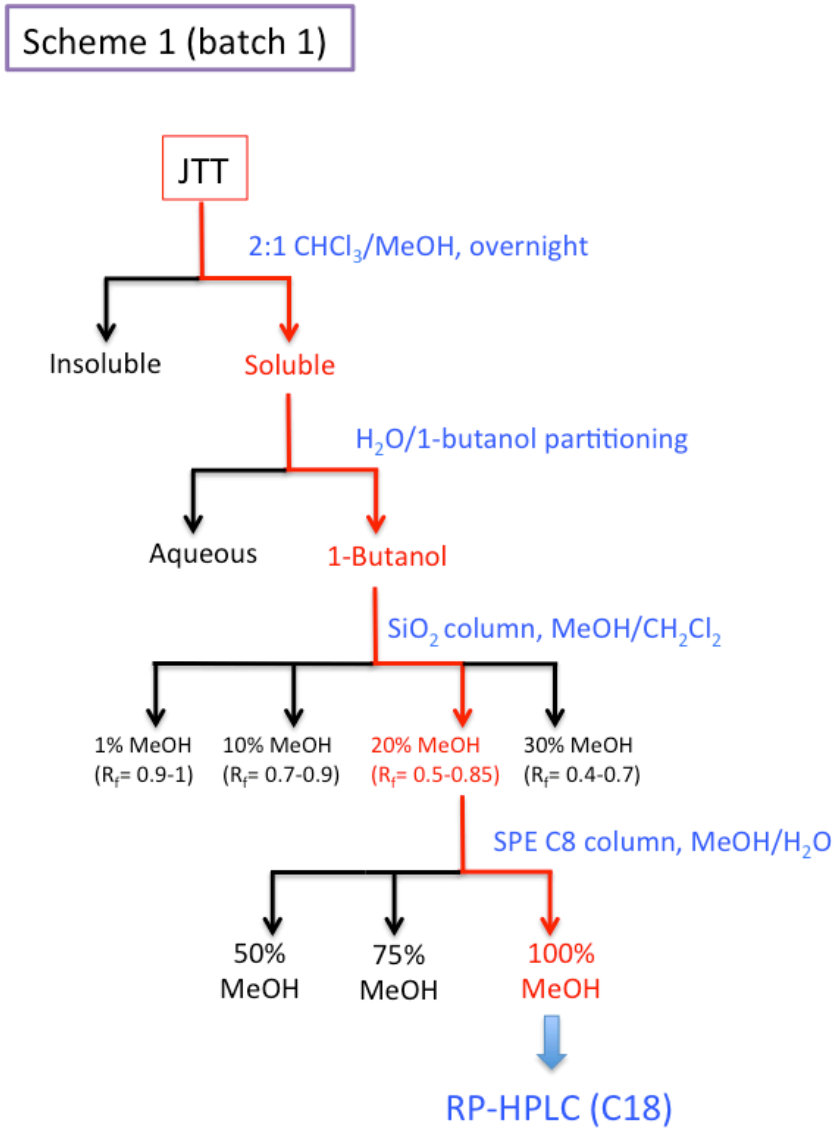

Scheme II.1: Fractionation schemes for JTT batch 1. R_f values indicated in the scheme were based on TLC developed in 20% methanol in CH_2Cl_2 and visualized using cerium molybdate.

Further purification of MΦ-stimulatory activity from this 100% MeOH fraction turned out to be difficult. Preliminary analysis of this fraction using both normal and reversed-phase HPLC suggested that the MΦ-stimulatory activity did not correlate with UV/vis absorption as monitored by a photodiode array detector.[38,39] To overcome this

problem, the subsequent HPLC was carried out using an evaporative light scattering detector (ELSD), which is widely used to detect UV-inactive compounds, such as carbohydrates and some steroids.[42–46] To our surprise, however, the maximum MΦ-stimulatory activity did not correlate with the ELSD profile (Figure II.4, a, b). Thus, the region with potent MΦ-stimulatory activity was separated into five fractions (Fractions B-F) for chemical constituent analyses (Figure II.4, b).

Structural characterization of constituent chemicals was carried out for Fractions C, D, and E. Fractions B and F were not studied in detail because Fraction B was still a complex mixture, whereas Fraction F did not have enough material for structural analysis.[38,39] NMR and ESI-MS revealed that the structures of the compounds in the active fractions, listed in Table II.2. Many of the compounds in the active fractions were amphiphilic, such as monostearin, β-glucocerebrosides (β-GlcCer), and sterolins (phytosteryl-glycoside), such as β-sitosteryl β-D-glucoside (BSSG), stigmasteryl β-D-glucoside, campesteryl β-D-glucoside, and 22,23-dihydrobrassicasteryl β-D-glucoside. Most of these compounds do not possess strong UV-absorbing chromophores. Major components of ELSD peaks were a mixture of four sterolins, as mentioned earlier.

Using biomarker-guided screening, we were able to identify components in the MΦ-stimulatory fraction in JTT, yet the reproducibility still remained as a major concern because identification of compounds from one batch does not ensure that they are truly the active components. The second round of purification was necessary using another batch of JTT.

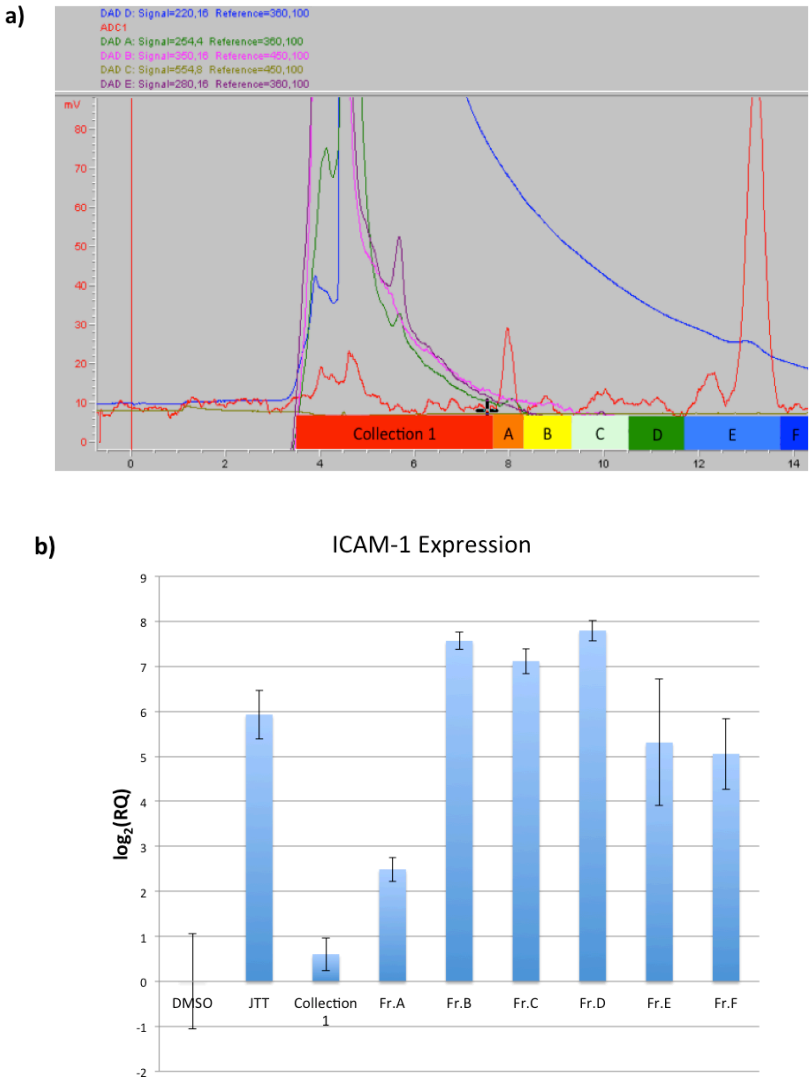

Figure II.4: HPLC profiles and ICAM-1 real-time PCR assays of Batch 1: a) An HPLC chromatogram of 100% MeOH fraction. Conditions: Alltech Econosil C_{18} 10 × 250 mm 10 µ (semi-preparative column) The column was operated at room temperature. Isocratic run of 100% MeOH with a flow rate of 3.0 mL/min. The eluent was detected with photodiode array (220 nm, 235 nm, 254 nm) and ELSD (Gain 16, Nitrogen flow at 4.3 barr, and 44°C). b) ICAM-1 qRT-PCR of collected fraction. THP-1 cells were treated with DMSO, negative control; JTT (100 µg/mL), positive control; Collection 1 and Fr. A-F (5 µg/mL)

Table II.2: Chemical constituents identified from active fractions of JTT (batch1)

Fraction	Name	Structure	Method(s) used
C	Monostearin	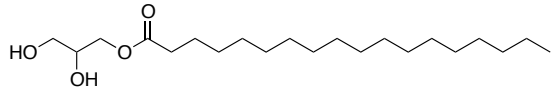	NMR/MS
	β-Glucocerebrosides (4-*trans*, 8-*cis*/*trans*)	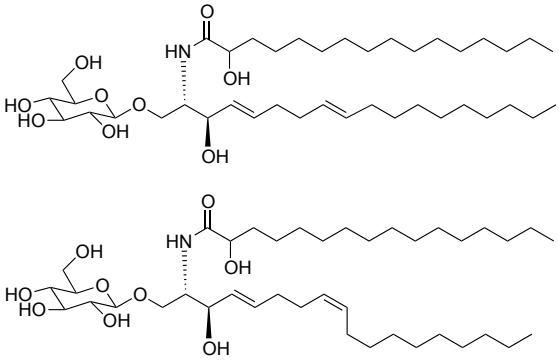	NMR/MS
D	Monostearin	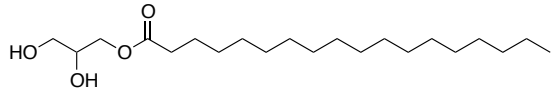	NMR/MS
	Stigmasteryl β-D-glucoside	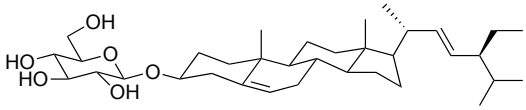	MS
	β-Glucocerebroside (4-*trans*)	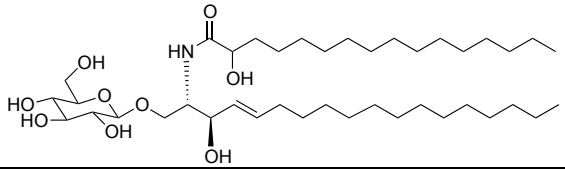	MS
E	Sterolins (phytosterylglycosides)	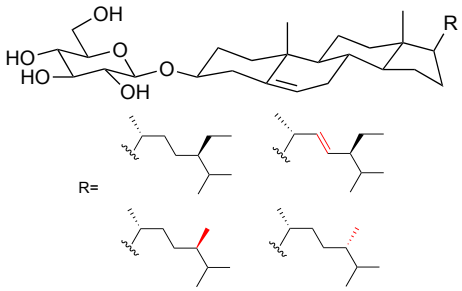	NMR/MS

II.2.2: Chemical constituents in the JTT fraction enriched with MΦ stimulatory activity (the second batch)

In order to assess the batch-to-batch variability of JTT, a second batch of JTT was obtained. The second batch of JTT was first examined by qRT-PCR of ICAM-1, which confirmed that batch 2 contains a comparable level of immunostimulatory activity to that of the batch 1 (Figure II.5).

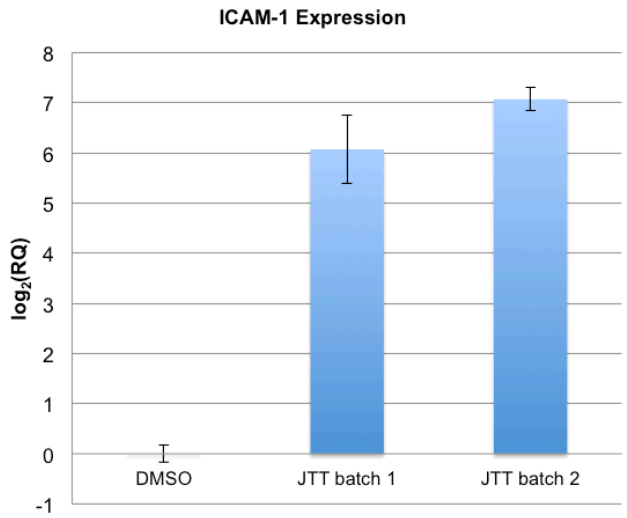

Figure II.5: ICAM-1 real-time PCR analysis of JTT batch 1 and batch 2. THP-1 cells were treated with DMSO, negative control; JTT batch 1 (100 μg/mL), and JTT batch 2 (100 μg/mL).

Purification of the MΦ stimulants from batch 2 was carried out using a slightly different scheme (Scheme II.2). In this new scheme, an acetone-precipitation step was inserted before the silica gel column chromatography to fractionate the butanol layer into acetone soluble (AS) and acetone insoluble (AI) fractions. This acetone precipitation simplified the compound mixture prior to the silica gel column chromatography. More

potent MΦ stimulatory activity was observed in the AI fraction, although the AS fraction also retained some activity (Figure II.6).

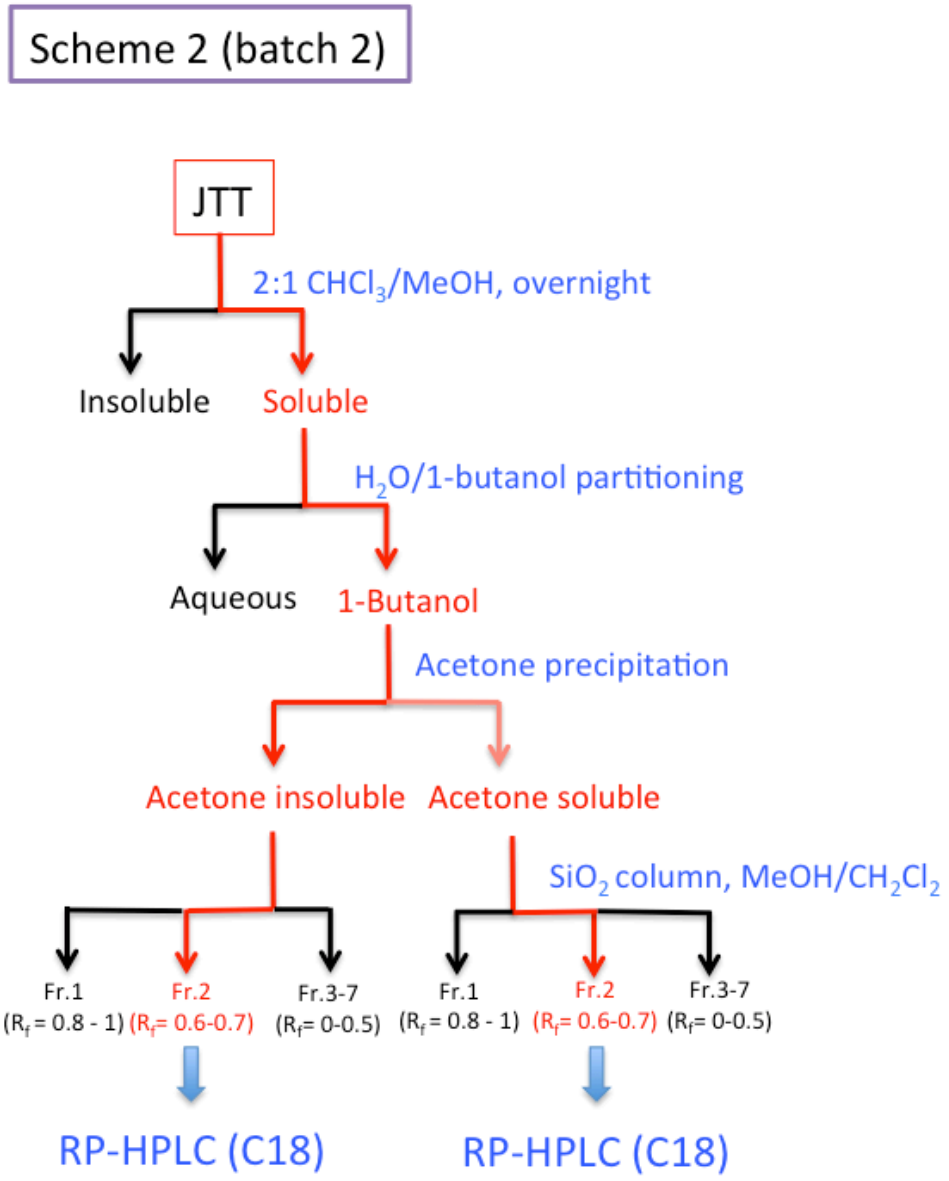

Scheme II.2: Fractionation schemes for JTT batch 2. R_f values indicated in the scheme were based on TLC developed with 20% methanol in CH_2Cl_2 and visualized using cerium molybdate.

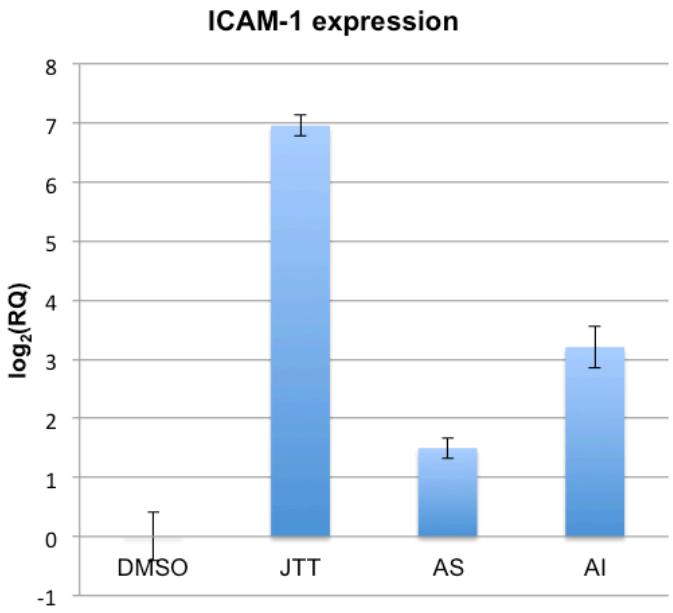

Figure II.6: ICAM-1 real-time PCR analysis of AS and AI. THP-1 cells were treated with DMSO, negative control; JTT (100 µg/mL), positive control, AS (acetone soluble fraction), and AI (acetone insoluble fraction) (10 µg/mL).

AI, a fraction that retained higher activity, was then further separated by silica gel column chromatography. The AI fraction was eluted with 5%-10% MeOH/CH_2Cl_2, and the contents were separated as individual spots on TLC (Figure II.7 a). The AI fraction was separated into seven fractions (Fr. 1-7). Among those seven fractions, Fraction 2, which contained compounds with R_f = 0.6-0.7, retained the highest activity (Figure II.7 b). Since a highly purified sample was obtained at the stage of this silica gel column chromatography, we eliminated the SPE C8 step and proceeded directly to HPLC.

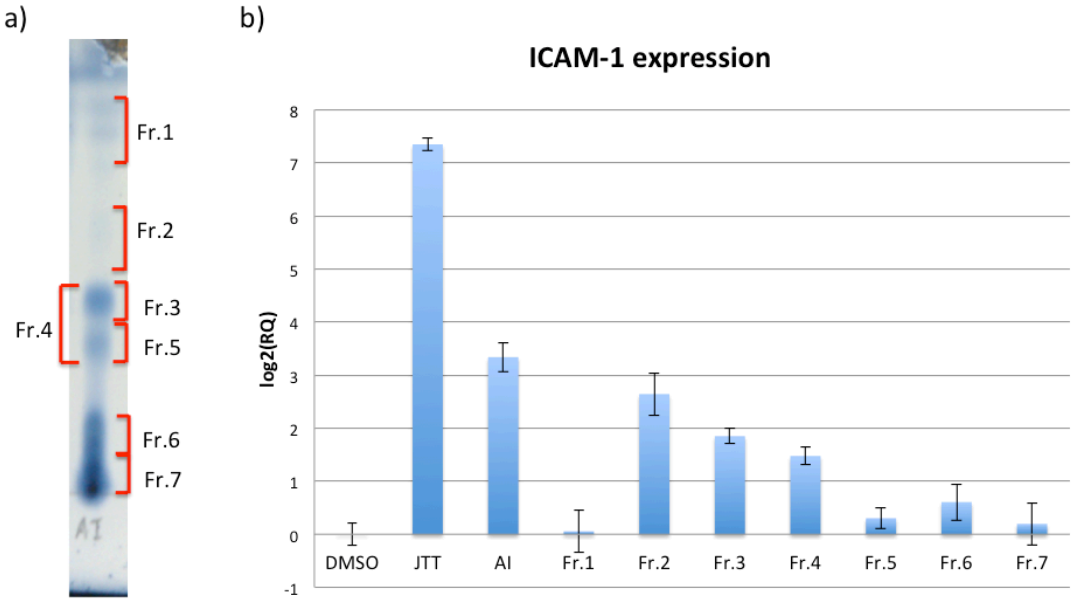

Figure II.7: Fractionation of active compounds by open silica column. a) TLC (20% methanol in methylene chloride) of acetone-insoluble fraction, visualized using cerium molybdate. b) ICAM-1 qRT-PCR analysis of collected fractions from an open silica column. THP-1 cells were treated with DMSO, negative control; JTT (100 µg/mL), positive control, AI (acetone-insoluble fraction) (10 µg/mL), and Fr. 1-7 (10 µg/mL).

The fraction was then further fractionated using HPLC equipped with ELSD. Unlike scheme 1, Fraction 2 from the AI fraction lacked the ELSD peaks around 12 -14 min, which correspond to sterolins (Figure II.8 a). The activity still eluted as a broad peak, in which the highest activity was observed around 10-12 min (Fr. C) (Figure II.8 b).

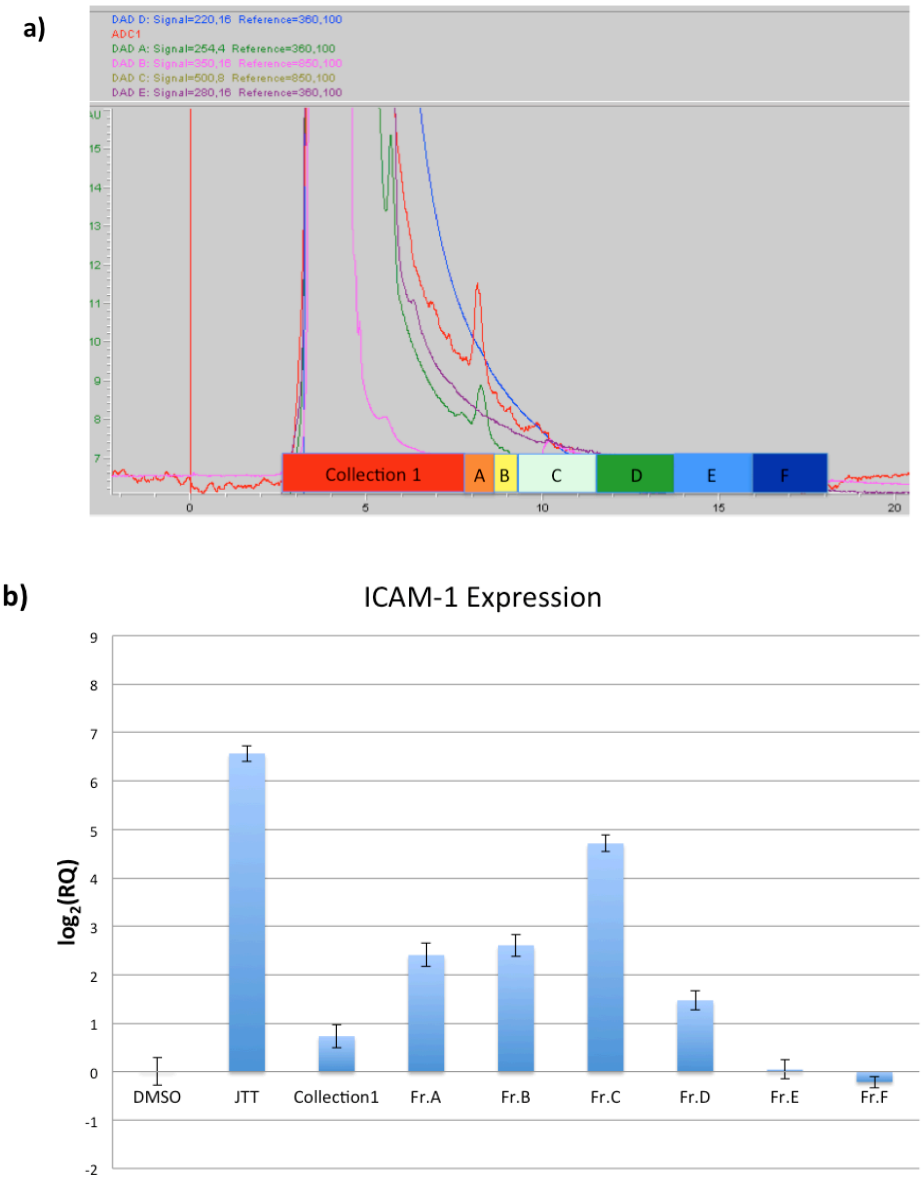

Figure II.8: HPLC profile of AI fraction and ICAM-1 real-time PCR analysis of HPLC fractions. a) HPLC analysis of Fr. 2 of an AI silica column. Conditions: Alltech Econosil C_{18} 10 × 250 mm 10µ (semi-preparative column) The column was operated at room temperature. Isocratic run of 100% MeOH with a flow rate of 3.0 mL/min. The eluent was detected with photodiode array (220 nm, 235 nm, 254 nm) and ELSD (Gain 16, Nitrogen flow at 4.3 barr, and 44°C). b) THP-1 cells were treated with DMSO, negative control; JTT (100 µg/mL), positive control; Collection 1 and Fr. A-F (5 µg/mL).

Structural characterization of the constituents in the active fraction was carried out for Fr. C, which is the fraction exhibiting the highest activity among all of the HPLC fractions collected. NMR and MS analyses suggested that the fraction contains mixtures of monoacylglycerols such as monostearin, monbehenin, and monopalmitin. In addition, free fatty acids, such as stearic and palmitic acid, were detected. There were also MS signals corresponding to β-GlcCer and sterolins, such as BSSG (β-sitosteryl β-D-glucoside) and stigmasteryl β-D-glucoside (Table II.3).

Table II.3: Chemical constituents identified from active fractions of JTT (batch2)

Fraction	Name	Structure	Method(s) used
C	Monostearin	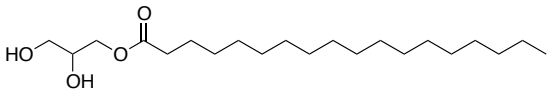	NMR/MS
	Stearic acid	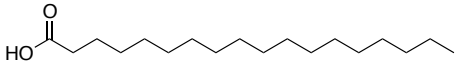	MS
	Monobehehine	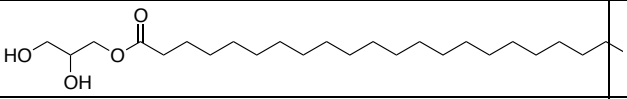	MS
	Monopalmitin	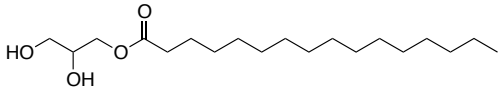	MS
	Palmitic acid	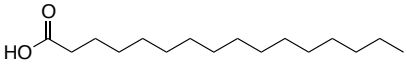	NMR/MS
	β-Glucocerebrosides (4-*trans*, 8-*cis*/*trans*)	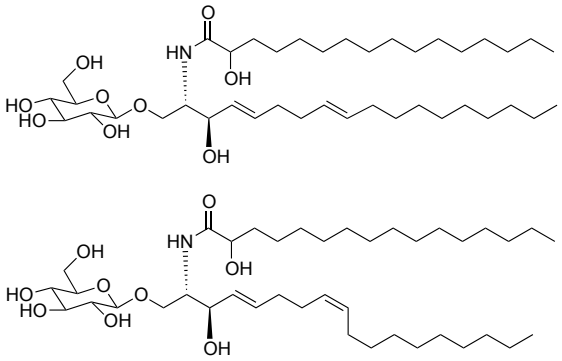	NMR/MS
	Stigmasteryl β-D-glucoside	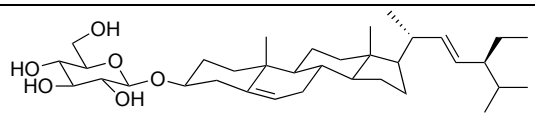	MS
	BSSG	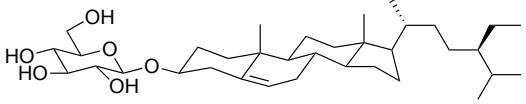	MS

By using two different batches of JTT and two slightly different purification schemes, we were able to enrich the active fraction in the same region on HPLC profile. The active fractions from two batches of JTT contained amphiphilic compounds, such as monostearin, β-GlcCer and sterolins, such as BSSG and stigmasteryl β-D-glucoside (Summarized in Table II.4).

Table II.4: Chemical constituents commonly observed in both batch1 and batch2

Name	Structure
Monostearin	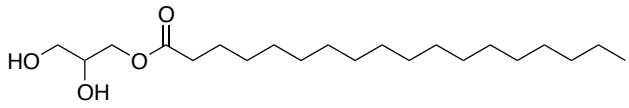
β-Glucocerebrosides (4-*trans*, 8-*cis*/*trans*)	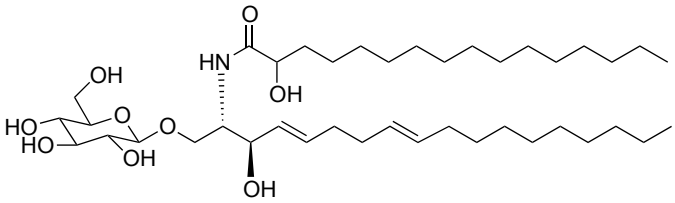 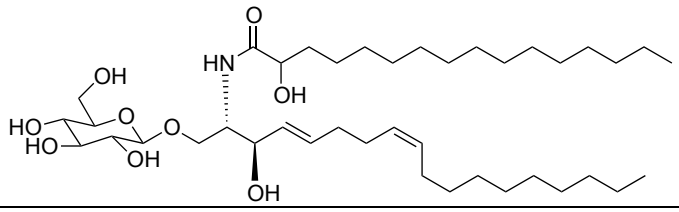
Sterolins (Stigmasteryl β-D-glucoside, BSSG)	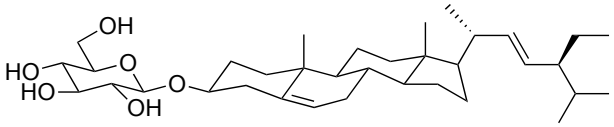 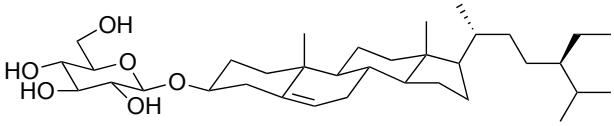

II.3: Biological assessment of active fractions from JTT

After obtaining active fractions from JTT, we next assess the biological relevance of the active fractions using human CD14+ (monocytes/MΦ) and DC isolated from human PBMC. The assays using primary cells were necessary because THP-1 is a cancer cell line and it was only used for the convenience for the screening. Thus, the biological relevance of the active fraction needed to be determined using primary cell lines. To this

end, we have examined Fr. D from batch 1. Here, Fr. D was used because it contained most of the major constituents identified in our study.

First, the mRNA expression level of ICAM-1 was examined by qRT-PCR. JTT was shown to be as potent as LPS, the positive control. ICAM1 expression was induced more than 9-fold in both CD14+ cells and DC upon JTT treatment. In addition, Fr. D was also capable of inducing immune response in human primary cell lines. ICAM-1 was induced more than 4-fold in CD14+ cells, and slightly less (~2 fold) in DC (Figure II.9).

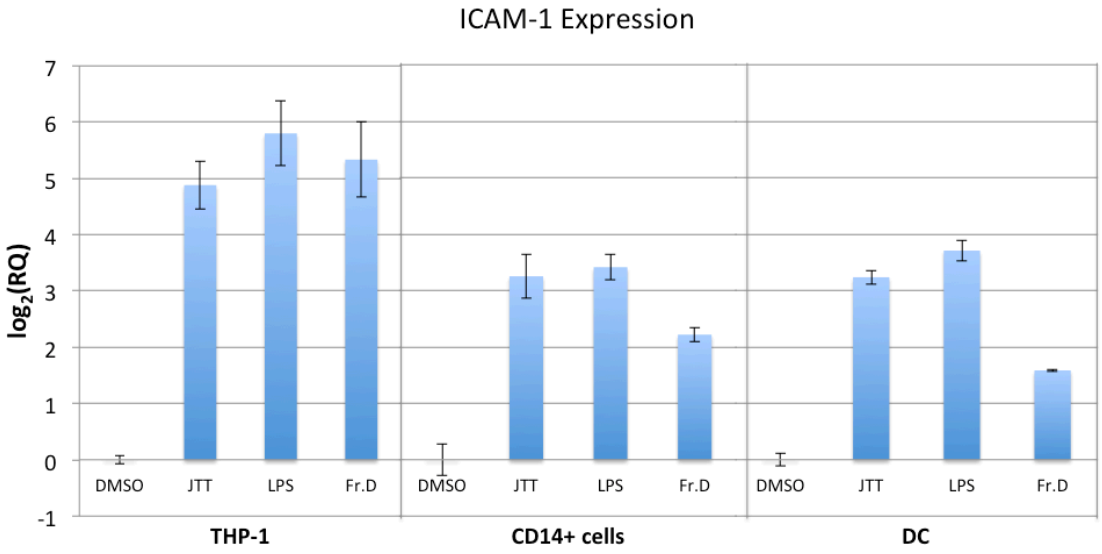

Figure II.9: ICAM-1 mRNA expression after 4 hr of treatment: THP-1, CD14+ cells, and DC were treated with DMSO, negative control; JTT (100 μg/mL), positive control; LPS (0.5 μg/mL); Fr. D (5 μg/mL).

In addition, ICAM-1 protein expression was determined by FACS. Since ICAM-1 is a transmembrane protein,[47] FACS could readily determine the ICAM-1 protein expression level using fluorescent-tagged antibodies. The mean fluorescence intensity (MFI) of ICAM-1 was determined for DMSO (negative control), LPS (positive control), JTT, and Fr. D. It turned out that JTT and Fr. D induced ICAM-1 protein level in all of

the cell line tested. Consistent with the ICAM-1 mRNA expression level, the ICAM-1 protein expression level was induced more than 4-fold on CD14+ cells, and about 2-fold on DC by the treatment with Fr. D (Figure II.10). The assay on the primary lymphocytes demonstrated that the fractions identified from our biomarker-guided screening have biological importance.

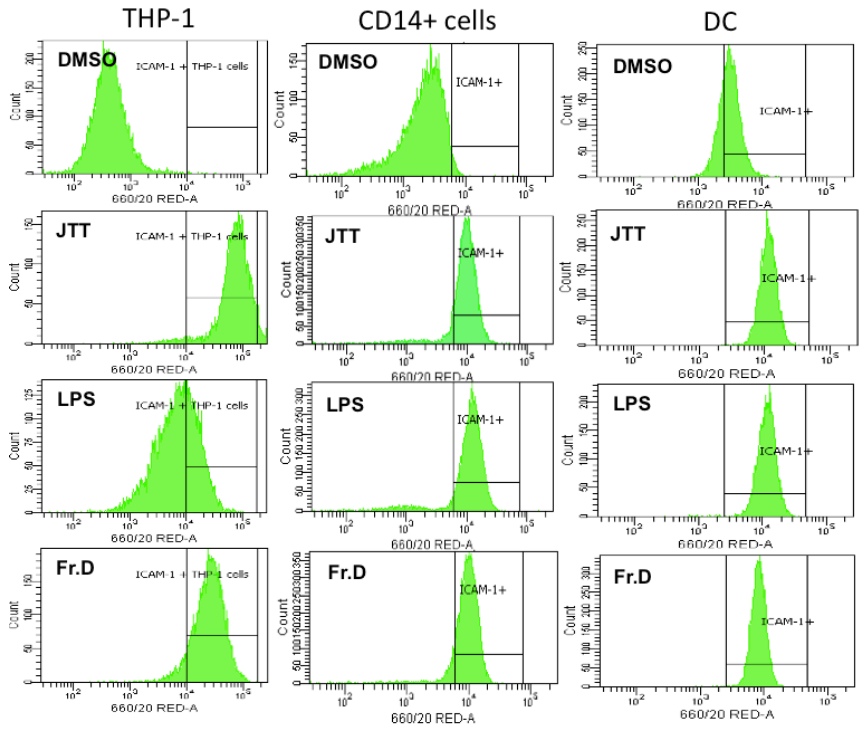

Treatment (24hrs)	THP-1 MFI	CD14+ MFI	DC MFI
DMSO	10791	1899	3108
JTT 100μg/ml	65451	8661	11463
LPS 0.5μg/ml	12697	9722	11653
Fr.D 5μg/ml	25289	8840	8253

Figure II.10: ICAM-1 expression at protein level evaluated by FACS

ICAM-1 expression on THP-1, CD14+ cells, and DC after a 24-hr treatment. THP-1 cells, CD14+ cells, and DC were treated with DMSO, negative control; JTT (100 μg/mL) and LPS (0.5 μg/mL), positive control; Fraction D (5 μg/mL).

II.4: Discussion

Through the studies described in this chapter, we were able to purify MΦ-stimulatory activity from two different batches of JTT. Although purification schemes for the two batches were slightly different, we were able to identify compounds that were common in both batches, namely monostearin, β-GlcCer and sterolins. This suggests that the issue of reproducibility has been resolved. This is an important achievement because batch-to-batch variation is a well-recognized problem in studies of herbal medicines.

In addition to the commonly observed compounds in two batches, several compounds that were uniquely identified in batch 2 are worthy of further consideration. For example, fatty acids, such as stearic and palmitic acid, were observed in the second batch. These fatty acids are known pro-inflammatory compounds (*vide infra*) that can be derived from the hydrolysis of monoacylglycerols. Although the study on batch 1 identified only monostearin, it is possible that fatty acids and other monoacylglycerols also existed in small quantities in batch 1. Thus, biological characterization (Chapter 3) included various fatty acids and monoacylglycerols.

Another issue addressed in this chapter was the characterization of MΦ-stimulatory factor using primary human leukocytes, namely CD14+ cells and DC. As described earlier, our screening required the use of THP-1 cells, although immortalized cell lines like THP-1 might lack some of the key characteristics of primary lymphocytes. To our relief, Fr. D was able to induce ICAM-1 expression not only in THP-1 but also in both CD14+ cells and DC at both mRNA and protein levels. These findings demonstrated that our biomarker-guided screening could successfully enrich biologically relevant

immunostumilants from JTT. The study also showed that JTT indeed was a source of MΦ-stimulatory compounds.

Most of the identified compounds were known to have important biological properties, according to the available literature. Lipids, such as monoacylglycerols, are known to enhance the bioavailability of hydrophobic drugs, and they are often used in food and cosmetics as emulsifying agents.[48–51] Monostearin and monopalmitin are known to attenuate the activity of membrane transporters. Monoglycerides are believed to facilitate drug-uptake.[50] In addition, monoacylglycerols such as monostearin and monopalmitin, might serve as the source of fatty acids in the active fractions. It is likely that these compounds could be hydrolyzed to form fatty acids during storage and treatment. In fact, saturated fatty acids, such as stearic and palmitic acid, have been suggested to be involved in modulation of the immune system.[52] Lauric acid, myristic acid, and palmitic acid have been shown to induce a proinflammatory response mediated by Toll-like receptor (TLR) 4 in adipose tissue.[53] Increased levels of fatty acids, cytokines, and chemokines are critical factors in the development of obesity-induced inflammation and insulin resistance.[54] Fatty acids derived from monostearin and monopalmitin, therefore, might be factors contributing to the MΦ-stimulatory activity in JTT.

Glycosphingolipids, such as glucocerebrosides (GlcCer), are also considered as immunostimulatory compounds for many years. Glycosphingolipids are composed of a sugar moiety (galactose or glucose) bound to ceramide in the α or β configuration. α-Galactosylceramides (α-GalCer) and its structural analogues are potent immunostimulants that bind to CD1d on antigen-presenting cells and activating NKT

cells.[13,55–57] β-GlcCer identified from MΦ-stimulatory fractions (4-*trans*, 8-*cis*/8-*trans*, a.k.a. soya GlcCer) have been previously isolated from soybean and garlic[58,59] and are commercially available. There are conflicting reports in regard to the immunostimulatory activity of β-GlcCer.[12–14] β-GlcCer has been suggested in epidemiological studies of Gaucher's disease. Gaucher's disease is caused by a deficiency of β-glucocerebrosidase, the enzyme that cleaves the β-glucosidic linkage of β-GlcCer,[60] and accumulation of β-GlcCer leads to an enlarged spleen and swelling of lymph nodes.[60,61] The inflammatory response is also observed in cells that have a β-glucocerebrosidase knock-down. Patients undergoing the enzyme replacement therapy for Gaucher's disease have a higher incidence of various diseases, including cancer and diabetes.[61,62] Thus it is likely that β-GlcCer plays a physiological role in the regulation of the immune system.

In addition to β-GlcCer, a metabolite generated from β-GlcCer may be important for the observed immunostimulatory activity. β-GlcCer can be metabolized to glucose and ceramide (Cer) by β-glucocerebrosidase in the lysosomal membrane.[63,64] Cer is a signaling molecule that activates many protein kinases and protein phosphatases. It is also suggested to mediate some of the early responses to TNF-α, which activates the NF-κB pathway.[65,66] Cer is involved in the regulation of cellular homeostasis.[67–70] It is also known to stabilize to membrane structures such as lipid rafts, and is capable of changing membrane permeability.[71] Cer, therefore, is included in the biological studies (Chapter 3).

The biological properties of sterolins have also been reported in literature. Phytosterols, and its glycoside (sterolins) such as β-sitosterol (BSS) and β-sitosterol β-D-glucoside (BSSG), are synthesized in plants and widely known as cholesterol-lowering agents.[72,73] Some studies, however, also report their anti-cancer properties.[74–76]

Immunomodulatory activity of a mixture containing BSS and BSSG was reported by Bouic *et al*. In their study, a proliferative response of human peripheral blood lymphocytes was increased by several fold by the mixture.[77] Bouic *et al.* also reported clinical benefits of this BSS/BSSG mixture, such as improved management of pulmonary tuberculosis, allergic rhinitis, and sinusitis in HIV-infected patients.[78,79] The BSS/BSSG mixture used in these studies, however, was a crude extract that could contain many other compounds.

Identification of the lipidic compounds gave us an opportunity to characterize and compare their biological activities in our assay system. In addition, it is now possible to examine the potential synergism of these compounds. Synergism of herbal medicine, which has long been suspected, is difficult to study because of the chemical complexity and variability of herbs. The series of compounds identified in this study provide a rare opportunity to systematically explore the synergism of herbal medicine. In the next chapter, we will discuss the biological characterization of the individual compounds and their mixtures.

II.5: Materials and methods

Materials: The solvents for extraction/purification were HPLC grade and were purchased from VWR and Fisher Scientific. *Juzen-taiho-to* (JTT) formulation was purchased from Honso Pharmaceutical Co. (Nagoya, Japan) as a dry water extract. Unless specified otherwise, all other chemicals and reagents were obtained from Fisher Scientific and VWR and used without further purification. HPLC analysis and purification were carried on an Agilent 1100 series, using Chem Station operating system. HPLC was equipped with an Agilent 1100 photodiode array detector and an Evaporative Light Scattering detector (ELSD) model 800 (Alltech®) and semi-preparative C18 column (Alltech®). NMR spectra were recorded on a Brüker 500-MHz instrument.

Cell culture: THP-1 cell were purchased from American Type Culture Collection (ATCC). Cells were propagated in RPMI-1640 media containing 25 mM HEPES and L-glutamine (HyClone), 10% fetal bovine serum (Fisher), 1% penicillin streptomycin and amphotericin B (VWR) and 0.005 mM β-mercaptoethanol. Cells were maintained in a 37 °C humidified 5% CO_2 incubator.

GeneChip: THP-1 cells were cultured in RPMI medium supplemented with 10% fetal bovine serum and 1x penicillin-streptomycin (100 units/mL and 100 μg/mL, respectively) and maintained in a 37 °C humidified 5% CO_2 incubator. On the day before the gene expression profiling, 2 million THP-1 cells were plated on a T-75 flask. After 24 hr THP-1 cells were treated with JTT (100 μg/mL) or DMSO vehicle controls for 4 hr in a 37 °C

humidified 5% CO_2 incubator. At this dosage (100 μg/mL) JTT did not inhibit the growth of THP-1 cells as determined by the MTS assay (data not shown).[80] The 4 hr time point was used to detect the early (primary) transcriptional events, which are less susceptible to experimental errors compared to later (secondary) transcriptional responses. Total RNA was purified with a Qiagen RNeasy mini kit. Expression profiling was carried out by following the Affymetrix GeneChip Expression Profiling manual. Briefly, synthesis of biotinylated cRNA via double-strand cDNA with T7 promoter was carried out with Affymetrix One-Cycle Target Labeling and Control Reagent kit. Biotinylated cRNA samples were fragmented. Fragmented samples were submitted to the Rockefeller University Genomics Center for hybridization to Human Genome U133 Plus 2.0 array, staining, washing, and scanning. The resulting data were analyzed with Affymetrix GeneChip® Operating Software and ArrayAssit Lite (Stratagene). Two independent experiments were carried out for each treatment condition: JTT-treated and DMSO (control)-treated THP1 cells. This enabled four comparisons between TSS-treated and control groups. Genes that were called "I (increase)" or "D (decrease)" by Affymetrix GeneChip® Operating Software in at least three out of four comparisons were selected. In order to obtain the most reliable genes for the subsequent real-time PCR guided fractionation, stringent criteria (Change p-value smaller than 0.001 or larger than 0.999) were used to further narrow down the genes. The table lists the genes with |Log ratio| of 3 or higher (Fold change 8 or higher). None of the down-regulated genes had a |Log ratio| of 3 or higher.

Cell treatment and lysis: THP-1 cells were split one day before the treatment at the

concentration of 0.2-0.5 × 10^6 in 2 mL of media in 6- or 12-well plates. After 24 hr, THP-1 were treated with fractions/treatment a (s), JTT (positive control, 100 μg/mL), and DMSO vehicle control for 4 hours in a 37 °C humidified 5% CO_2 incubator. The fractions (dry)/treatment sample(s) were quantified with analytical scale and then dissolved in biological grade DMSO for the treatment. The final DMSO concentration for each treatment was kept at or less than 0.5%. After the 4 hr incubation, the cell suspension was transferred to a 15 mL falcon tube and centrifuged at 1,300 rpm for 5 min. The medium was aspirated. The cell pellet was lysed with 350 μL of TRK lysis butter (containing 2% β-mercaptoethanol). The cell lysate was then loaded onto an Omega® Homogenizer column (Omega Bio-Tek) and centrifuged at 13,200 rpm for 2 min. The homogenized lysate was either stored at -80°C or immediately processed for RNA purification.

RNA purification and quantification: A total RNA kit (Omega Bio-Tek) was used to purify total RNA from the THP-1 cell lysate. Then 70% ethanol (350 μL) was added to the cell lysate (350 μL) and the mixture was loaded into a HiBind® RNA mini-column. The mixture was centrifuged at 13,200 rpm for 1 min and the flow-through was discarded. RNA Wash Buffer I (RNA wash buffer for the RNA kit, 500μL) was added to the column and centrifuged at 13,200 rpm for 1 min. The flow-through was discarded and the column was then washed twice with 500 μL of RNA Wash Butter II, and then was centrifuged for 1 minute at 13,200 rpm. The flow-through was discarded, then the column was centrifuged for additional 2 min in order to dry the membrane. Then, the HiBind® RNA mini-column was placed in a new collection tube and 25 μL of RNAse-free water

was added. The column was incubated at room temperature for 5 min and then centrifuged at 13,200 rpm for 1 min. The resulting RNA sample was quantified using absorbance at 260 nm. Samples with 260 nm/280 nm ratio ~1.8 or higher were used for subsequent studies. Purified RNA samples were used for cDNA synthesis.

Reverse Transcription: For reverse transcription reaction, the total RNA concentration between 0.5-4 μg was used. For each RT reaction, the following materials were used: 1 μL of a 10 mM dNTP mixture, 2 μL of Random hexamers (0.3 μg/μL, Invitrogen), the appropriate amount of purified RNA (to make the desired concentration) and complete with Nuclease-free water in order to reach a total volume of the mixture equal to 16 μL. The mixture was placed at 70 °C for 3 min in a thermocycler and then cooled down to 4 °C for 1 min. After that, the following reagents were added to the mixture: 4 μL of 5× RT buffer, 0.5 μL of 200U/μL M-MLV (Promega). The mixture was incubated at 42 °C for 1 hr and then was heated at 95 °C for 10 min. The sample was further incubated at 37 °C for 20 min in order to eliminate RNA-DNA hybrids. Synthesized cDNA was either immediately used for real-time PCR analysis or stored at -20 °C. cDNA was diluted with RNase-free water before real-time PCR, and the final concentration of cDNA was ~0.02 μg/μL.

Real-time polymerase chain reaction (Real-Time PCR): Taqman® Gene Expression assays (Applied Biosystems) was carried out on an Applied Biosystems 7500 Real-Time PCR system using pre-optimized assays for selected genes and GAPDH (endogenous control). For every gene of interest and GAPDH assay the following reagents were

mixed: 10 μL (per reaction) of Taqman® master mix 2× and 1 μL (per reaction) of each probe. From each of the previous probes mixtures, 11 μL was transferred to corresponding optical PCR tubes. From each cDNA mixture, 9 μL was added to the proper PCR tubes. The PCR experiment was divided into three stages: 1. 2 min at 50°C (one cycle), 2. 10 min at 95 °C (one cycle) and 3. 15 s at 95°C followed by 1 min at 60°C (40 cycles). The $\Delta\Delta C_T$ was employed to quantify the selected genes induction. The raw data were first normalized by the endogenous control (GAPDH) for individual samples. Then the relative quantification (RQ) values, i.e. the ratio, were obtained by comparing the normalized data against the DMSO vehicle control. At least duplicate experiments were carried out for each fraction.

Extraction and purification of active fraction from JTT (Batch1): The JTT sample for this study was already the water extract (dried powder) prepared by Honso Pharmaceutical (Nagoya, Japan). Every 400 grams of JTT sample was extracted with chloroform/methanol (2:1). The mixture (3 L total volume) was stirred for 24 hr at room temperature, in a covered 5 L-round bottom flask. The insoluble material was filtered and the solvent of the soluble fraction was evaporated using a rotatory evaporator. The dried fraction was further simplified by *n*-butanol-water partitioning. The 1-butanol layer was separated from the aqueous layer, and evaporated. The dried 1-butanol fraction was applied to an open silica column (amount of silica = 100 g) and eluted with 1%, 10%, 20%, and 30% methanol in dichloromethane (480 mL each). The 20% methanol in dichloromethane fraction was evaporated under vacuum. The dried 20% fraction was further purified with a SPE C8 column with 50%, 75%, and 100% methanol in water. The

100% methanol fraction contained a mixture of sterolins, and the individual compounds were isolated by HPLC.

HPLC and ELSD (Batch 1): The reversed-phase HPLC purification was carried out using an Agilent 1100 HPLC equipped with a photodiode array detector (PDA) and ELSD. Samples subjected to HPLC purification were dissolved in biological grade DMSO and filtered through a 0.22-μm PTFE membrane filter (Whatman). The reverse-phase purification was carried out on an Alltech Econosil semi-preparative C18 10 mm × 250 mm column (Alltech) with isocratic elution using 100% methanol in water at an operating temperature 26°C. Isocratic elution was carried out over a period of 30 min with a flow rate of 3 mL/min. Injection volume was 80-100 μL (into a 200 μL loop), which contained ~1 mg of sample. UV signals were collected at 220 nm, 280 nm, 254 nm, and 350 nm. The data were recorded and processed using Agilent ChemStation software. ELSD analysis was performed on an Alltech ELSD 800 detector, with nitrogen in a drift temperature of 43°C and nebulizer pressure of 4.4 bar. Fractions A-F were collected.

Isolation and identification of soya GlcCer in Fr. C (Batch 1): Soya GlcCer was isolated and identified by acetylating the constituents in HPLC Fraction C. Briefly, acetylation of Fr. C was done by treating a solution of Fr. C (1 mg) in pyridine (1 mL) with acetic anhydride (200 μg) and left overnight at room temperature. The mixture was diluted with 1 mL of water and extracted with dichloromethane. The dried sample was purified on a silica gel column chromatography (5mm i.d. × 30mm).

Extraction and purification of active fraction from JTT (Batch 2): The JTT sample for this study was the water extract (dried powder) prepared by Honso Pharmaceutical (Nagoya, japan). Every 500 grams of JTT sample was extracted with chloroform/methanol (2:1). The mixture (3 L total volume) was stirred for 24 hr at room temperature, in covered 4 L-flask. The insoluble material was removed by filtering out and was subjected to a second extraction with 1 L of chloroform/methanol (2:1) overnight. The solvents of the soluble fraction of both the first and second extractions were combined and were evaporated under vacuum. The dried fraction was further simplified by 1-butanol-water partitioning. The 1-butanol layer was separated from the aqueous layer, and the solvents were evaporated under vacuum. The dried 1-butanol fraction was then reconstituted with cold acetone (100 mL of cold acetone was used for ~8 g of 1-butanol fraction) and kept at 4°C for 24 hr. The acetone-soluble and acetone-insoluble fractions were separated by centrifugation (10 min @ 2000 rpm, 4°C) and decanting. The acetone-insoluble fraction was applied by silica column chromatography (amount of silica = ~250 g for every 5 g of acetone-insoluble fraction), and eluted with 7.5% methanol in dichloromethane. The fraction containing compound(s) with R_f values 0.6-0.7 (developing solvent, 20% methanol in dichloromethane, eluted twice) retained the highest immunostimulatory activity (determined by ICAM-1 real-time PCR), and were subjected to further purification by HPLC.

HPLC and ELSD (Batch 2): Refer to p.46 of HPLC and ELSD (Batch 1)

NMR: Samples were dissolved in methanol-d_4, $CDCl_3$, or a mixture of methanol-

d_4/$CDCl_3$. NMR spectra were measured by Brüker Avance 500-MHz spectrometer equipped with a dual [^{13}C, ^{1}H] CryoProbe. Data were acquired and processed with the Brüker XWIN-NMR software package.

CD14+ cells and DC: CD14+ cells and DC were kindly provided by Dr. Xiangming Li and Prof. Moriya Tsuji (Aaron Diamond AIDS Research Center). Briefly, CD14+ monocytes were isolated from human PBMC using CD14 MicroBeads. DC was prepared by culturing CD14+ monocytes in the presence of GM-CSF and Il-4.

Treatment of CD14+ cells and DC: Freshly isolated CD14+ cells were treated with Fraction D (5 μg/mL), DMSO, JTT; positive control (100 μg/mL), and LPS; (0.5 μg/mL). After 4 hr of treatment, qRT-PCR was performed to examine the ICAM-1 expression level.

FACS: In order to determine the ICAM-1 protein expression level, CD14+ cells and DCs were treated by the active fraction D for 24 hr. Then cells were transferred into Eppendorf tubes (~0.16×10^6/tube), and spun for 5 min at 2500 rpm. After the supernatant was discarded, then 40 μL (1 μg of Fc blocking antibody for 0.5×10^6 cells, diluted in FACS buffer) of Fc blocking antibody was added, and incubated for 15 min at room temperature. FACS buffer (750 μL) was added to each Eppendorf tubes, and spun for 5 min at 2700 rpm. The supernatant was aspirated. The cells were then incubated with anti-ICAM-1 conjugated with APC (Allophycocyanin) in the dark at room temperature. After 15 min of incubation, FACS buffer (750 μL) was added, followed by centrifugation

for 5 min at 2700 rpm. The supernatant was aspirated, and 250 μL of FACS buffer was added, followed by mixing by pipetting up and down. The solution with cells (250 μL) was transferred to a FACS tube.

II.6: References

1. Sumner, J. *The Natural History of Medicinal Plants*. (Timber Press: 2000).

2. Newman, D. J. & Cragg, G. M. Natural products as sources of new drugs over the last 25 years. *J. Nat. Prod.* **70**, 461–477 (2007).

3. Ginsburg, H. & Deharo, E. A call for using natural compounds in the development of new antimalarial treatments - an introduction. *Malar. J.* **10 Suppl 1**, S1 (2011).

4. Harvey, A. L. Natural products in drug discovery. *Drug Discov. Today* **13**, 894–901 (2008).

5. Shu, Y. Z. Recent natural products based drug development: a pharmaceutical industry perspective. *J. Nat. Prod.* **61**, 1053–1071 (1998).

6. Kawamura, A., Brekman, A., Grigoryev, Y., Hasson, T.H., Takaoka, A., Wolfe, S. & Soll, C.E. Rediscovery of natural products using genomic tools. *Bioorg. Med. Chem. Lett.* **16**, 2846–2849 (2006).

7. Kawamura, A., Iacovidou, M., Takaoka, A., Soll, C. E. & Blumenstein, M. A polyacetylene compound from herbal medicine regulates genes associated with thrombosis in endothelial cells. *Bioorg. Med. Chem. Lett.* **17**, 6879–6882 (2007).

8. Kensil, C. R., Patel, U., Lennick, M. & Marciani, D. Separation and characterization of saponins with adjuvant activity from Quillaja saponaria Molina cortex. *J. Immunol.* **146**, 431–437 (1991).

9. Wang, G.-X., Li, F.-Y., Cui, J., Wang, Y., Liu, Y.-T., Han, J. & Lei, Y. Immunostimulatory Activities of a Decapeptide Derived from Alcaligenes faecalis FY-3 to Crucian Carp. *Scand. J. Immunol.* **74**, 14–22 (2011).

10. Jacobsen, N. E. Fairbrother, W.J., Kensil, C.R., Lim, A., Wheeler, D.A. & Powell, M.F. Structure of the saponin adjuvant QS-21 and its base-catalyzed isomerization product by 1H and natural abundance 13C NMR spectroscopy. *Carbohyd. Res.* **280**, 1–14 (1996).

11. Natori, T., Morita, M., Akimoto, K. & Koezuka, Y. Agelasphins, novel antitumor and immunostimulatory cerebrosides from the marine sponge Agelas mauritianus. *Tetrahedron* **50**, 2771–2784 (1994).

12. Motoki, K., Morita, M., Kobayashi, E., Uchida, T., Akimoto, K., Fukushima, H. & Koezuka, Y. Immunostimulatory and antitumor activities of monoglycosylceramides having various sugar moieties. *Biol. Pharm. Bull.* **18**, 1487–1491 (1995).

13. Tsuji, M. Glycolipids and phospholipids as natural CD1d-binding NKT cell ligands. *Cell. Mol. Life Sci.* **63**, 1889–1898 (2006).

14. Kobayashi, E., Motoki, K., Uchida, T., Fukushima, H. & Koezuka, Y. KRN7000, a novel immunomodulator, and its antitumor activities. *Oncol. Res.* **7**, 529–534 (1995).

15. Taylor, P. R., Martinez-Pomares, L., Stacey, M., Lin, H.-H. Brown, G. D. & Gordon, S. Macrophage receptors and immune recognition. *Annu. Rev. Immunol.* **23**, 901–944 (2005).

16. Kaufmann, S. H. E., Medzhitov, R. & Gordon, S. *The Innate Immune Response to Infection*. (ASM Press: 2004).

17. Paul, W. E. *Fundamental Immunology*. (Lippincott Williams & Wilkins: 2008).

18. Beutler, B. & Rietschel, E. T. Innate immune sensing and its roots: the story of endotoxin. *Nat. Rev. Immunol.* **3**, 169–176 (2003).

19. Waller, E. K. The Role of sargramostim (rhGM-CSF) as immunotherapy. *The Oncologist* **12**, 22–26 (2007).

20. Haworth, C., Brennan, F.M., Chantry, D., Turner, M., Maini, R.N. & Feldmann, M. Expression of granulocyte-macrophage colony-stimulating factor in rheumatoid arthritis: Regulation by tumor necrosis factor-α. *Eur. J. Immunol.* **21**, 2575–2579 (1991).

21. Takeuchi, O., Sato, S., Horiuchi, T., Hoshino, K., Takeda, K., Dong, Z., Modlin, R.L. & Shizuo, A. Cutting edge: role of toll-like receptor 1 in mediating immune response to microbial lipoproteins. *J. Immunol.* **169**, 10–14 (2002).

22. da Silva Correia, J., Soldau, K., Christen, U., Tobias, P. S. & Ulevitch, R. J. Lipopolysaccharide is in close proximity to each of the proteins in its membrane receptor complex. transfer from CD14 to TLR4 and MD-2. *J. Biol. Chem.* **276**, 21129–21135 (2001).

23. Ulevitch, R. J. & Tobias, P. S. Receptor-dependent mechanisms of cell stimulation by bacterial endotoxin. *Annu. Rev. Immunol.* **13**, 437–457 (1995).

24. Greenberg, J. W., Fischer, W. & Joiner, K. A. Influence of lipoteichoic acid structure on recognition by the macrophage scavenger receptor. *Infect. Immun.* **64**, 3318–3325 (1996).

25. Liu, W., Yin, L., Chen, C. & Dai, Y. Function modification of SR-PSOX by point mutations of basic amino acids. *Lipids in Health and Disease* **10**, 59 (2011).

26. Heine, H., El-Samalouti, V.T., Notzel, C., Pfeiffer, A., Lentschat, A., Kusumoto, S., Schmitz, G., Hamann, L. & Ulmer, A.J. CD55/decay accelerating factor is part of the lipopolysaccharide-induced receptor complex. *Eur. J. Immunol.* **33**, 1399–1408 (2003).

27. Sankala, M., Brannstrom, A., Schulthess, T., Bergmann, U., Morgunova, E., Engle, J., Tryggvason, K. & Pikkarainen, T. Characterization of recombinant soluble macrophage scavenger receptor MARCO. *J. Biol. Chem.* **277**, 33378–33385 (2002).

28. Nielsen, M. J., Madsen, M., Møller, H. J. & Moestrup, S. K. The macrophage scavenger receptor CD163: endocytic properties of cytoplasmic tail variants. *J. Leukoc. Biol.* **79**, 837–845 (2006).

29. Daws, M. R., Sullam, P.M., Niemi, E.C., Chen, T.T., Tchao, N.K. & Seaman, W.E. Pattern recognition by TREM-2: binding of anionic ligands. *J. Immunol.* **171**, 594–599 (2003).

30. Saiki, I. A Kampo medicine 'Juzen-taiho-to'--prevention of malignant progression and metastasis of tumor cells and the mechanism of action. *Biol. Pharm. Bull* **23**, 677–688 (2000).

31. Ohnishi, Y., Fujii, H., Hayakawa, Y., Sakukawa, R., Yamaura, T., Sakamoto, T., Tsukada, K., Fujimaki, M., Nunome, S., Komatsu, Y. & Saiki, I. Oral administration of a Kampo (Japanese herbal) medicine Juzen-taiho-to inhibits liver metastasis of colon 26-L5 carcinoma cells. *Cancer Science* **89**, 206–213 (1998).

32. Tagami, K., Niwa, K., Lian, Z., Gao, J., Mori, H. & Tamaya, T. Preventive effect of Juzen-taiho-to on endometrial carcinogenesis in mice is based on Shimotsu-to constituent. *Biol. Pharm. Bull.* **27**, 156–161 (2004).

33. Lian, Z., Niwa, K., Onogi, K., Mori, H., Harrigan, R.C. & Tamaya, T. Anti-tumor effects of herbal medicines on endometrial carcinomas via estrogen receptor-alpha-related mechanism. *Oncol. Rep* **15**, 1133–1136 (2006).

34. Kiyohara, H., Matsumoto, T. & Yamada, H. Combination effects of herbs in a multi-herbal formula: expression of Juzen-taiho-to's immuno-modulatory activity on the intestinal immune system. *Evid. Based Complement Alternat. Med.* **1**, 83–91 (2004).

35. Yamada, H. & Saiki, I. *Juzen-taiho-to (Shi-Quan-Da-Bu-Tang): Scientific Evaluation and Clinical Applications*. (CRC Press: 2005).

36. Gertsch, J., Viveros-Paredes, J. M. & Taylor, P. Plant immunostimulants—Scientific paradigm or myth? *J. Ethnopharmacol.* **136**, 385–391 (2011).

37. Capasso, R., Izzo, A.A., Pinto, L., Bifulco, T., Vitobello, C. & Mascolo, N. Phytotherapy and quality of herbal medicines. *Fitoterapia* **71, Supplement 1**, S58–S65 (2000).

38. Hasson, T. H. *Isolation and Characterization of Immunomodulatory Compounds from Juzen-Taiho-To: Novel Understanding of Phytosteryl Glucosides Nano-Aggregates and Synergism.* (The Graduate Center of CUNY: New York, 2009).

39. Iacovidou, M. *Uncovering hidden potential of natural products*. (The Graduate Center of CUNY: New York, 2010).

40. Van De Stolpe, A., Caldenhoven, E., Stade, B.G., Koenderman, L., Raaijmakers, J.A., Johnson, J.P. & Van Der Saag, P.T. 12-O-Tetradecanoylphorbol-13-acetate- and tumor necrosis factor alpha-mediated induction of intercellular adhesion molecule-1 is inhibited by dexamethasone. Functional analysis of the human intercellular adhesion molecular-1 promoter. *J. Biol. Chem.* **269**, 6185–6192 (1994).

41. Folch, J., Lees, M. & Sloane Stanley, G. H. A simple method for the isolation and purification of total lipides from animal tissues. *J. Biol. Chem.* **226**, 497–509 (1957).

42. Lucena, R., Cárdenas, S. & Valcárcel, M. Evaporative light scattering detection: trends in its analytical uses. *Anal. Bioanal. Chem.* **388**, 1663–1672 (2007).

43. Wei, Y.-J., Qi, L.-W., Li, P., Luo, H.-W., Yi, L. & Sheng, L.-H. Improved quality control method for Fufang Danshen preparations through simultaneous determination of phenolic acids, saponins and diterpenoid quinones by HPLC coupled with diode array and evaporative light scattering detectors. *J. Pharm. Biomed. Anal.* **45**, 775–784 (2007).

44. Niiho, Y., Nakajima, Y., Yamazaki, T., Okamoto, M., Tsuchihashi, R., Kodera, M., Kinjo, J. & Nohara, T. Simultaneous analysis of isoflavones and saponins in *Pueraria* flowers using HPLC coupled to an evaporative light scattering detector and isolation of a new isoflavone diglucoside. *J. Nat. Med.* **64**, 313–320 (2010).

45. Almeling, S. & Holzgrabe, U. Use of evaporative light scattering detection for the quality control of drug substances: influence of different liquid chromatographic and evaporative light scattering detector parameters on the appearance of spike peaks. *J. Chromatogr. A* **1217**, 2163–2170 (2010).

46. Fuzzati, N. Analysis methods of ginsenosides. *J. Chromatogr. B Analyt. Technol. Biomed. Life Sci.* **812**, 119–133 (2004).

47. Dustin, M. L., Rothlein, R., Bhan, A. K., Dinarello, C. A. & Springer, T. A. Induction by IL 1 and interferon-gamma: tissue distribution, biochemistry, and function of a natural adherence molecule (ICAM-1). *J. Immunol.* **137**, 245–254 (1986).

48. Mattson, F. H. & Volpenhein, R. A. Synthesis and properties of glycerides. *J. Lipid Res.* **3**, 281 –296 (1962).

49. Haften, J. L. Fat-based food emulsifiers. *J Am Oil Chem Soc* **56**, 831A–835A (1979).

50. Jia, J. X. & Wasan, K. M. Effects of monoglycerides on rhodamine 123 accumulation, estradiol 17 beta-D-glucuronide bidirectional transport and MRP2 protein expression within Caco-2 cells. *J. Pharm. Pharm. Sci.* **11**, 45–62 (2008).

51. Porter, C. J. H., Trevaskis, N. L. & Charman, W. N. Lipids and lipid-based formulations: optimizing the oral delivery of lipophilic drugs. *Nat. Rev. Drug Discov.* **6**, 231–248 (2007).

52. Håversen, L., Danielsson, K. N., Fogelstrand, L. & Wiklund, O. Induction of proinflammatory cytokines by long-chain saturated fatty acids in human macrophages. *Atherosclerosis* **202**, 382–393 (2009).

53. Han, C. Y., Kargi, A.Y., Omer, M., Chan, C.K., Webitsch, M., O'Brien, K.D., Wight, T.N. & Chait, A. Differential effect of saturated and unsaturated free fatty acids on the generation of monocyte adhesion and chemotactic factors by adipocytes: dissociation of adipocyte hypertrophy from inflammation. *Diabetes* (2009).doi:10.2337/db09-0925

54. Weisberg, S. P., McCann, D., Desai, M., Rosenbaum, M., Leibel, R.L. & Ferrante, A.W. Obesity is associated with macrophage accumulation in adipose tissue. *J. Clin. Invest.* **112**, 1796–1808 (2003).

55. Natori, T., Koezuka, Y. & Higa, T. Agelasphins, novel α-galactosylceramides from the marine sponge Agelas mauritianus. *Tetrahedron Letters* **34**, 5591–5592 (1993).

56. Margalit, M., Abu Gazala, S., Alper, R., Elinav, E., Klein, A., Doviner, V., Sherman, Y., Thalenfeld, B., Engelhardt, D., Rabbani, E. & Ilan, Y. Glucocerebroside treatment ameliorates ConA hepatitis by inhibition of NKT lymphocytes. *Am. J. Physiol. Gastrointest. Liver Physiol.* **289**, G917–925 (2005).

57. Parekh, V. V., Singh, A.K., Wilson, M.T., Olivares-Villagomez, D., Bezbradica, J.S., Inazawa, H., Ehara, H., Sakai, T., Serizawa, I., Wu, L., Wang, C.-R., Joyce, S. & Van Kaer, L. Quantitative and qualitative differences in the in vivo response of NKT cells to distinct alpha- and beta-anomeric glycolipids. *J. Immunol.* **173**, 3693–3706 (2004).

58. Shibuya, H., Kawashima, K., Sakagami, M., Kawashima, H., Shimomura, M., Ohashi, K. & Kitagawa, I. Sphingolipids and glycerolipids. I. Chemical structures and ionophoretic activities of soya-cerebrosides I and II from soybean. *Chem. Pharm. Bull.* **38**, 2933–2938 (1990).

59. Inagaki, M., Harada, Y., Yamada, K., Isobe, R., Higuchi, R., Matsuura, H. & Itakura, Y. Isolation and structure determination of cerebrosides from Garlic, the bulbs of Allium sativum L. *Chem. Pharm. Bull.* **46**, 1153–1156

60. Ilan, Y., Elstein, D. & Zimran, A. Glucocerebroside: an evolutionary advantage for patients with Gaucher disease and a new immunomodulatory agent. *Immunol. Cell Biol.* **87**, 514–524 (2009).

61. Bertram, H. C., Eldibany, M., Padgett, J. & Dragon, L. H. Splenic lymphoma arising in a patient with Gaucher disease. A case report and review of the literature. *Arch. Pathol. Lab. Med.* **127**, e242–245 (2003).

62. Lo, S. M., Stein, P., Mullaly, S., Bar, M., Jain, D, Pastores, G.M. & Mistry, P.K. Expanding spectrum of the association between Type 1 Gaucher disease and cancers: a series of patients with up to 3 sequential cancers of multiple types--correlation with genotype and phenotype. *Am. J. Hematol.* **85**, 340–345 (2010).

63. Brady, R. O., Kanfer, J. N. & Shapiro, D. Metabolism of glucocerebrosides. II. Evidence of an enzymatic deficiency in gaucher's disease. *Biochem. Biophys. Res. Commun.* **18**, 221–225 (1965).

64. Vanderjagt, D. J., Fry, D. E. & Glew, R. H. Human glucocerebrosidase catalyses transglucosylation between glucocerebroside and retinol. *Biochem. J.* **300 (Pt 2)**, 309–315 (1994).

65. Hannun, Y. A. & Obeid, L. M. The Ceramide-centric universe of lipid-mediated cell regulation: stress encounters of the lipid kind. *J. Biol. Chem.* **277**, 25847–25850 (2002).

66. Demarchi, F., Bertoli, C., Greer, P. A. & Schneider, C. Ceramide triggers an NF-|[kappa]|B-dependent survival pathway through calpain. *Cell Death Differ.* **12**, 512–522 (2005).

67. Ruvolo, P. P. Intracellular signal transduction pathways activated by ceramide and its metabolites. *Pharmacological Research* **47**, 383–392 (2003).

68. Hannun, Y. A. Functions of ceramide in coordinating cellular responses to stress. *Science* **274**, 1855+ (1996).

69. Ruvolo, P. P. Ceramide regulates cellular homeostasis via diverse stress signaling pathways. *Leukemia* **15**, 1153–1160 (2001).

70. Smyth, M. J., Obeid, L. M. & Hannun, Y. A. Ceramide: a novel lipid mediator of apoptosis. *Adv. Pharmacol.* **41**, 133–154 (1997).

71. Ruiz-Argüello, M. B., Basáñez, G., Goñi, F. M. & Alonso, A. Different Effects of Enzyme-generated Ceramides and Diacylglycerols in Phospholipid Membrane Fusion and Leakage. *J. Biol. Chem.* **271**, 26616–26621 (1996).

72. Tapiero, H., Townsend, D. M. & Tew, K. D. Phytosterols in the prevention of human pathologies. *Biomed. Pharmacother.* **57**, 321–325 (2003).

73. Bouic, P. J. & Lamprecht, J. H. Plant sterols and sterolins: a review of their immune-modulating properties. *Altern Med Rev* **4**, 170–177 (1999).

74. Bradford, P. G. & Awad, A. B. Phytosterols as anticancer compounds. *Mol Nutr Food Res* **51**, 161–170 (2007).

75. Awad, A. B. & Fink, C. S. Phytosterols as Anticancer Dietary Components: Evidence and Mechanism of Action. *J. Nutr.* **130**, 2127–2130 (2000).

76. Ling, W. H. & Jones, P. J. Dietary phytosterols: a review of metabolism, benefits and side effects. *Life Sci.* **57**, 195–206 (1995).

77. Bouic, P. J., Etsebeth, S., Liebenberg, R.W., Albrecht, C.F., Pegel, K. & Ven Jaarsveld, P.P. beta-Sitosterol and beta-sitosterol glucoside stimulate human peripheral blood lymphocyte proliferation: implications for their use as an immunomodulatory vitamin combination. *Int. J. Immunopharmacol.* **18**, 693–700 (1996).

78. Bouic, P. J. D. Sterols and sterolins: new drugs for the immune system? *Drug Discov. Today* **7**, 775–778 (2002).

79. Bouic, P. J. The role of phytosterols and phytosterolins in immune modulation: a review of the past 10 years. *Curr Opin Clin Nutr Metab Care* **4**, 471–475 (2001).

80. Malich, G., Markovic, B. & Winder, C. The sensitivity and specificity of the MTS tetrazolium assay for detecting the in vitro cytotoxicity of 20 chemicals using human cell lines. *Toxicology* **124**, 179–192 (1997).

Chapter III: Characterization of individual compounds and mixtures of identified compounds in MΦ-stimulating fractions from JTT

Chapter III

III.1: Introduction

Chapter 2 presented the identification of lipid compounds in MΦ-stimulatory fractions from JTT. Although some of these compounds have been described as immunostimulants,[1–5] it was still necessary to determine their activities using our assay system for several reasons.

First, the immunostimulatory activities were characterized in assays and conditions that are different from ours. For example, Lee *et al.* observed inflammatory responses initiated by saturated fatty acids, in which saturated fatty acids induced the expression of COX-2, inducible nitric oxide synthase (iNOS), and IL-1α in a murine macrophage-like cell line, RAW264.7 cells.[1] On the other hand, we utilize THP-1 cells (and human primary monocytes/MΦ and DC). THP-1 cells were employed in another study, in which fatty acids were used to induce inflammatory responses.[2] However, the study differed from ours in terms of treatment conditions and the genes to monitor the activity;[2] the cells were treated for 8 hr (instead of 4 hr), and the expression of IL-8 and macrophage inflammatory protein (MIP-1) were examined (as opposed to ICAM-1). The method to prepare samples was different in many studies: fatty acids were first solubilized using bovine serum albumin (BSA) prior to the cell treatment.[1–3,6] In our system, samples were simply dissolved in DMSO before the treatment.

Second, some of the compounds were never tested individually for the immunostimulatory activity. For example, sterolins, which have been reported to possess immunostimulatory activity, have been tested only as crude mixtures.[4,5,7,8] Likewise, even

a "purified" immunostimulatory lipid can still be a mixture of structural isomers. For example, commercial soya GlcCer was found to be a mixture of two isomers in the sphingoid backbone, namely 8-*cis* and 8-*trans*.[9] It is not clear whether double bond configuration is important for immunostimulatory activity. Instead of double-bond configuration of the sphingoid backbone, past structure-activity relationship studies of this class of compounds (cerebrosides) focused on the sugar moiety, *N*-acyl chain, and the polar region of the sphingoid backbone.[10–13]

The issues listed above made it necessary to evaluate and compare the immunostimulatory activity of the compounds identified in Chapter 2 using our assays. The study was also expected to help us assess the contribution of individual compounds to the observed immunostimulatory activity of JTT.

Characterization of individual compounds also opened an opportunity to conduct a study of their mixtures. Motivation of this study stemmed from the fact that oriental herbal medicine, including JTT, is formulated by mixing multiple herbs.[14–18] Although it is believed that synergistic interactions among multiple herbs are important for the therapeutic effects of oriental herbal medicine,[17,18] few studies have quantitatively analyzed such "mixture effects." In our case, however, it was possible to conduct a quantitative analysis of mixture effects because chemical constituents in the active fractions have been identified. As described in this chapter, our screening uncovered one mixture that consistently exhibited a higher potency than expected from the individual constituents.

III.2: Results

III.2.1: Preparation of individual compounds for biological characterization

In order to assess the activity of individual compounds, it was necessary to obtain pure samples. While some compounds identified in Chapter 2 were available in pure form from commercial sources, others had to be either purified from commercial samples or chemically synthesized. Commercially available fatty acids and monoacylglycerols (or "monoglycerides") were sufficiently pure (≥ 99%) to be used for the assay without further purification.

Soya GlcCer (β-GlcCer, with 4-*trans* and 8-*cis*/8-*trans* double bonds) from a commercial source, however, turned out to be a mixture of the *cis* and *trans* isomers. The two isomers, therefore, were separated by reverse-phase HPLC using a condition reported previously (Figure III.1, a).[19] Briefly, the 8-*cis* and 8-*trans* isomers in soya GlcCer were separated by HPLC using a semi-preparative column with $CHCl_3$/MeOH/H_2O (1:10:1) as the isocratic eluent. After the HPLC purification, the 8-*trans* isomer was nearly pure as evidenced by ^{13}C-NMR, whereas the 8-*cis* isomer was ~90% pure (Figure III.1, b).

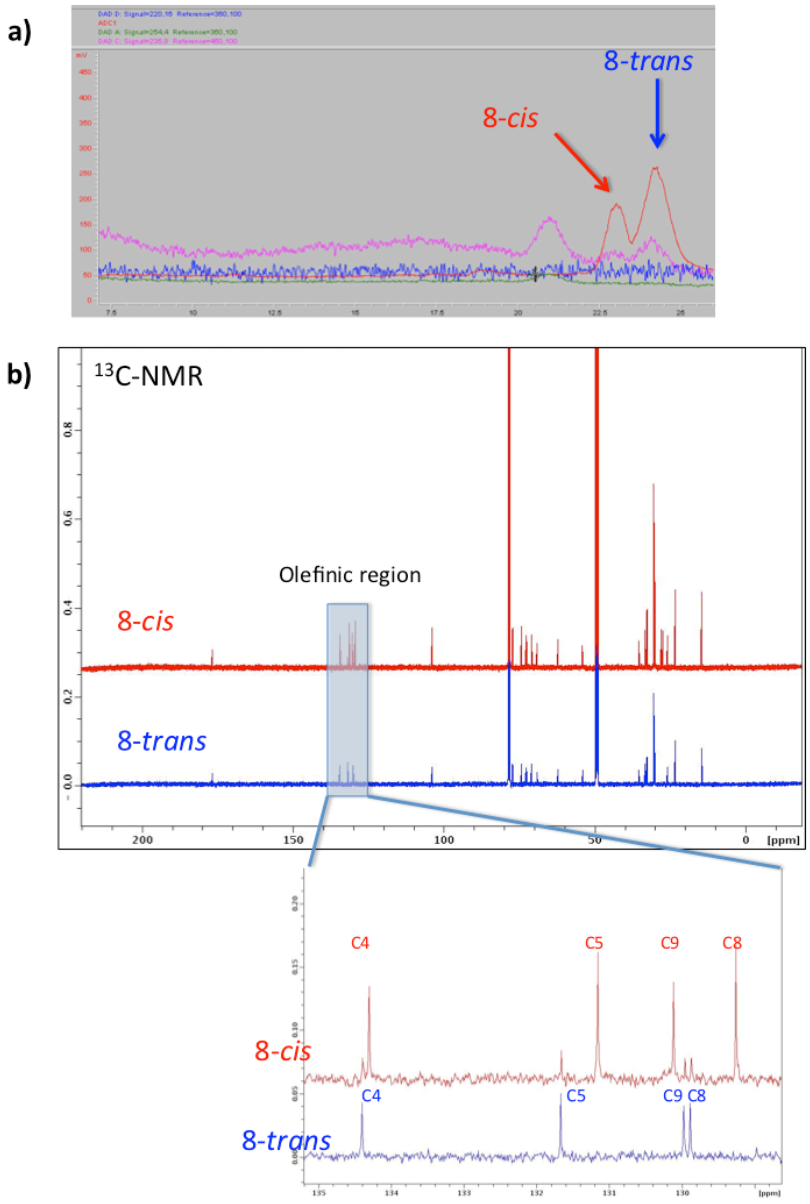

Figure III.1: Isolation and characterization of 8-*cis*/8-*trans* GlcCer. a) An HPLC chromatogram of soya GlcCer (commercial sample, mixture of 8-*cis*/8-*trans*) Conditions: Alltech Econosil C_{18} 10 × 250 mm 10 µ (semi-preparative column). The column was operated at room temperature. Isocratic run of $CHCl_3$/MeOH/H_2O (1:10:1) with a flow rate of 3.0 mL/min. The eluent was detected with photodiode array (220 nm, 235 nm, 254 nm) and ELSD (Gain 16, Nitrogen flow at 4.3 barr, and 44°C). b)^{13}C-NMR of 8-*cis* and 8-*trans* GlcCer, overall spectra, and the olefinic region (magnified).

Sterolins were chemically synthesized using a short scheme as outlined in Scheme III.1. Briefly, β-D-glucose pentaacetate (**3**) in CH_2Cl_2 was reacted with β-sitosterol/stigmasterol in the presence of a Lewis acid catalyst, resulting in the α and β isoforms of each sterolins. β-Isomer formation was favored due to neighboring group participation (Figure III.2).[20] The peracetylated form of theα and β isomers were separated by silica gel column chromatography (elution with 10% ethyl acetate 90% petroleum ether) and deprotected with base to produce the final products, BSSG (**1**) and stigmasteryl β-D-glucoside (**2**) (Scheme III.1, b).

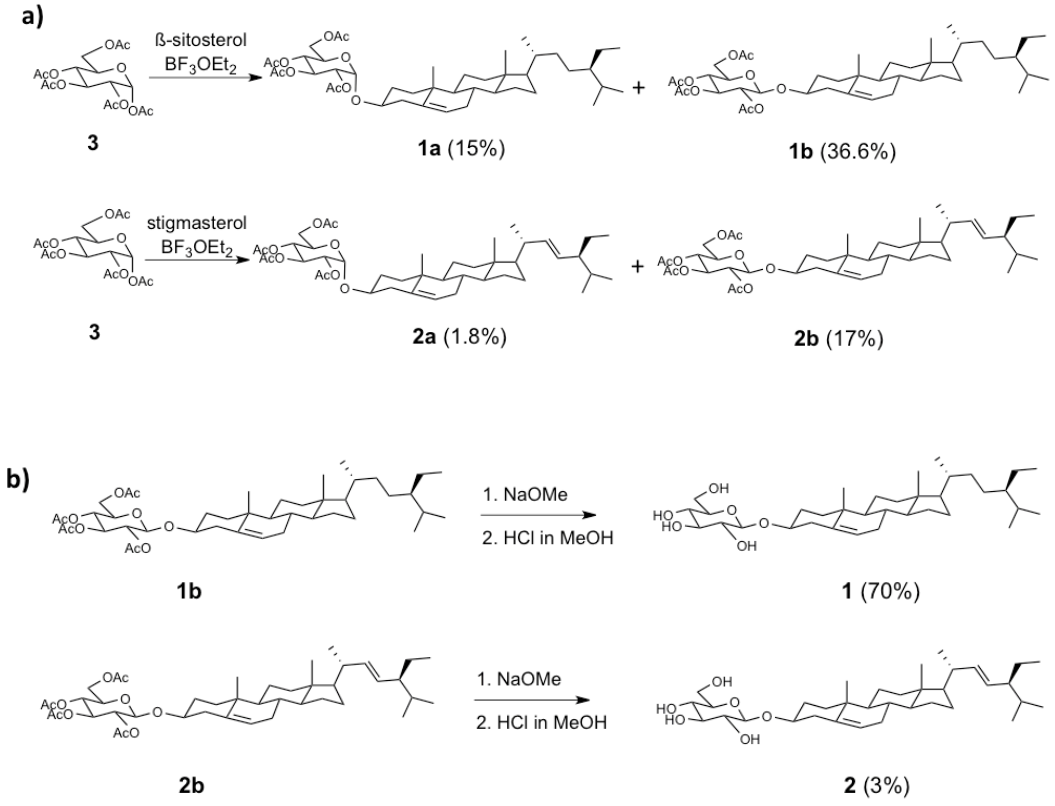

Scheme III.1: Synthesis of β-phytosteryl-glucosides. (a) Syntheses of BSSG peracetate, **1b**, and stigmasteryl β-D-glucoside peracetate, **2b**. Minor α-isomers, **1a** and **2a** were also produced. (b) Base hydrolysis of acetyl groups on the glucose moiety, yields **1**; BSSG, **2**; Stigmasteryl β-D-glucoside.

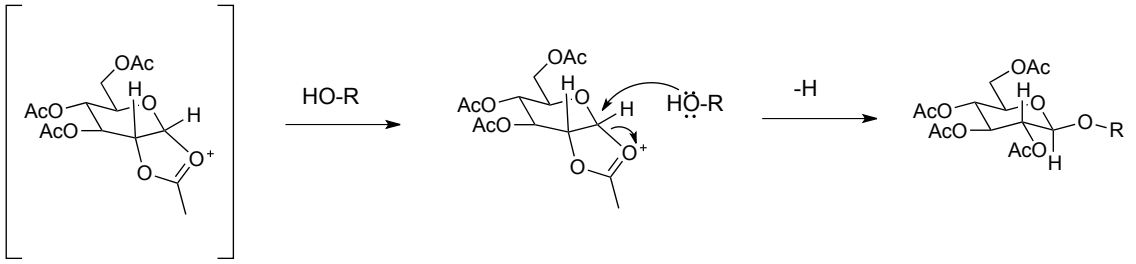

Figure III.2: Neighboring group participation favoring β-isomer formation

III.2.2: Characterization of individual compounds

The qRT-PCR of ICAM-1 was used to characterize the MΦ stimulatory activity of individual compounds. The samples were dissolved in DMSO. The resulting DMSO solutions were used to treat THP-1 cells. After 4 hr of incubation, ICAM-1 expression was determined by qRT-PCR.

First, the MΦ-stimulatory activity of monoacylglycerides, such as monostearin, monobehenin, monopalmitin, and fatty acids, such as stearic acid, were examined. Commercially available monostearin, monobehenin, monopalmitin and stearic acid were subjected to the qRT-PCR assay, which exhibited no significant change in ICAM-1 expression in THP-1 cells. Although these compounds have been reported to stimulate MΦ, many investigators used BSA as the solubilizing agent of fatty acids.[1–3] We, therefore, prepared the stearic acid-BSA complex in our hands. However, no significant induction of ICAM-1 was observed in our assay system.

Second, soya GlcCer was tested for MΦ-stimulatory activity. The commercial sample, which is a mixture of 8-*cis* and 8-*trans* isomers, induced ICAM-1 significantly higher than the DMSO control (Figure III.3). Although the activity was modest (~1.7

fold, 5 μg/mL) and could not account for the potency of JTT, GlcCer was the first sample that reproducibly induced ICAM-1 in THP-1 cells in our hands.

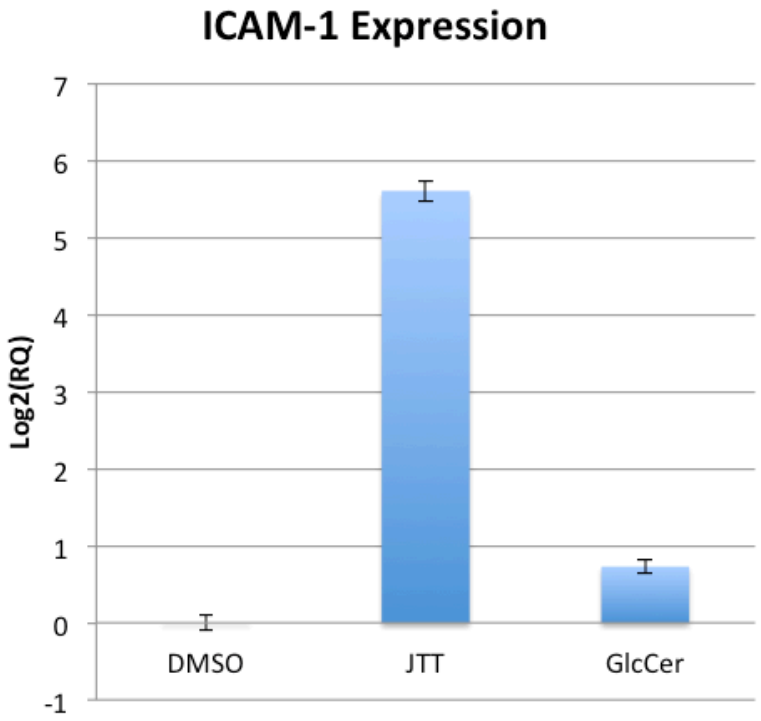

Figure III.3: ICAM-1 real-time PCR assays of GlcCer. THP-1 cells were treated with DMSO, negative control; JTT (100 μg/mL); GlcCer (5 μg/mL). n = 5 for each sample.

The commercial soya GlcCer sample was further characterized with CD14+ cells and DC from human blood to determine whether the GlcCer sample can also stimulate the primary cells. CD14+ cells and DC were freshly prepared and treated with soya GlcCer for 24 hr. The expression of ICAM-1 protein was determined by FACS. The FACS analysis revealed that the commercial GlcCer sample indeed induced ICAM-1 expression, although the activity was modest compared to JTT and LPS (Figure III.4).

Thus GlcCer was confirmed to be the first lipid factor that contributes to the MΦ-stimulatory activity of JTT.

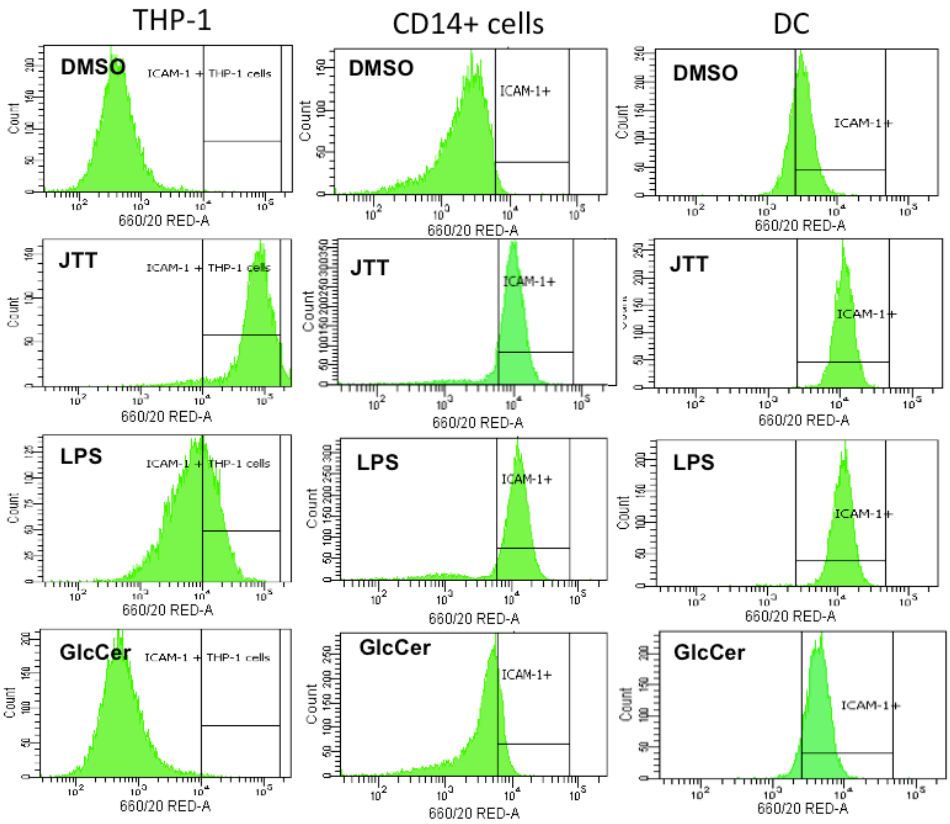

Treatment (24hr)	THP-1 MFI	CD14+ MFI	DC MFI
DMSO	10791	1899	3108
JTT 100 µg/mL	65451	8661	11463
LPS 0.5 µg/mL	12697	9722	11653
GlcCer 5 µg/mL	9907	3324	4278

Figure III.4: ICAM-1 expression at protein level evaluated by FACS. THP-1, CD14+ and DC cells were treated with DMSO, negative control; JTT (100 µg/mL); LPS, positive control (0.5 µg/mL), GlcCer (5 µg/mL) for 24 hr.

As mentioned above, however, the commercial soya GlcCer sample is a mixture of 8-*cis* and 8-*trans* isomers, in which the *trans*-isomer is the major constituent (Figure III.1). On the other hand, GlcCer in the active fraction of JTT contained more *cis*-isomer than the *trans*-isomer.[9] The difference in the *cis*/*trans* ratio in the two samples raised a possibility that the *cis*-isomer might be important for the immunostimulatory activity.

Although, the difference between the 8-*cis* and 8-*trans* isomers of GlcCer had not been characterized at that point, the activity differences of *cis* and *trans* fatty acids were demonstrated by many researchers. It is known that *trans*-unsaturated fatty acids possess adverse effects on human health.[21,22] For example, *trans*-fatty acids have been considered to contribute to the cause of coronary heart disease.[23] Since the structures of 8-*cis* GlcCer and 8-*trans* GlcCer are distinctively different, it would not be surprising if they showed differences in activity. We, therefore, set out to investigate the activity of individual isomers.

The activity of individual 8-*cis* and 8-*trans* isomers was characterized using the samples purified by HPLC as described above (Figure III.1). The qRT-PCR analysis revealed that the difference was not statistically significant, although the 8-*cis* isomer tended to show higher activity than the 8-*trans* isomer (Figure III.5).

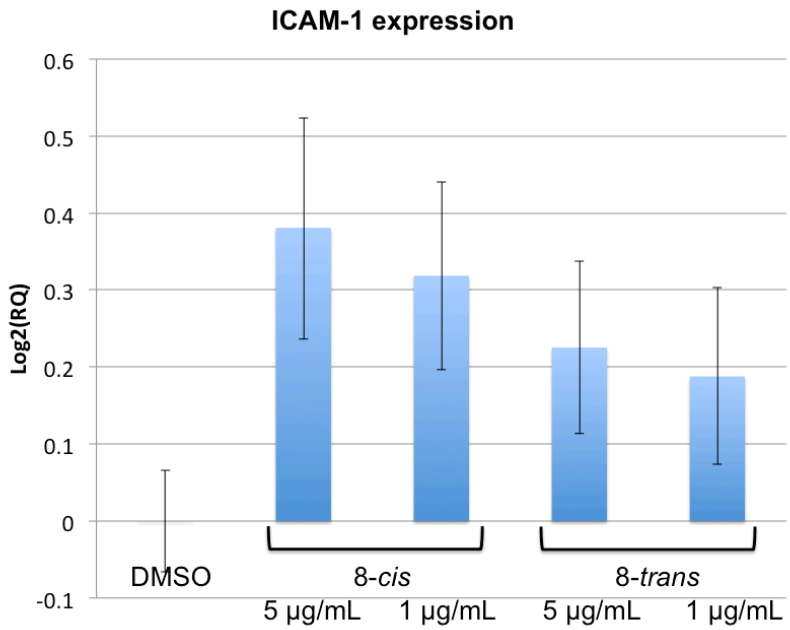

Figure III.5: ICAM-1 real-time PCR assays of individual GlcCer isomers. THP-1 cells were treated with DMSO, negative control; 8-*cis* GlcCer (5 µg/mL and 1 µg/mL); 8-*trans* GlcCer (5 µg/mL and 1 µg/mL); n = 5 for each sample.

Sterolins are another group of compounds that were characterized in this study. As noted earlier, a number of studies have reported various immunostimulatory activities of sterolins.[5,7,8] However, these studies were carried out using crude mixtures of sterolins and other lipids. In a study conducted previously in our group, sterolins were the first group of compounds that were identified in the fractions with MΦ-stimulatory activity from JTT.[24] However, these fractions contained small amounts of additional lipids that were difficult to remove. Chemical synthesis, as outlined above, gave us the opportunity to study the MΦ-stimulatory activity of each sterolin without the concern of potential contaminants in samples.

Synthesized BSSG and stigmasteryl β-D-glucoside samples were dissolved in DMSO and used directly for the qRT-PCR assay using THP-1 cells. The qRT-PCR assay revealed that synthetic sterolins did not possess MΦ-stimulatory activity (Figure III.6). These results suggested that sterolins were not the main active constituents in JTT, although they might have some secondary roles, such as formulation agents.

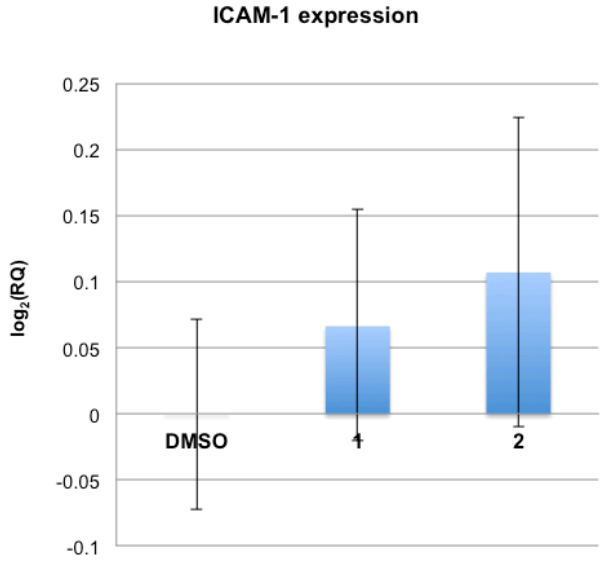

Figure III.6: ICAM-1 real-time PCR analysis of BSSG (1) and stigmasteryl β-D-glucoside (2). THP-1 cells were treated with DMSO, negative control; (1 µg/mL), JTT; (100 µg/mL), and BSSG (**1**) and stigmasteryl β-D-glucoside (**2**); (5 µg/mL) n = 4 for each sample.

Table III.1 summarizes the results of characterization of individual compounds. Among the compounds tested soya GlcCer (as a mixture of 8-*cis* and 8-*trans*) showed reproducible MΦ-stimulatory activity.

Table III.1: Individual characterization of compounds in active fractions

Compound	Activity
Monostearin	-
Monobehenin	-
Monopalmitin	-
Stearic acid	-
Soya GlcCer (Mixture of 8-*cis* and 8-*trans* isomers)	+
GlcCer (8-*cis*)	-
GlcCer (8-*trans*)	-
BSSG	-
Stigmasteryl β-D-glucoside	-

(-) : No statistical difference compared to DMSO control

(+): $p<0.005$ from DMSO control

III.2.3: Preparation of the compound mixtures for biological screening

Characterization of the individual compounds revealed that soya GlcCer possessed MΦ-stimulatory activity. However, the activity of GlcCer alone could not explain the potency of the fractions purified from JTT. Thus, we turned our focus toward the mixture effect of these compounds. The mixtures could be categorized into four different groups. The first group was the GlcCer mixtures that differed in the ratio of 8-*cis* and 8-*trans* isomers. The second group was the mixtures designed to replicate the NMR profiles of the active fractions. The third group was the mixture prepared with borate and/or zinc ion (the rationale behind the use of borate/zinc ions will be described later in this chapter). Finally, the fourth group is the mixtures prepared randomly from compounds identified in Chapter 2.

The first group of mixtures focused on GlcCer, which was identified to be an active factor in a JTT fraction with potent MΦ-stimulatory activity. As noted earlier, GlcCer in this active fraction is a 2:1 mixture of 8-*cis* and 8-*trans* isomers.[9] On the other

hand, the commercial soya GlcCer, which exhibited much weaker activity, contained predominantly the *trans* isomer. Here, the working hypothesis was that the 2:1 mixture was important for the potent immunostimulatory activity. To test this hypothesis, we prepared two mixtures of these isomers in different ratios (Table III.2).

Another group of mixtures was prepared to replicate the NMR profile of an active fraction (Fr. C of the first batch) obtained from JTT. According to NMR and MS, the active fraction C, contained predominantly monostearin and GlcCer. The ratio of the compounds was estimated to be about 5:1 monostearin/GlcCer. Using commercially available monostearin and soya GluCer, we prepared the mixture of the two compounds. The resulting mixture exhibited a ^{1}H-NMR profile that was nearly identical to the profile of fraction C (Figure III.7). In addition, structurally similar monoacylglycerides, such as monobehenin and monopalmitin, as well as individual GlcCer, were combined to produce analogous mixtures for biological characterization (Table III.2).

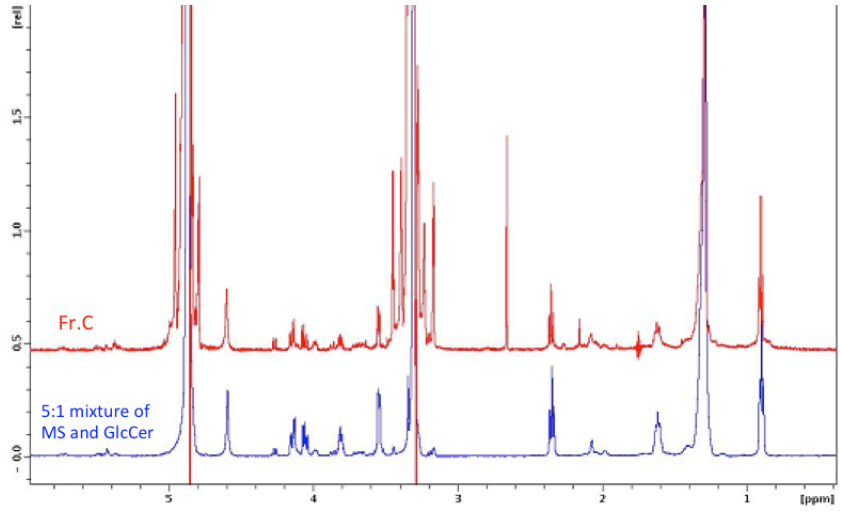

Figure III.7: ^{1}H NMR comparison of fraction C (in red) and 5:1 mixture of monostearin (MS) and commercially available β-glucosylceramides (GlcCer) (in blue).

Table III.2: Mixtures prepared for activity assay (molar ratio)

Monostearin	Monobhenin	Monopalmitin	GlcCer	8-*cis*	8-*trans*
				1	1
				2	1
5			1		
2	2	2	1		
2	2	2		1	
2	2	2			1

The third group is the mixtures of lipids containing borate and/or zinc. Borate is a ubiquitous species that can form complexes with the hydroxyl group of organic molecules. We considered the complex formation by borate because we routinely use borosilicate glass vials and glass test tubes for sample collection during the silica column chromatography. There are cases in which a small quantity (in the order of μg) of polyhydroxylated molecules formed complexes with borate leached out from borosilicate tubes.[25] If borate complexes exist, such complexes may have different biological activities. Thus, we prepared various lipid mixtures containing borate for biological characterization (Table III.3).

Table III.3: Mixtures prepared for activity assay (molar ratio)

Monostearin	GlcCer	BSSG	Borate
8			1
4			1
2			1
1			1
1			2
1			4
	1		0.1
		1	1
5	1		0.25
5		1	0.25
5	1	1	0.25
	1	1	0.1

The presence of zinc ion was also considered because of our preliminary analysis of active fractions using Inductively Coupled Plasma Mass Spectrometer (ICP-MS). The ICP-MS analysis suggested the presence of 83 elements. Among them, zinc was most prominently detected in the active fraction. It was interesting to observe zinc in the active fractions because recent studies found that zinc ion could induce ICAM-1 expression through activation of the NF-κB pathway.[26,27] In order to examine the possible roles of zinc, Zn^{2+} was added to some lipid mixtures. (BSSG was not added in these mixtures because the active fraction submitted to the ICP-MS analysis was Fr. C from the first batch, which did not contain BSSG.) Some mixtures were prepared with zinc ion alone, and some were prepared with both borate and zinc ion (Table III.4).

The final group was the 15 mixtures prepared from the compounds identified in Chapter 2 (Table III.5). Here, Cer was included in this study because it could be formed by the hydrolysis of GlcCer during storage or during the cell treatment.

Table III.4: Mixtures prepared for activity assay (molar ratio)

Monostearin	GlcCer	Borate	Zn
5			1
5			0.5
2	1		1
5	1		2
	2		1
5	1		0.5
5	1		1
5		1	1
10		1	1
5		0.5	1
5		1	0.5
5	1	0.5	0.5
5	1	1	1
5	1	1	0.5
5	1	0.5	1

Table III.5: Mixtures prepared for activity assay (molar ratio)

Monostearin	Monobehenin	Monopalmitin	GlcCer	BSSG	Cer
1	1	1			
1	1	1	1		
1	1	1		1	
1	1	1	1	1	
1	1	1			1
1	1	1		1	1
1	1	1	1		1
1	1	1	1	1	1
0.33	0.33	0.33	1		
0.33	0.33	0.33		1	
0.33	0.33	0.33			1
			1	1	
			1		1
				1	1
			1	1	1

III.2.4: Biological screening of lipid mixtures

In order to identify possible synergism among compounds identified in Chapter 2, various mixtures were prepared as described above and subjected to the qRT-PCR assay using THP-1 cells. The activities of most mixtures could be explained by the sum of the individual constituents. However, one notable exception was identified by this screening. A 1:1 mixture of GlcCer and Cer (total 5 μg/mL) exhibited substantially higher activity than GlcCer (5 μg/mL) and Cer (5 μg/mL), both of which showed comparable activity (Figure III.8 and III.9). This is a synergism because if the 1:1 mixture has an additive effect, a total of 5 μg/ml of the mixture (2.5 μg/mL of each lipid) is expected to show the activity comparable to that of GlcCer and Cer (5 μg/mL). However, the mixture reproducibly exhibited significantly higher activity than expected from the additive effect.

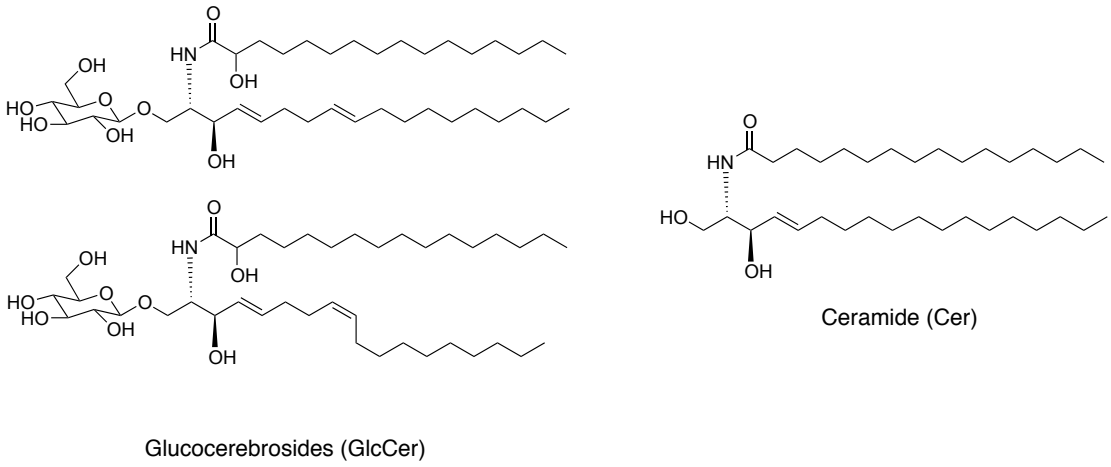

Figure III.8: Structures of commercially available GlcCer (8-*trans* and 8-*cis*) and C16:0-ceramide (Cer)

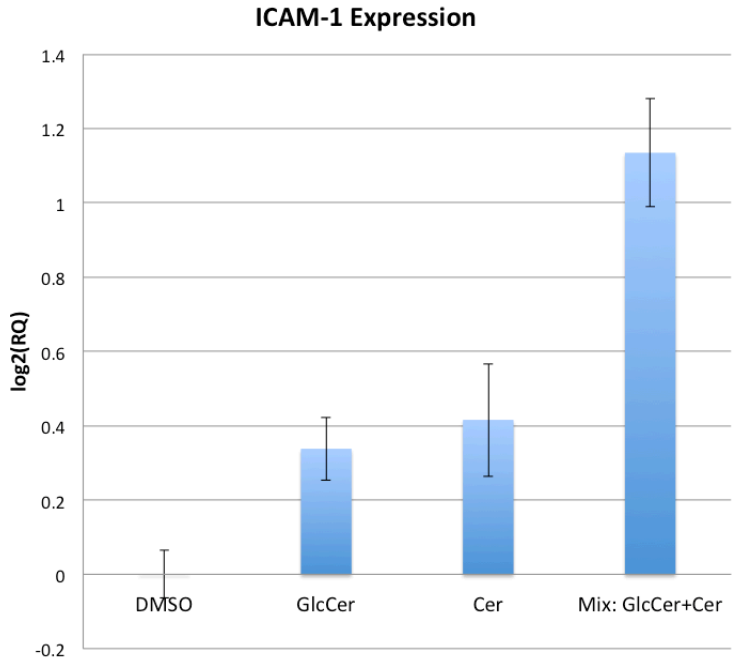

Figure III.9: ICAM-1 real-time PCR assays of GlcCer, Cer and 1:1 mixture of GlcCer and Cer. THP-1 cells were treated with DMSO, negative control; GlcCer (5 μg/mL); Cer (5 μg/ml); and a 1:1 mixture of GlcCer and Cer (total 5 μg/mL). To make the 1:1 mixture, ethanol solutions of GlcCer and Cer were first prepared. Then the solutions were combined to make the 1:1 mixture, which was dried and dissolved in DMSO for cell treatment. Likewise, GlcCer and Cer samples were also prepared from the ethanol solution.

III.2.5: Same sample exhibiting different activity

In the course of assessing the MΦ-stimulatory activity of a GlcCer/Cer mixture, we made a curious observation. The activity of the GlcCer/Cer mixture turned out to be very unstable. When the sample solution in DMSO is freshly prepared, the mixture consistently exhibited distinct MΦ-stimulatory activity. On the other hand, when the sample solution in DMSO was left at room temperature for 3 hr the activity diminished

substantially (Figure III.10). Thus, this GlcCer/Cer mixture presented an interesting example of the same sample exhibiting very different biological activity.

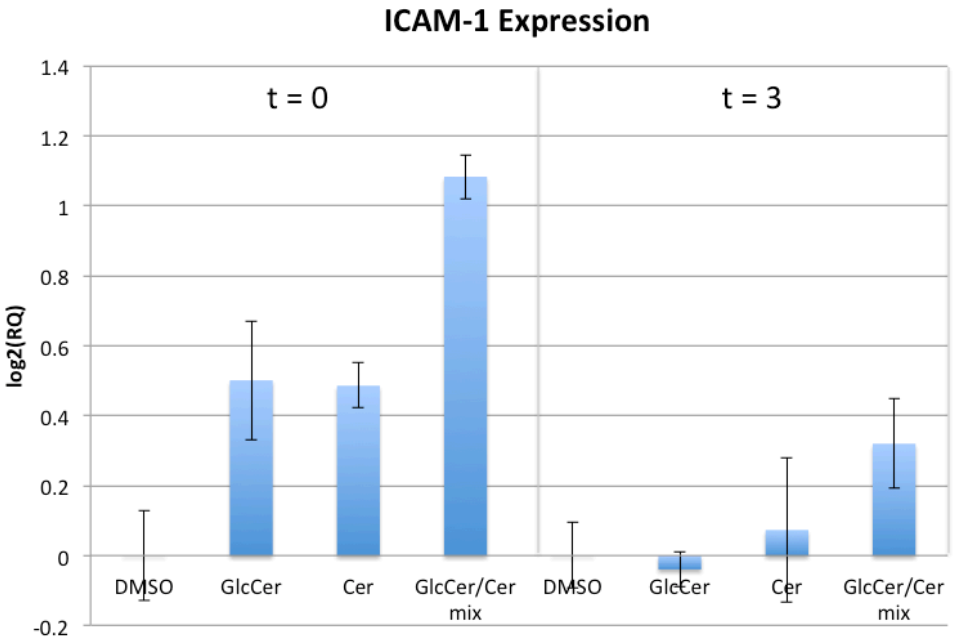

Figure III.10: ICAM-1 real-time PCR assays of GlcCer, Cer and 1:1 mixture of GlcCer and Cer at t = 0 and t = 3. THP-1 cells were treated with DMSO, negative control; GlcCer (5 μg/mL); Cer (5 μg/mL); and 1:1 mixture of GlcCer and Cer (5 μg/mL). THP-1 cells were treated immediately after the dried GlcCer, Cer, and GlcCer/Cer mix was reconstituted (t = 0). For t = 3, DMSO reconstituted GlcCer, Cer, and the GlcCer/Cer mix was kept in room temperature for 3 hr before the treatment.

III.3: Discussion

The study of individual compounds identified GlcCer as a MΦ-stimulatory constituent in JTT. GlcCer has been linked to MΦ in many reports in the context of Gaucher's disease. In Gaucher's disease, the inherited deficiency of β-glucocerebrosidase

results in lipid-laden MΦ, also known as "Gaucher cells" that accumulate GlcCer and other lipids.[28–30] The accumulation of GlcCer is believed to trigger various abnormal immune responses, including induction of pro-inflammatory cytokines, such as TNF and IL-8.[31–34]

What we observed in our study, however, might not be directly relevant to the various immunological abnormalities in Gaucher's disease. In Gaucher's disease, the cellular concentration of GlcCer is chronically high. According to a cell line model of Gaucher's disease, the cellular GlcCer level is ~12-fold higher than the normal level.[35] On the other hand, the induction of ICAM-1 in THP-1 cells, as we observed in our study, was caused by the one time treatment of GlcCer at low micromolar concentration, which does not cause the formation of Gaucher-like cells. In fact, few studies have examined the effect of such a transient, low dose of GlcCer on MΦ. Further studies on low dose GlcCer, therefore, may provide clues to understand the safe and effective immunostimulatory activity of JTT.

The identification of GlcCer, however, does not eliminate the possibility of additional MΦ-stimulatory factors in JTT. In fact, mass spectrometric analyses of the active fractions suggest the presence of as yet uncharacterized compounds (data not shown). Further structural analyses of those compounds are currently underway to obtain the complete picture of chemical constituents in the active fractions from JTT.

Characterization of individual compounds allowed us to investigate the mixture effect among the compounds we identified. Our screening of 48 mixtures revealed a synergistic interaction between GlcCer and Cer. Synergistic stimulation of MΦ has been observed among ligands of Toll-like receptors (TLR) and scavenger receptors (SR) in the

context of various pathological conditions, such as inflammation and atherosclerosis.[36–39] Many TLR/SR ligands, such as LPS, muropeptides, oxidized low-density lipoprotein, dsRNA, and CpG sequences are heterogeneous mixtures of large molecules, which make it difficult to characterize the synergism in a reproducible manner. The GlcCer/Cer mixture, on the other hand, is a mixture of chemically well-defined small molecules. Synergism by the GlcCer/Cer mixture is reproducible and suitable for mechanistic studies. Further examination of the GlcCer/Cer mixture, therefore, is expected to provide clues to understand the molecular basis of the observed synergism. Our observation may also explain the reason why there have been many controversial reports regarding the immunostimulatory activity of GlcCer. The activity of GlcCer could be substantially altered by the presence of additional lipids or even by the manner in which the sample is formulated.

Another important finding was that the activity of the GlcCer/Cer mixture disappeared over time. Inconsistent activity is an old problem in immunology research, such as studies involving vaccine adjuvant.[40] Adjuvant must be appropriately formulated for stability and maximum effect.[41] The unstable activity of the GlcCer/Cer mixture may serve as a useful system to gain novel mechanistic insights into such inconsistent activity of organic molecules, which are often observed but poorly documented.

The reason why the GlcCer/Cer mixture lost the activity is a major mystery. Such loss of activity over time was not observed with the original JTT or the MΦ-stimulating fractions purified from JTT, even when the samples were kept dissolved in DMSO for longer periods of time. It is unlikely that the GlcCer/Cer mixture underwent a chemical

reaction in only 3 hr. Our next question was, “What could change over time within the mixture?”

A clue to address this question came from a somewhat analogous observation made previously in our group. During the first purification round of JTT, it was found that an active fraction formed nanoparticles in DMSO and in water, and the size of the particles appeared to correlate with the biological activity. When the particle size was small (< 10 nm in diameter), the sample showed potent MΦ-stimulatory activity. On the other hand, larger particles (~100 nm in diameter) exhibited much weaker activity. We, therefore, postulated that similar molecular assembly and their changes might explain the observed synergism and its disappearance. The next chapter will discuss the investigation on the molecular assembly of GlcCer/Cer and how it relates to the observed loss of activity.

III.4: Materials and methods

Materials: The solvents/reagents for HPLC and synthesis of sterolins were purchased from VWR and Fisher Scientific. C16:0-ceramide was purchased from VWR.

Cell culture: Refer to p.41

Cell treatment and lysis: Refer to p.43

RNA purification and quantification: Refer to p.43-44

Reverse transcription: Refer to p.44

Real-time polymerase chain reaction (Real-Time PCR): Refer to p.44-45

CD14+ cells and DC: Refer to p.48

Treatment of CD14+ cells and DC: Freshly isolated CD14+ cells were treated with Fraction D (5 μg/mL), DMSO, JTT; positive control (100 μg/mL), and LPS; (0.5 μg/mL). After 4 hr of treatment, qRT-PCR was performed to examine the ICAM-1 expression level.

FACS: Refer to p.48

Separation of 8-*cis*/8-*trans* GlcCer: Soya GlcCer (commercial sample, mixture of 8-*cis* and 8-*trans*) was analyzed on an Econosil C18 10 × 250 mm semi-preparative column with an injection volume of 15 μL. The column was operated at 25°C, using an isocratic run of $CHCl_3$:MeOH:H_2O (1:10:1) with a flow rate of 3.0 mL/min. Detection was done with photodiode array 61 (220 nm, 235 nm, 254 nm) and ELSD (Gain 16, Nitrogen flow at 4.3 barr, and 44°C). ELSD visible peaks at 22.5-23.5 min and 23.5-25 min were collected.

Synthesis of β-sitosteryl-β-D-glucoside pentaacetate: β-sitosterol (100mg) and 4 equivalents (380 mg) of β-D-glucose pentaacetate were placed in a 25-mL round bottom flask with a magnetic stirrer. Benzene (5mL) was added to remove water from the reaction mixture. Then 12 mL CH_2Cl_2 was added to make the reaction mixture of 0.02 M. The reaction mixture was placed on ice and BF_3OEt_2 was added. The reaction was stirred for 10-15 min and removed from the ice bath, then run at room temperature overnight. The progress of the reaction was tested by TLC, with 20% ethyl acetate/80% petroleum ether as the developing solvent. When the reaction was completed, aqueous saturated $NaHCO_3$ solution was added to quench the reaction. The product was extracted with CH_2Cl_2. The organic layer was dried using anhydrous magnesium sulfate, and filtered. The solvent was evaporated under vacuum and the residue was dissolved in 1:1 CH_2Cl_2/petroleum ether, and loaded onto an open silica column and eluted with 100 mL 10% of ethyl acetate/90% petroleum ether. Another 100 mL of 10% ethyl acetate/90% petroleum ether was added to the silica column, and 8 mL fractions were collected. The fractions were tested using TLC (developing solvent mixture, 20% ethyl acetate/80%

petroleum ether). The polarity of the eluting solvent mixture was gradually increased to 17.5% ethyl acetate/82.5% petroleum ether. The fractions for the β-sitosteryl α-D-glucoside pentaacetate and β-sitosteryl β-D-glucoside pentaacetate were combined and the solvent was evaporated under vacuum.

Synthesis of stigmasteryl β-D-glucoside pentaacetate: Refer to p.79. Smaller scale glycosylation was performed with stigmasterol. The reaction mixture contained 50 mg of stigmasterol and 6 equivalents (280 mg) of β-D-glucose pentaacetate. Chemicals used were 3 mL of benzene, 3 mL of CH_2Cl_2, 220 μL of BF_3OEt_2.

Deprotection of phytosterylglucoside pentaacetate: For every 350 μg of phytosteryl glucoside pentaacetate, 100 μL of dry methanol was added. Then ~50 μL of sodium methoxide (NaOMe) in MeOH was added, and the mixture was sonicated for 30 min. After 30 min of sonication, the mixture was acidified by adding HCl in MeOH. The degree of protection was verified by running the sample on TLC using 100% ethyl acetate. Once the complete deprotection had been verified, the solvent was evaporated under vacuum.

HPLC purification of synthesized sterolins: Refer to p.46

NMR: Refer to p.48

Preparation of a mixture using the identified compounds: Stock samples of lipids (monostearin, monobehenin, monopalmitin, stearic acid, GlcCer, BSSG, and Cer) were prepared by dissolving each lipid in 100% EtOH. The final concentration of each lipid was 1 μg/μL. An appropriate volume of each lipid solution was was added in Eppendorf tube, and the EtOH was evaporated under vacuum. The dried samples were re-constituted in DMSO (final concentration, 1 μg/μL). An aqueous solution of $NaB_4O_7 \bullet H_2O$ (10 μg/μL) was used as the source of borate. $ZnCl_2$ (1 mM) was used as the source of Zn^{2+}.

III.5: References

1. Lee, J. Y., Sohn, K. H., Rhee, S. H. & Hwang, D. Saturated Fatty Acids, but Not Unsaturated Fatty Acids, Induce the Expression of Cyclooxygenase-2 Mediated through Toll-like Receptor 4. *J. Biol. Chem.* **276**, 16683–16689 (2001).

2. Choi, S.-E. Kim, T.H., Yi, S.-A., Hwang, Y.C., Hwang, W.S., Choe, S.J., Han, S.J., Kim, H.J., Kim, D.J., Kang, Y. & Lee, K.-W. Capsaicin attenuates palmitate-induced expression of macrophage inflammatory protein 1 and interleukin 8 by increasing palmitate oxidation and reducing c-Jun activation in THP-1 (human acute monocytic leukemia cell) cells. *Nutr. Res.* **31**, 468–478 (2011).

3. Håversen, L., Danielsson, K. N., Fogelstrand, L. & Wiklund, O. Induction of proinflammatory cytokines by long-chain saturated fatty acids in human macrophages. *Atherosclerosis* **202**, 382–393 (2009).

4. Bouic, P. J., Etsebeth, S., Liebenberg, R.W., Albrecht, C.F. & Van Jaarsveld, P.P. beta-Sitosterol and beta-sitosterol glucoside stimulate human peripheral blood lymphocyte proliferation: implications for their use as an immunomodulatory vitamin combination. *Int. J. Immunopharmacol.* **18**, 693–700 (1996).

5. Bouic, P. J. The role of phytosterols and phytosterolins in immune modulation: a review of the past 10 years. *Curr Opin Clin Nutr Metab Care* **4**, 471–475 (2001).

6. Listenberger, L. L., Ory, D. S. & Schaffer, J. E. Palmitate-Induced Apoptosis Can Occur Through a Ceramide-Independent Pathway. *J. Biol. Chem.* **276**, 14890–14895 (2001).

7. Bouic, P. J. D. Sterols and sterolins: new drugs for the immune system? *Drug Discov. Today* **7**, 775–778 (2002).

8. Bouic, P. J. & Lamprecht, J. H. Plant sterols and sterolins: a review of their immune-modulating properties. *Altern Med Rev* **4**, 170–177 (1999).

9. Iacovidou, M. *Uncovering hidden potential of natural products*. (The Graduate Center of CUNY: New York, 2010).

10. Wu, D., Xing, G.-W., Poles, M. A., Horowitz, A., Kinjo, Y., Sullivan, B., Bodmer-Narkevitch, V., Plettenburg, O., Kronenberg, M., Tsuji, M., Ho, D. D. & Wong, C.-H. Bacterial glycolipids and analogs as antigens for CD1d-restricted NKT cells. *Proc. Natl. Acad. Sci. U.S.A.* **102**, 1351–1356 (2005).

11. Schmieg, J., Yang, G., Franck, R. W. & Tsuji, M. Superior protection against malaria and melanoma metastases by a C-glycoside analogue of the natural killer T cell ligand α-galactosylceramide. *J. Exp. Med.* **198**, 1631–1641 (2003).

12. Fujio, M., Wu, D., Garcia-Navarro, R., Ho, D. D., Tsuji, M. & Wong, C.-H. Structure-based discovery of glycolipids for CD1d-mediated NKT cell activation: tuning the adjuvant versus immunosuppression activity. *J. Am. Chem. Soc.* **128**, 9022–9023 (2006).

13. Yu, K. O. A., Im, J. S., Molano, A., Dutronc, Y., Illarionov, P. A., Forestier, C., Fujiwara, N., Arias, I., Miyake, S. & Yamamura, T. Modulation of CD1d-restricted NKT cell responses by using N-acyl variants of alpha-galactosylceramides. *Proc. Natl. Acad. Sci. U.S.A.* **102**, 3383–3388 (2005).

14. Azas, N., Laurencin, N., Delmas, F., Di, G. C., Gasquet, M., Laget, M. & Timon-David, P. Synergistic in vitro antimalarial activity of plant extracts used as traditional herbal remedies in Mali. *Parasitol. Res.* **88**, 165–171 (2002).

15. Hemaiswarya, S., Kruthiventi, A. K. & Doble, M. Synergism between natural products and antibiotics against infectious diseases. *Phytomedicine* **15**, 639–652 (2008).

16. Marchetti, O., Moreillon, P., Glauser, M. P., Bille, J. & Sanglard, D. Potent Synergism of the Combination of Fluconazole and Cyclosporine in Candida Albicans. *Antimicrob. Agents Chemother.* **44**, 2373–2381 (2000).

17. Williamson, E. M. Synergy and other interactions in phytomedicines. *Phytomedicine* **8**, 401–409 (2001).

18. Rasoanaivo, P., Wright, C. W., Willcox, M. L. & Gilbert, B. Whole plant extracts versus single compounds for the treatment of malaria: synergy and positive interactions. *Malaria J.* **10**, S4 (2011).

19. Shibuya, H., Kawashima, K., Sakagami, M., Kawanishi, H., Shimomura, M., Ohashi, K. & Kitagawa, I. Sphingolipids and glycerolipids. I. Chemical structures and ionophoretic activities of soya-cerebrosides I and II from soybean. *Chem. Pharm. Bull.* **38**, 2933–2938 (1990).

20. Goodman, L. Neighboring-Group Participation in Sugars. *Advances in Carbohydrate Chemistry* **Volume 22**, 109–175 (1967).

21. Ascherio, A. & Willett, W. C. Health effects of trans fatty acids. *Am. J. Clin. Nutr.* **66**, 1006S–1010S (1997).

22. Kinsella, J. E., Bruckner, G., Mai, J. & Shimp, J. Metabolism of trans fatty acids with emphasis on the effects of trans, trans-octadecadienoate on lipid composition, essential fatty acid, and prostaglandins: an overview. *Am. J. Clin. Nutr.* **34**, 2307–2318 (1981).

23. Mensink, R. P., Zock, P. L., Katan, M. B. & Hornstra, G. Effect of dietary cis and trans fatty acids on serum lipoprotein[a] levels in humans. *J. Lipid Res.* **33**, 1493–1501 (1992).

24. Hasson, T. H. *Isolation and Characterization of Immunomodulatory Compounds from Juzen-Taiho-To: Novel Understanding of Phytosteryl Glucosides Nano-Aggregates and Synergism.* (The Graduate Center of CUNY: New York, 2009).

25. Kawamura, A., Guo, J., Itagaki, Y., Bell, C., Wang, Y., Haupert, G. T., Magil, S., Gallagher, R. T., Berova, N. & Nakanishi, K. On the structure of endogenous ouabain. *P. Natl. Acad. Sci. U.S.A.* **96**, 6654–6659 (1999).

26. Li, C.-H., liao, P.-L., Shyu, M.-K., Liu, C.-W., Kao, C.-C., Huang, S.-H., Cheng, Y.-W. & Kang, J.-J. Zinc oxide nanoparticles–induced intercellular adhesion molecule 1 expression requires Rac1/Cdc42, mixed lineage kinase 3, and c-Jun N-terminal kinase activation in endothelial cells. *Toxicol. Sci.* **126**, 162–172 (2012).

27. Tsou, T.-C., Chao, H.-R., Yeh, S.-C., Tsai, F.-Y. & Lin, H.-J. Zinc induces chemokine and inflammatory cytokine release from human promonocytes. *J. Hazard. Mater.* **196**, 335–341 (2011).

28. Bertram, H. C., Eldibany, M., Padgett, J. & Dragon, L. H. Splenic lymphoma arising in a patient with Gaucher disease. A case report and review of the literature. *Arch. Pathol. Lab. Med.* **127**, e242–245 (2003).

29. Gery, I., Zigler, J. S., Brady, R. O. & Barranger, J. A. Selective Effects of Glucocerebroside (Gaucher's Storage Material) on Macrophage Cultures. *J. Clin. Invest.* **68**, 1182–1189 (1981).

30. Ilan, Y., Elstein, D. & Zimran, A. Glucocerebroside: an evolutionary advantage for patients with Gaucher disease and a new immunomodulatory agent. *Immunol. Cell Biol.* **87**, 514–524 (2009).

31. Barak, V., Acker, M., Nisman, B., Kalickman, I., Abrahamov, A., Zimran, A. & Yatziv, S. Cytokines in Gaucher's disease. *Eur. Cytokine Netw.* **10**, 205–210 (1999).

32. Hollak, C. E. M., Evers, L., Aerts, J. M. F. G. & van Oers, M. H. J. Elevated Levels of M-CSF, sCD14 and IL8 in Type 1 Gaucher Disease. *Blood Cells Mol. Dis.* **23**, 201–212 (1997).

33. Allen, M. J., Myer, B. J., Khokher, A. M., Rushton, N. & Cox, T. M. Pro-inflammatory cytokines and the pathogenesis of Gaucher's disease: increased release of interleukin-6 and interleukin-10. *QJM* **90**, 19–25 (1997).

34. Pandey, M. K., Rani, R., Zhang, W., Setchell, K. & Grabowski, G. A. Immunological cell type characterization and Th1–Th17 cytokine production in a mouse model of Gaucher disease. *Molecular Genetics and Metabolism* **106**, 310–322 (2012).

35. Hein, L. K., Meikle, P. J., Hopwood, J. J. & Fuller, M. Secondary sphingolipid accumulation in a macrophage model of Gaucher disease. *Mol. Genet. Metab.* **92**, 336–345 (2007).

36. Whitmore, M. M., Deveer, M. J., Edling, A., Oates, R. K., Simons, B., Lindner, D. & Williams, B. R. G. Synergistic activation of innate immunity by double-stranded RNA and CpG DNA promotes enhanced antitumor activity. *Cancer Res.* **64**, 5850–5860 (2004).

37. Wiesner, P., Choi, S.-H., Almazan, F., Benner, C., Huang, W., Diehl, C. J., Gonen, A., Butler, S., Witztum, J. L., Glass, C. K. & Miller, Y. I. Low doses of lipopolysaccharide and minimally oxidized low-density lipoprotein cooperatively activate macrophages via nuclear factor κb and activator protein-1 possible mechanism for acceleration of atherosclerosis by subclinical endotoxemia. *Circ. Res.* **107**, 56–65 (2010).

38. Traub, S., Kubasch, N., Morath, S., Kresse, M., Hartung, T., Schmidt, R. R. & Hermann, C. Structural requirements of synthetic muropeptides to synergize with lipopolysaccharide in cytokine induction. *J. Biol. Chem.* **279**, 8694–8700 (2004).

39. Into, T., Fujita, M., Okusawa, T., Hasebe, A., Morita, M. & Shibata, K. Synergic effects of mycoplasmal lipopeptides and extracellular ATP on activation of macrophages. *Infect. Immun.* **70**, 3586–3591 (2002).

40. Watson, D. S., Endsley, A. N. & Huang, L. Design considerations for liposomal vaccines: Influence of formulation parameters on antibody and cell-mediated immune responses to liposome associated antigens. *Vaccine* **30**, 2256–2272 (2012).

41. Reed, S. G., Bertholet, S., Coler, R. N. & Friede, M. New horizons in adjuvants for vaccine development. *Trends Immunol.* **30**, 23–32 (2009).

Chapter IV: Mechanistic study of the GlcCer/Cer mixture

Chapter IV

IV.1: Introduction

Synergy is defined as the interaction of multiple substances to produce an effect that exceeds the sum of individual effects. Chapter 3 described a synergistic interaction between GlcCer and Cer, which disappeared over a period of three hours. In order to understand the synergism and its disappearance, it was necessary to conduct further mechanistic studies. Mechanistic understanding of synergism is important because it could provide a new basis of novel combination therapies, which aim at maximizing therapeutic effects while minimizing adverse side-effects and resistance.[1]

The mechanism of synergism can be classified into two different types, namely pharmacodynamic synergy and pharmacokinetic synergy. In pharmacodynamic synergy, multiple ingredients are formulated to target different receptors that are involved in the disease, thereby enhancing the overall therapeutic effect.[1,2] Examples are methotrexate (MTX) and anti-TNF therapeutics (such as infliximab and adalimumab). MTX is a potent dihydrofolate reductase (DHFR) inhibitor, used in the treatment of rheumatoid arthritis.[3–5] Its mechanism of action is believed to be the suppression of cutaneous lymphocyte-associated antigen (CAL) and ICAM-1 expression. The anti-TNF therapeutics, on the other hand, neutralizes TNF, a well-known cytokine involved in inflammation. A combination of these two drugs synergistically attenuates the progression of arthritis, which is an inflammatory disease (Figure IV.1 left).[5] Another example of pharmacodynamic synergism is the combination of a narcotic, such as codeine, and an analgesic, such as acetaminophen. Codeine attenuates the pain-related signals in the

central nervous system. Acetaminophen works as an inhibitor of cyclooxygenase 1 and 2, which are involved in prostaglandin biosynthesis[6]. Although codeine and acetaminophen work through different mechanisms, the combination of the two drugs results in a better analgesic effect (Figure IV, right).[7]

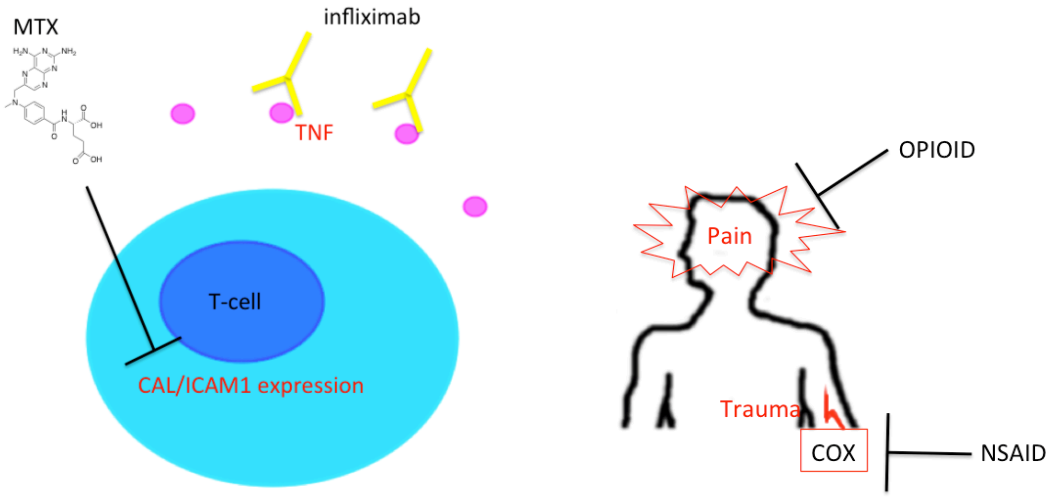

Figure IV.1: Examples of pharmacodynamic synergy. Two drugs with different targets but similar therapeutic effects can be combined to attain pharmacodynamic synergism. Left: MTX and infliximab suppressing the inflammatory response of immune cells. Right: Opioid and non-steroidal anti-inflammatory drug in the pain treatment.

In pharmacokinetic synergy, the bioavailability or delivery of the main active ingredient is aided by the presence of another compound that does not exhibit therapeutic activity. The inactive ingredients, for example, inhibit secretion or metabolism of the main active ingredients.[2] One of the examples is the combination of curcumin and piperin. Curcumin is a polyphenolic compound from turmeric, and has anti-malaria activity.[8,9] Due to the high glucuronidation in the small intestine, curcumin has poor oral bioavailability by itself, but piperine from black pepper inhibits UDP-glucuronyl

transferase. Therefore, when piperine is administered together with curcumin, it enhances the bioavailability of curcumin by 2000% (Figure IV.2).[10–12] Similarly, piperine improves the bioavailability of epigallocatechine gallate (EGCG), which binds to P-glycoprotein (P-gp), an efflux pump of anticancer agents, and reverses multidrug resistance of cancer.[13]

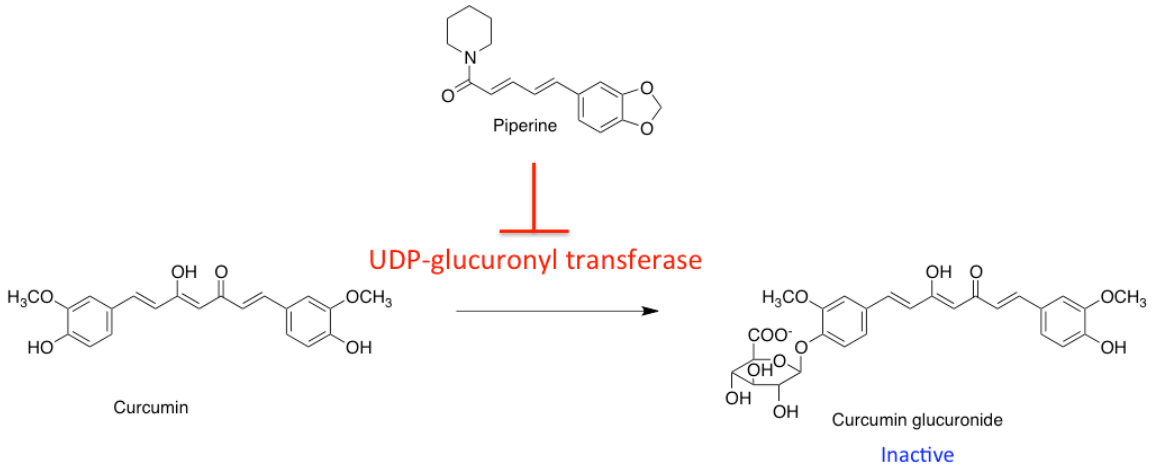

Figure IV.2: Pharmacokinetic synergy of curcumin and piperine. Inhibition of UDP-glucuronyl transferase, which converts curcumin to its inactive form, curcumin glucornide by piperine increases bioavailability of curcumin.

Although the mechanism of the observed synergism between GlcCer and Cer could be either pharmacodynamic or pharmacokinetic, one of our earlier studies provided some interesting clues to formulate a hypothesis.[14] In this study, it was observed that the fraction E (Fr. E), an active fraction from JTT (Figure II.4 in Chapter 2), formed nanoparticles in DMSO (the vehicle solvent for cell treatment), and the activity of this fraction depended on the size of those particles. The size of these particles was affected by the solvent system that was used prior to dissolving in DMSO. For example, when Fr.

E was suspended in 90% MeOH in water, dried, and dissolved in DMSO, large particles in the order of 100 nm predominated as evidenced by atomic force microscopy (AFM) and dynamic light scattering (DLS) (Figure IV.3, a and b). On the other hand, smaller aggregates (~10 nm) were observed when the fraction was suspended in 100% MeOH, dried, and dissolved in DMSO. Importantly, the size of these aggregates was directly correlated with the activity (Figure IV.4). The smaller aggregates (~10 nm) showed potent immunostimulatory activity, whereas the larger aggregates (~100 nm) had little or no activity.

Based on this earlier study, we hypothesized that the synergism between GlcCer and Cer might also be due to nanoparticle formation. In fact, if we consider the amphiphilic nature of GlcCer and Cer, it would not be surprising to observe the mixture forming nanoaggregates once the mixture is introduced into an aqueous environment. Thus, in this hypothesis, when the mixture of these two compounds is dissolved in DMSO and immediately suspended into the aqueous medium, biologically active nanoparticles are formed. This nanoparticle hypothesis could also explain the disappearance of the synergism after three hours of the sample storage in DMSO. Although DMSO is a hygroscopic solvent, in which long-term storage could lead to degradation of solutes, the three-hour storage in DMSO seemed too short for decomposition. In fact, in a study to examine the stability of compounds in DMSO, it was found that short-term storage (~3 months) would cause no more than 8% of degradation at room temperature.[15] Instead, it was more likely that the disappearance of activity was caused by changes in molecular aggregation.

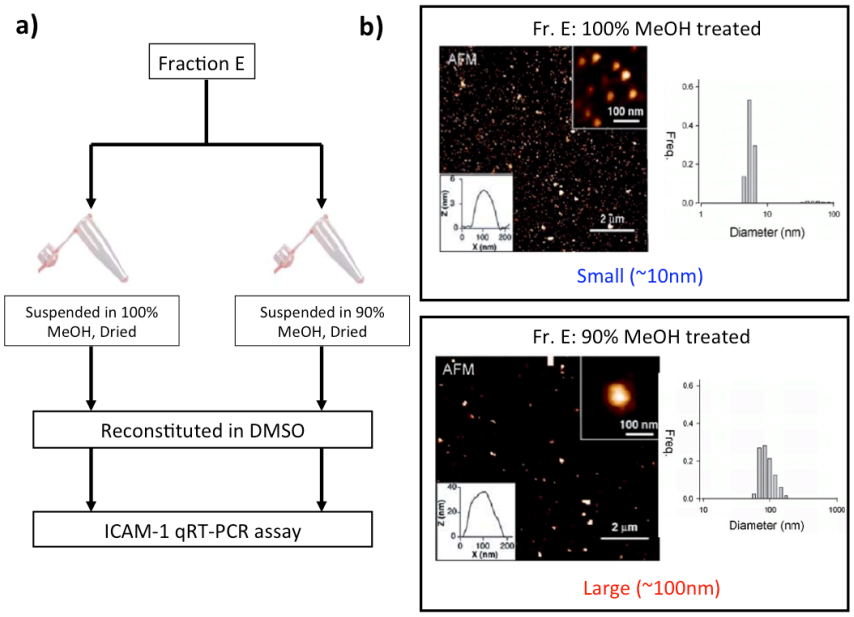

Figure IV.3: a) Sample preparation scheme. b) AFM and DLS analyses of Fr. E prepared in different solvent conditions. a) Active Fr. E was aliquoted into two. One was suspended in 100% MeOH, dried then reconstituted in DMSO (Fr. E 100% MeOH treated). The other one was suspended in 90% MeOH, dried then reconstituted in DMSO (Fr. E 90% MeOH treated). b) AFM: 2 µL of each sample prepared in a) was spotted on clean mica and was allowed to sit overnight. Image illustrates two different scales 2 µm wide view, and particle analysis at 200 nm. X axis particle length in nm. Z-axis particle height in nm. DLS: 2 µL of 90% and 100% purified BSSG in DMSO (2.33 µg/mL) was diluted in 78 µL of pure DMSO. DMSO control sample contained 80 µL of DMSO. The entire sample was loaded to a DLS cuvette and analyzed at room temperature. The entire analysis was done over a period of 1 hr. The data shown were obtained from three independent experiments. As shown above, 90% sample contained particle size of about 90 nm while the 100% sample contained particles of less than 10 nm. The X-axis illustrates diameter size and the Y-axis illustrates the frequency.

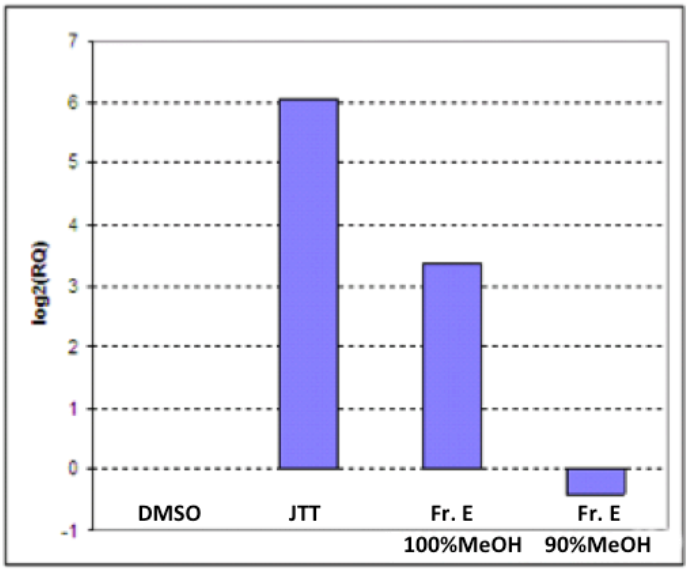

Figure IV. 4: ICAM-1 real-time PCR assay of Fr. E. THP-1 cells were treated with DMSO, negative control; JTT, positive control (100 μg/mL), Fr. E 100% MeOH treated sample, and Fr. E 90% MeOH treated sample. Incubated for 4 hr.

This chapter describes the characterization of molecular assembly of the GlcCer/Cer mixture. Microscopic and spectroscopic analyses revealed time-dependent changes in the molecular assembly of the mixture, which allowed us to develop a new model to understand the synergism between GlcCer and Cer and its disappearance.

IV.2: Results

IV.2.1: Determination of molecular assembly of the GlcCer/C16:0-Cer mixture by TEM

In order to visualize the possible molecular assembly of GlcCer/Cer mixture, the mixture was subjected to the analysis by transmission electron microscopy (TEM).

Negative staining (1% sodium phosphotungstate solution in water (w/v)) was used in this study because organic compounds like GlcCer and Cer are difficult to visualize under TEM due to their low electron density.

This TEM study examined two time points, namely, t = 0 hr and t = 3 hr. The t = 0 hr sample refers to the GlcCer/Cer mixture that was dissolved in DMSO and immediately suspended in water for TEM measurement. This t = 0 sample represents the sample that exhibited synergistic stimulation of MΦ. On the other hand, the t = 3 hr sample refers to the GlcCer/Cer mixture that was dissolved in DMSO, stored at room temperature for 3 hr, and then suspended in water for TEM measurement. Once the sample was placed on a copper grid, the sample was stained by 1% phosphotungstate solution, and then the grid was air-dried completely.

Figure IV.5 shows the TEM images at these two time points and energy dispersive X-ray spectroscopy, which was used for the elemental analysis. TEM at t = 0 revealed light grey particles as well as the dark background that appear to be electron-dense phosphotungstate. Energy dispersive X-ray spectroscopy by EDAX confirmed that the dark background was indeed the element tungsten (W), indicating that the grey particles were negatively stained aggregates of the GlcCer/Cer mixture. The population of nanoparticles seemed to be poly-dispersed. Particle distribution was measured using ImageJ64. The smaller nanoparticles were about 10 nm in diameter, and the larger particles were around 400 nm in diameter.

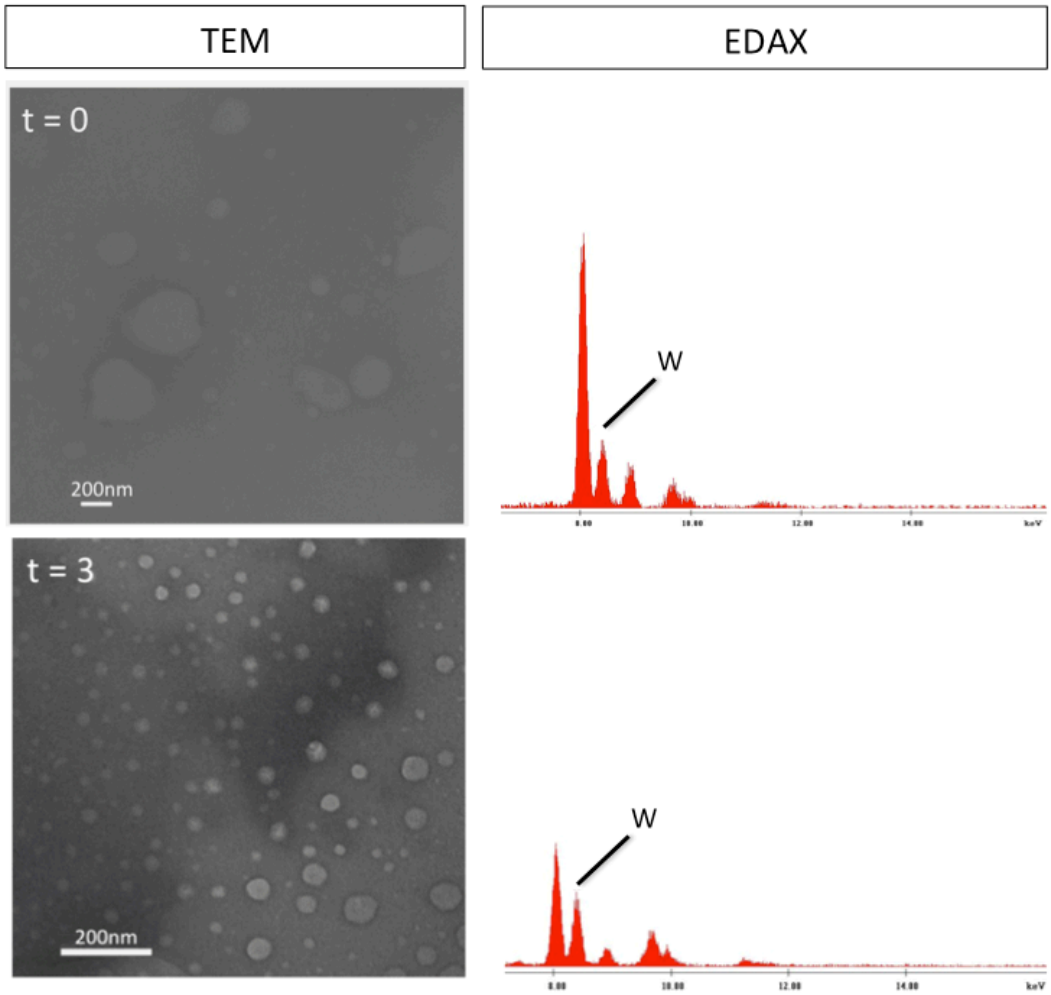

Figure IV.5: TEM images of GluCer/Cer mixture at t = 0 and 3 hr (left) and EDAX Netcounts spectra (right). GlcCer/Cer was re-constituted in DMSO (1 µg/µL) then diluted in Millipore water (final concentration, 0.05 µg/µL). Two 8 µL of GlcCer/Cer mixture was placed on a grid, then 8 µL of 1% sodium phosphotungstate solution was added. The grid was air dried before the measurement.

At t = 3 hr a change in the particle size was evident. Particles around 400 nm in diameter were no longer apparent, and a population of smaller particles (diameter less than 100 nm) had increased. The largest particle observed in t = 3 sample was approximately 70 nm (Figure IV.5).

It is important to note that the size measured by TEM might be smaller than the actual size due to the drying process, which could cause the particles to shrink.

IV.2.2: Determination of molecular assembly of the GlcCer/Cer mixture by DLS

In addition to TEM, the molecular assembly of the GlcCer/Cer mixture was determined by dynamic light scattering (DLS). DLS measures light scattered by small particles in solution. More specifically, DLS measures a time-dependent fluctuation of the scattered light, from which the particle distribution in the solution can be estimated.[16] Since the measurement is carried out in solution, there is no need to worry about the particle shrinkage.

DLS was first used to characterize DMSO solutions of the GlcCer/Cer mixture. Here two different measurements were carried out. In one measurement, DLS was measured immediately after dissolving the sample in DMSO (t = 0). In another experiment, DLS was measured 3 hr after dissolving the sample in DMSO (t = 3). Figure IV.6 shows the DLS profiles of the GlcCer/Cer mixture at t = 0 and t = 3. DLS revealed that, at t = 0, the GlcCer/Cer mixture predominantly formed aggregates around 200-600 nm in diameter. About 10% of the population showed the size of 20-50 nm in diameter (Figure IV.6, middle). At t = 3, however, nearly 50% of the nanoparticle population was smaller than 50 nm in diameter. Only 40% of the population was larger than 200 nm in diameter (Figure IV.6, bottom).

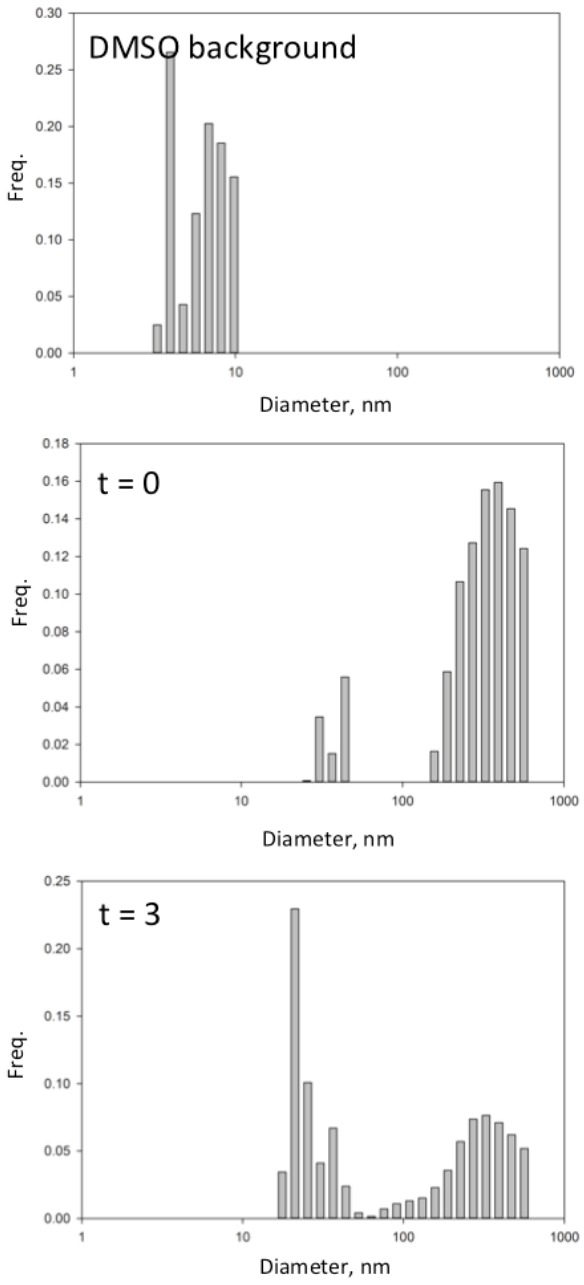

Figure IV.6: DLS analysis of GlcCer/Cer mixture in DMSO (1 µg/µL) at t = 0 and 3 hr. DMSO control sample contained 80 µL of DMSO. GlcCer/Cer mixture was dissolved in DMSO (1 µg/µL). DMSO-dissolved sample (40 µL) was loaded onto a DLS cuvette and analyzed at room temperature. The X-axis illustrates diameter size. The Y-axis illustrates the frequency.

After the measurements in DMSO, DLS was carried out with the sample diluted in water as well. As before, this DLS study examined two time points, namely t = 0 and t = 3. The t = 0 sample refers to the GlcCer/Cer mixture that was dissolved in DMSO and immediately suspended in water for DLS measurement. The t = 3 sample refers to the GlcCer/Cer mixture that was dissolved in DMSO, stored at room temperature for 3 hr, and then suspended in water for DLS measurement. At t = 0, DLS showed that molecular assembly of the GlcCer/Cer mixture is poly-dispersed. Approximately 22% of the population was larger than 1000 nm in diameter, 60% of aggregates was within 100-500 nm in diameter (Figure IV.7, middle). At t = 3 hr, the population of smaller aggregates (around 100-500 nm) increased whereas the population of the larger aggregates (around 1,000 nm) decreased. Only 4% of aggregates were larger than 1,000 nm in diameter. The majority of the population was within the range of 130-300 nm in diameter (Figure IV 7, bottom).

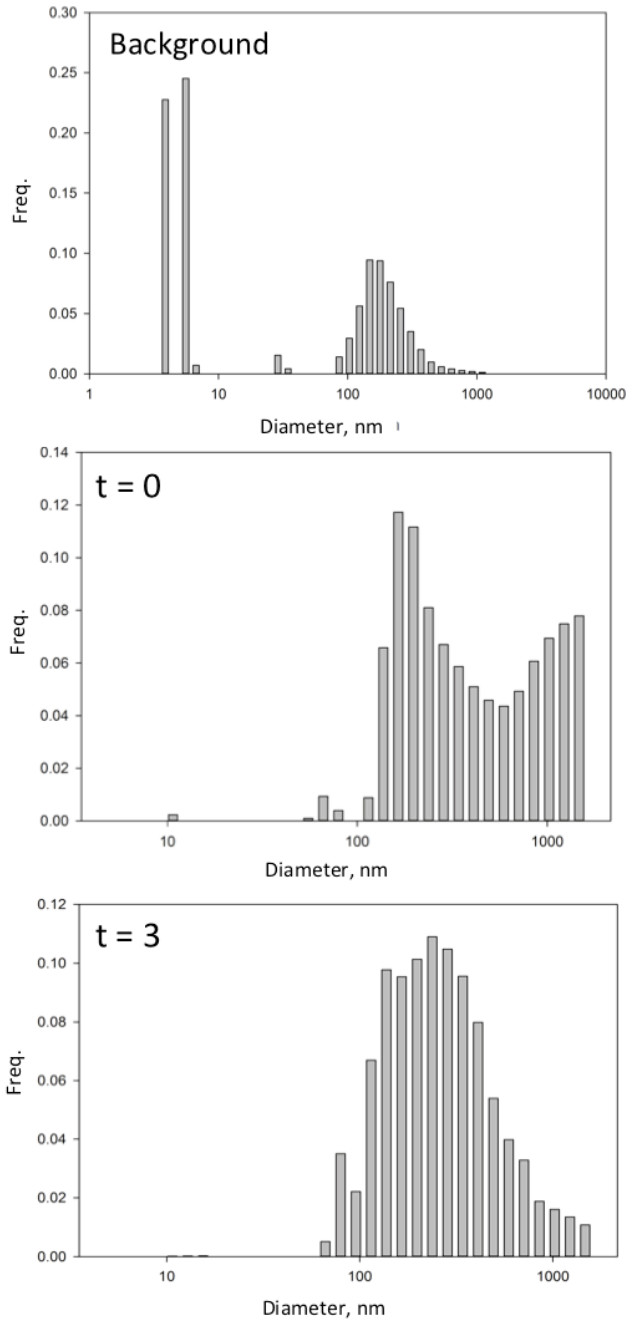

Figure IV.7: DLS analysis of GlcCer/Cer mixture in water (0.05 µg/µL) at t = 0 and 3 hr. Control sample contained 2.5 µL of DMSO and 47.5 µL of Millipore water. GlcCer/Cer mixture was dissolved in DMSO (1 µg/µL), then suspended in Millipore water to the final concentration of GlcCer/Cer mixture = 0.05 µg/µL. The sample (40 µL) was loaded onto a DLS cuvette and analyzed at room temperature. The X-axis illustrates diameter size. The Y-axis illustrates the frequency.

IV.3: Discussions

In our study on the molecular assembly of the GlcCer/Cer mixture, we observed that the mixture formed nanoparticles in an aqueous environment. It is likely that the particles are micelles because amphiphilic compounds, such as GlcCer and Cer, spontaneously organize themselves into micelles in aqueous media, in which their hydrophilic regions are oriented outside, and the hydrophobic tails are packed in the core. Alternatively, some particles could also be liposomes, which are spherical vesicles composed of a lipid bilayer.[17]

It was also observed that the distribution of the particle size changed dramatically over 3 hr. Importantly, the particle size seemed to correlate with the MΦ-stimulatory activity. The t = 0 sample, which exhibited the synergistic MΦ-stimulatory activity, contained a substantial population of large particles (~1,000 nm in solution, ~400 nm when it is dried). On the other hand, the t=3 hr sample, which did not exhibit the synergism, consisted mainly of a population of smaller particles (100-500 nm in solution, < 100 nm when it is dried). Taken together, these results indicated that the activity of the GlcCer/Cer mixture might be attributed to the larger particles.

The size of particles (micelles and liposomes) has substantial effects on biological activity.[18] Many studies have noted such correlations,[19–21] in which particle size was varied by changing lipid composition and other factors, such as surface charges, and biological activities were examined. Yet there is no clear trend between particle size and biological activity.[21] In some studies larger particles show higher activity,[22] as was the case for the GlcCer/Cer mixture in this study. On the other hand, in other studies,

including our previous study on Fr. E,[14] smaller particles exhibited more potent activity.[23,24]

The observed correlation is an important finding because it gives us a new clue to understand the synergism and its disappearance in terms of molecular assembly. Figure IV.8 illustrates the changes in molecular assembly as indicated by the TEM and DLS experiments. The GlcCer/Cer mixture, when first dissolved in DMSO, already forms aggregates in the size of 300-700 nm (Figure IV.6). When these initial aggregates in DMSO are suspended in water, some of them further assemble to form larger aggregates (~1,000 nm) (Figure IV.7), which correlated with the synergism. On the other hand, the initial aggregates in DMSO are not very stable and dissociate into smaller particles (40-80 nm) in 3 hr. These smaller particles do not form the larger aggregates when the DMSO solution is suspended in water.

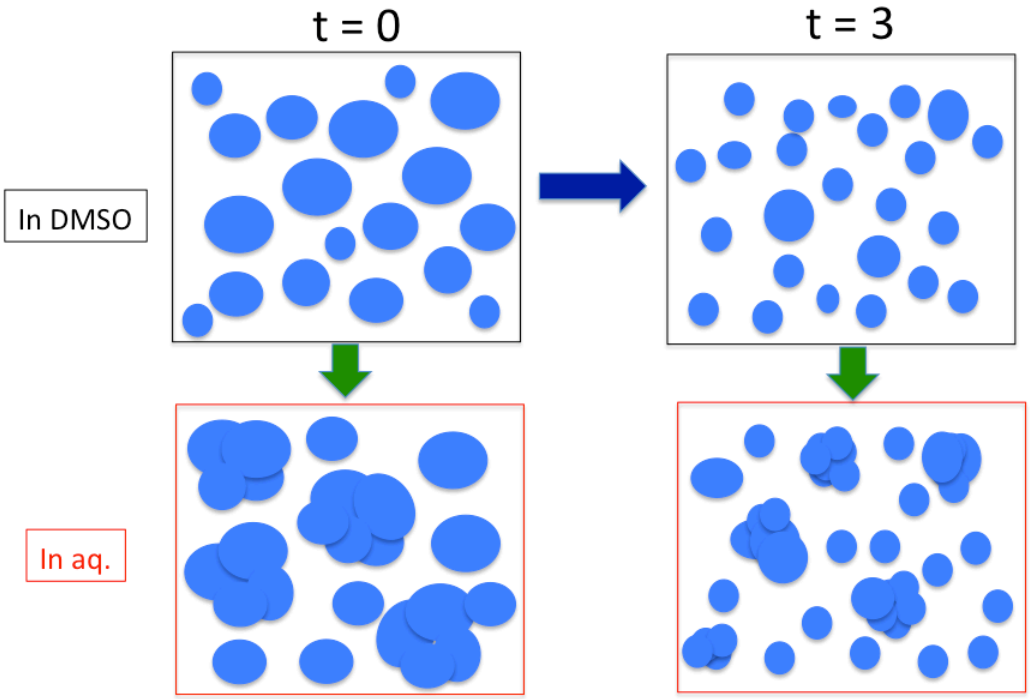

Figure IV.8: Illustration of change in aggregation size in DMSO and in an aqueous environment. Top, left: DMSO reconstituted GlcCer/Cer mixture at t = 0. Top, right: DMSO re-constituted GlcCer/Cer mixture at t = 3. Bottom, left: DMSO reconstituted GlcCer/Cer mixture (t = 0) suspended in water. Bottom, right: DMSO reconstituted GlcCer/Cer mixture (t = 3) suspended in water.

While the larger aggregates correlate with the immunostimulatory activity, the biological mechanism is still unclear. One possible explanation is the involvement of nanoparticle internalization by cells. MΦ and other mammalian cells are capable of internalizing macromolecules and nanoparticles via endocytosis, which is classified into two categories, namely pinocytosis and phagocytosis.[25] Pinocytosis ("cell drinking") is an uptake of fluid and solutes from extracellular environment, and is conducted by all cell types. Phagocytosis ("cell eating") is considered to be the uptake of materials that are larger than 500 nm and is only conducted by specialized cells, such as MΦ, monocytes,

and neutrophils, whose functions are the clearance of pathogens, viruses, apoptotic cells, and cancer cells.[26] Pinocytosis and phagocytosis are essential to control physiological processes, and they are highly regulated by the receptor recognition and sophisticated signaling pathways.[25] The mannose receptor, complement receptor, Fcγ receptor, and scavenger receptor are such examples.

Recognition of nanoparticles on these receptors depends on the size of the particles, and signaling cascades initiated by the ligation of each receptor could be different. For example, phagocytosis via the mannose receptor, complement receptor, and Fcγ receptor has been reported to result in induction of pro-inflammatory response.[21] Gluco-mannan particles that are ~200 nm in diameter is one example of nanoparticles that are internalized via the mannose receptor.[27] Lipid nanocapsules with 20, 50, and 100 nm in diameter are phagocytosed via the complement receptor-mediated pathway.[28] On the other hand, superparamagnetic iron oxide nanoparticles (~10-20 nm) and colloidal gold nanoparticles (~35 nm) are internalized via scavenger receptors.[21,29,30] The recognition of nanoparticles on scavenger receptor does not result in the activation of the pro-inflammatory response. In our study, the GlcCer/Cer mixture induced ICAM-1 expression. This suggests a receptor-mediated phagocytosis of the GlcCer/Cer nanoparticles.

Which compound is actually responsible for the activity? As mentioned before, both GlcCer and Cer could be immunostimulatory compounds. There is a possibility that phagocytosis of the larger aggregates by MΦ results in a sudden increase in cellular GlcCer concentration, which in turn triggers the immunostimulatory activity. As seen in Gaucher's disease, accumulation of GlcCer in the cell results in some beneficial effect,

such as protection against infection and cancer.[31] On the other hand, Cer is also a signaling molecule and is known to be involved in induction of inflammatory response.[32] Due to the formation of aggregates with GlcCer, it may have been internalized more efficiently than the Cer alone; therefore, the Cer concentration in the cell is increased.

Use of micelles and liposomes as drug carriers has attracted many researchers, and lipid nanoparticles have been utilized in drug development.[17,30,33,34] A nanoparticle drug delivery system is designed to overcome the issues with solubility, bioavailability, half-life, and shelf life of a drug.[35,36] In the context of herbal medicine, uses of nanoparticles begin to emerge, and the development of more effective formulations has been attempted,[37–40] although most of studies were conducted using crude mixtures/extracts. Without the use of liposomal formulation, however, herbal medicine might already have some "inactive" components that permit the formation of stable and active particles for efficient delivery and stability. Our current finding may be a new clue to unveil previously overlooked roles of various chemical constituents in herbal medicine.

IV. 4: Materials and methods

Transmission electron microscopy: After sample (1:1 mixture of GlcCer and C16:0-Cer) was dissolved in DMSO (1 μg/μL), it was diluted with Millipore water so that the final concentration was 0.05 μg/μL. All data were collected at 200kV on a JEM 2100 (Jeol) at the eucentric height to ensure that all measurements were accurate for comparison. An 8-μL drop of the sample was placed on a 300-mesh silicon monoxide coated copper grid (TED Pella, Redding, California, USA). Two 8-μL drops of a 1% aqueous solution of sodium phosphotungstate (stain) were added and then an 8-μL drop of deionized water was added. The sample was allowed to dry for 1 min under a protective cover. The remaining liquid was removed using filter paper. Average particle sizes were determined by counting at least 50 particles from the TEM images for the nanoparticle samples using "ImageJ" software (NIH). Energy dispersive X-ray spectroscopy was performed by EDAX to confirm the presence of the element W in the dark background surrounding the micelle-like structures. This confirmed that the sodium phosphotungstate solution negatively stained the sample.

Dynamic light scattering: A solution of the sample in DMSO (1 μg/μL) was diluted with Millipore water so that the final concentration was 0.05 μg/μL. Into each cuvette, a total of 40 μL of that sample (0.05 μg/μL) was added. In each experiment, the total acquisition time was 15 ms, for a total of 10 scans, which was repeated 5 times. The data were processed with SigmaPlot.™ Experiments were carried at room temperature. However if there is interference, there will be a deviation in refraction from the average value, which will cause light to be observed in different direction. Brownian motion

causes temporal fluctuations in the intensity of the light scattered. Since small molecules move faster in solution compared to larger ones, more particles will diffuse from high to low concentration in a given unit of time. With the use of intensity correlation function it is possible to evaluate the diffusion coefficient of the scattering particles. The relation between in spherical particles between the radius and the diffusion is given by Stokes-Einstein equation shown below.

$D=T\ K_B/6\pi\eta R$

K_B= Boltzmann constant

T=absolute temperature

η=viscosity of the solution

IV.5: References

1. Ginsburg, H. & Deharo, E. A call for using natural compounds in the development of new antimalarial treatments - an introduction. *Malar. J.* **10 Suppl 1**, S1 (2011).

2. Rasoanaivo, P., Wright, C. W., Willcox, M. L. & Gilbert, B. Whole plant extracts versus single compounds for the treatment of malaria: synergy and positive interactions. *Malar. J.* **10**, S4 (2011).

3. Ascierto, P. A. & Marincola, F. M. Combination therapy: the next opportunity and challenge of medicine. *J. Transl. Med.* **9**, 115 (2011).

4. Soliman, M. M., Ashcroft, D. M., Watson, K. D., Lunt, M., Symmons, D. P. M. & Hyrich, K. L. Impact of concomitant use of DMARDs on the persistence with anti-TNF therapies in patients with rheumatoid arthritis: results from the British Society for Rheumatology Biologics Register. *Ann. Rheum. Dis.* **70**, 583–589 (2011).

5. Johnston, A., Gudjonsson, J. E., Sigmundsdottir, H., Runar Ludviksson, B. & Valdimarsson, H. The anti-inflammatory action of methotrexate is not mediated by lymphocyte apoptosis, but by the suppression of activation and adhesion molecules. *Clin. Immunol.* **114**, 154–163 (2005).

6. Dionne, R. A., Campbell, R. A., Cooper, S. A., Hall, D. L. & Buckingham, B. Suppression of postoperative pain by preoperative administration of ibuprofen in comparison to placebo, acetaminophen, and acetaminophen plus codeine. *J. Clin. Pharmacol.* **23**, 37–43 (1983).

7. Raffa, R. B. Pharmacology of oral combination analgesics: rational therapy for pain. *J. Clin. Pharm. Ther.* **26**, 257–264 (2001).

8. Reddy, R. C., Vatsala, P. G., Keshamouni, V. G., Padmanaban, G. & Rangarajan, P. N. Curcumin for malaria therapy. *Biochem. Biophys. Res. Commun.* **326**, 472–474 (2005).

9. Cui, L., Miao, J. & Cui, L. Cytotoxic Effect of Curcumin on Malaria Parasite Plasmodium falciparum: Inhibition of Histone Acetylation and Generation of Reactive Oxygen Species. *Antimicrob. Agents Chemother.* **51**, 488–494 (2007).

10. Shoba, G., Joy, D., Joseph, T., Majeed, M., Rajendran, R. & Srinivas, P. S. Influence of piperine on the pharmacokinetics of curcumin in animals and human volunteers. *Planta Med.* **64**, 353–356 (1998).

11. Srinivasan, K. & Suresh, D. Influence of curcumin, capsaicin, and piperine on the rat liver drug-metabolizing enzyme system in vivo and in vitro. *Can. J. Physiol. Pharm.* **84**, 1259–1265 (2006).

12. Anand, P., Kunnumakkara, A. B., Newman, R. A. & Aggarwal, B. B. Bioavailability of Curcumin: Problems and Promises. *Mol. Pharmaceutics* **4**, 807–818 (2007).

13. Lambert, J. D., Hong, J., Kim, D. H., Mishin, V. M. & Yang, C. S. Piperine enhances the bioavailability of the tea polyphenol (-)-epigallocatechin-3-gallate in mice. *J. Nutr.* **134**, 1948–1952 (2004).

14. Hasson, T. H. *Isolation and Characterization of Immunomodulatory Compounds from Juzen-Taiho-To: Novel Understanding of Phytosteryl Glucosides Nano-Aggregates and Synergism.* (The Graduate Center of CUNY: New York, 2009).

15. Kozikowski, B. A., Burt, T. M., Tirey, D. A., Williams, L. E., Kuzmak, B. R., Stanton, D. T., Morand, K. L. & Nelson, S. L. The Effect of Room-Temperature Storage on the Stability of Compounds in DMSO. *J. Biomol. Screen* **8**, 205–209 (2003).

16. Berne, B. J. & Pecora, R. *Dynamic Light Scattering: With Applications to Chemistry, Biology, and Physics*. (Courier Dover Publications: 2000).

17. Letchford, K. & Burt, H. A review of the formation and classification of amphiphilic block copolymer nanoparticulate structures: micelles, nanospheres, nanocapsules and polymersomes. *Eur. J. Pharm. Biopharm.* **65**, 259–269 (2007).

18. Li, S.-D. & Huang, L. Pharmacokinetics and biodistribution of nanoparticles. *Mol. Pharmaceutics* **5**, 496–504 (2008).

19. Champion, J., Walker, A. & Mitragotri, S. Role of particle size in phagocytosis of polymeric microspheres. *Pharm. Res.* **25**, 1815–1821 (2008).

20. Singh, R. & Lillard Jr., J. W. Nanoparticle-based targeted drug delivery. *Exp. Mol. Pathol.* **86**, 215–223 (2009).

21. Dobrovolskaia, M. A. & McNeil, S. E. Immunological properties of engineered nanomaterials. *Nat. Nanotechnol.* **2**, 469–478 (2007).

22. van Zijverden, M. & Granum, B. Adjuvant activity of particulate pollutants in different mouse models. *Toxicology* **152**, 69–77 (2000).

23. Chong, C. S. W., Cao, M., Wong, W. W., Fischer, K. P., Addison, W. P., Kwon, G. S., Tyrrell, D. L. & Samuel, J. Enhancement of T helper type 1 immune responses against hepatitis B virus core antigen by PLGA nanoparticle vaccine delivery. *J. Control Release* **102**, 85–99 (2005).

24. Cui, Z. & Mumper, R. J. Coating of cationized protein on engineered nanoparticles results in enhanced immune responses. *Int. J. Pharm.* **238**, 229–239 (2002).

25. Conner, S. D. & Schmid, S. L. Regulated portals of entry into the cell. *Nature* **422**, 37–44 (2003).

26. Aderem, A. & Underhill, D. M. Mechanisms of phagocytosis in macrophages. *Annu. Rev. Immunol.* **17**, 593–623 (1999).

27. Cuña, M., Alonso-Sandel, M., Remunan-Lopez, C., Pivel, J. P., Alonso-Lebrero, J. L. & Alonso, M. J. Development of phosphorylated glucomannan-coated chitosan nanoparticles as nanocarriers for protein delivery. *J. Nanosci. Nanotechnol.* **6**, 2887–2895 (2006).

28. Vonarbourg, A., Passirani, C., Saulnier, P., Simard, P., Leroux, J. C. & Benoit, J. P. Evaluation of pegylated lipid nanocapsules versus complement system activation and macrophage uptake. *J. Biomed. Mater. Res. A.* **78**, 620–628 (2006).

29. von zur Muhlen, C., von Elverfeldt, D., Bassler, N., Neudorfer, I., Steitz, B., Petri-Fink, A., Hofmann, H., Bode, C. & Peter, K. Superparamagnetic iron oxide binding and uptake as imaged by magnetic resonance is mediated by the integrin receptor Mac-1 (CD11b/CD18): Implications on imaging of atherosclerotic plaques. *Atherosclerosis* **193**, 102–111 (2007).

30. Shukla, R., Bensal, V., Chaudhary, M., Basu, A., Bhonde, R. R. & Sastry, M. Biocompatibility of gold nanoparticles and their endocytotic fate inside the cellular compartment: a microscopic overview. *Langmuir.* **21**, 10644–10654 (2005).

31. Ilan, Y., Elstein, D. & Zimran, A. Glucocerebroside: an evolutionary advantage for patients with Gaucher disease and a new immunomodulatory agent. *Immunol. Cell Biol.* **87**, 514–524 (2009).

32. Demarchi, F., Bertoli, C., Greer, P. A. & Schneider, C. Ceramide triggers an NF-|[kappa]|B-dependent survival pathway through calpain. *Cell Death Differ.* **12**, 512–522 (2005).

33. Cui, Z. & Mumper, R. J. Microparticles and nanoparticles as delivery systems for DNA vaccines. *Crit. Rev. Ther. Drug Carrier Syst.* **20**, 103–137 (2003).

34. Peek, L. J., Middaugh, C. R. & Berkland, C. Nanotechnology in vaccine delivery. *Adv. Drug Deliv. Rev.* **60**, 915–928 (2008).

35. Kataoka, K., Harada, A. & Nagasaki, Y. Block copolymer micelles for drug delivery: design, characterization and biological significance. *Adv. Drug Deliv. Rev.* **47**, 113–131 (2001).

36. Torchilin, V. P. Micellar nanocarriers: pharmaceutical perspectives. *Pharm. Res.* **24**, 1–16 (2007).

37. Chen, M., Wang, S., Tan, M. & Wang, Y. Applications of nanoparticles in herbal medicine: zedoary turmeric oil and its active compound β-elemene. *Am. J. Chin. Med.* **39**, 1093–1102 (2011).

38. Tiyaboonchai, W., Tungpradit, W. & Plianbangchang, P. Formulation and characterization of curcuminoids loaded solid lipid nanoparticles. *Int. J. Pharm.* **337**, 299–306 (2007).

39. Su, Y. L., Fu, Z. Y., Zhang, J. Y., Wang, W. M., Wang, H., Wang, Y. C. & Zhang, Q. J. Microencapsulation of Radix salvia miltiorrhiza nanoparticles by spray-drying. *Powder Technol.* **184**, 114–121 (2008).

40. Yen, F.-L., Wu, T.-H., Lin, L.-T., Cham, T.-M. & Lin, C.-C. Nanoparticles formulation of Cuscuta chinensis prevents acetaminophen-induced hepatotoxicity in rats. *Food Chem. Toxicol.* **46**, 1771–1777 (2008).

Appendices

Appendix A: ESI-MS (positive) mode of an acetylation product from fraction C. Top: the entire ESI-MS spectrum. Bottom: zoomed spectrum

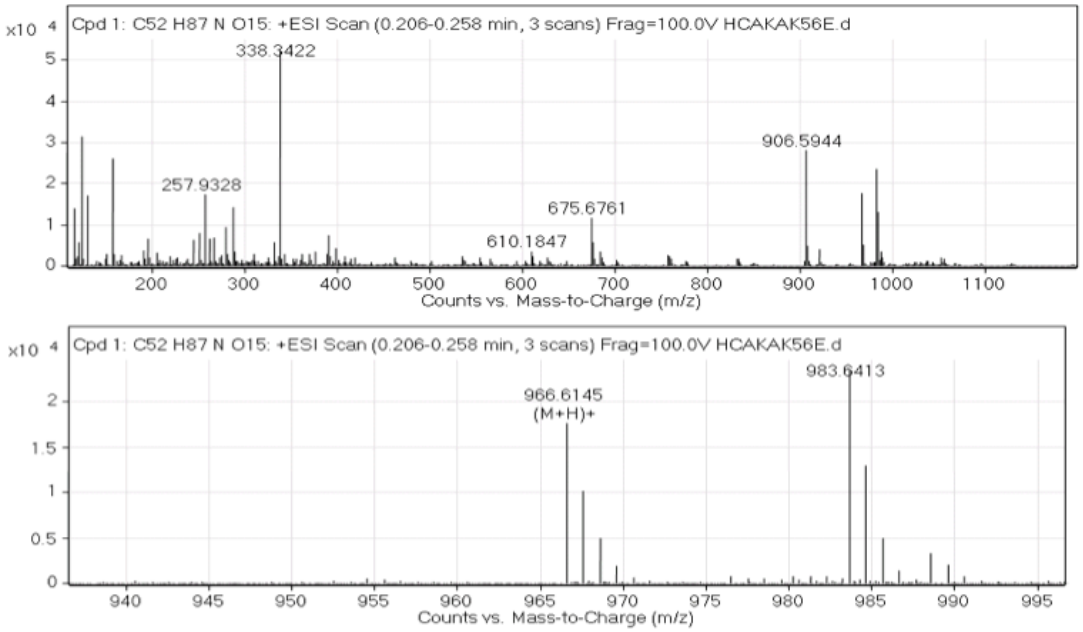

Appendix B: Partial structure COSY analysis of the acetylated product (acetylated fraction C). a) Magnified carbinol/olefin/amide region of COSY spectrum. b) Assembled partial structure of polar region fragment and olefinic fragments.

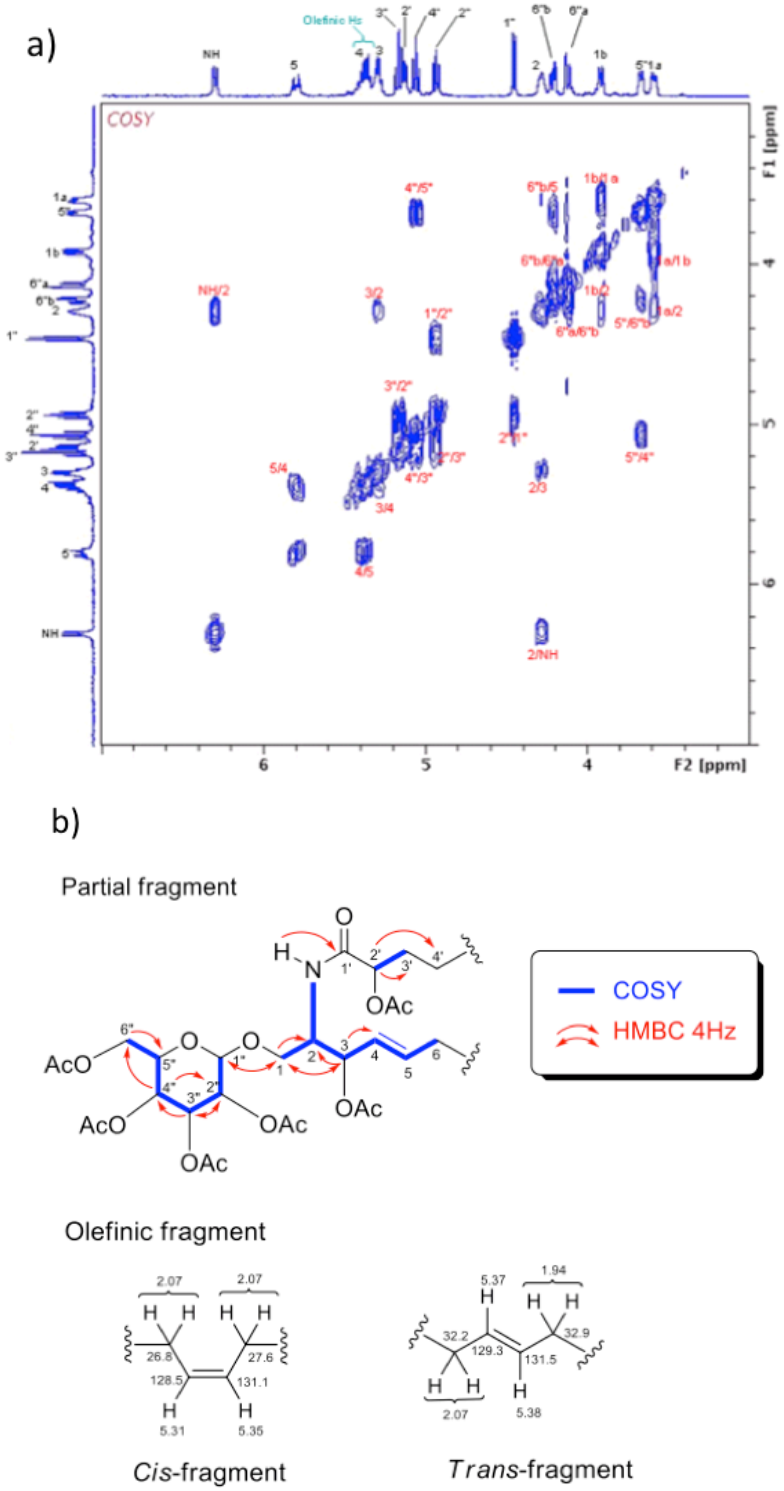

Appendix C: ESI MS/MS (positive mode) fragmentation analysis of acetylated fraction C. a) ESI MS/MS spectrum. b) Possible fragmentation sequence. In the box: fragment structures for ions at m/z = 331.1028.

a)

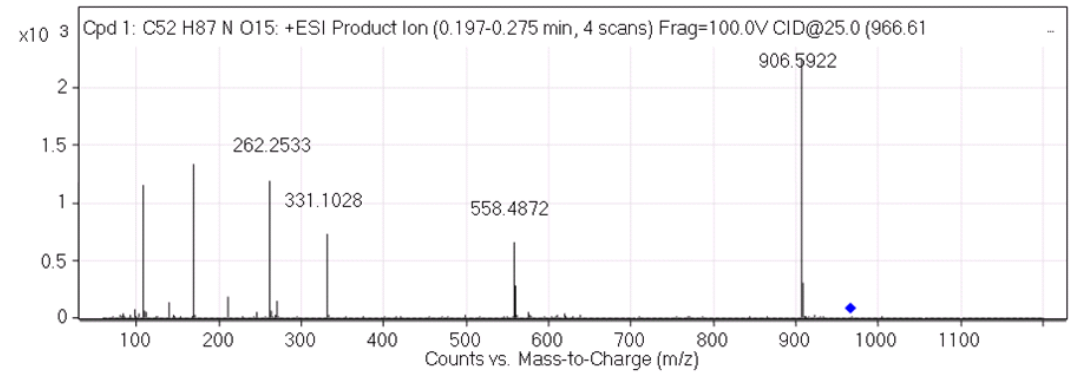

b)

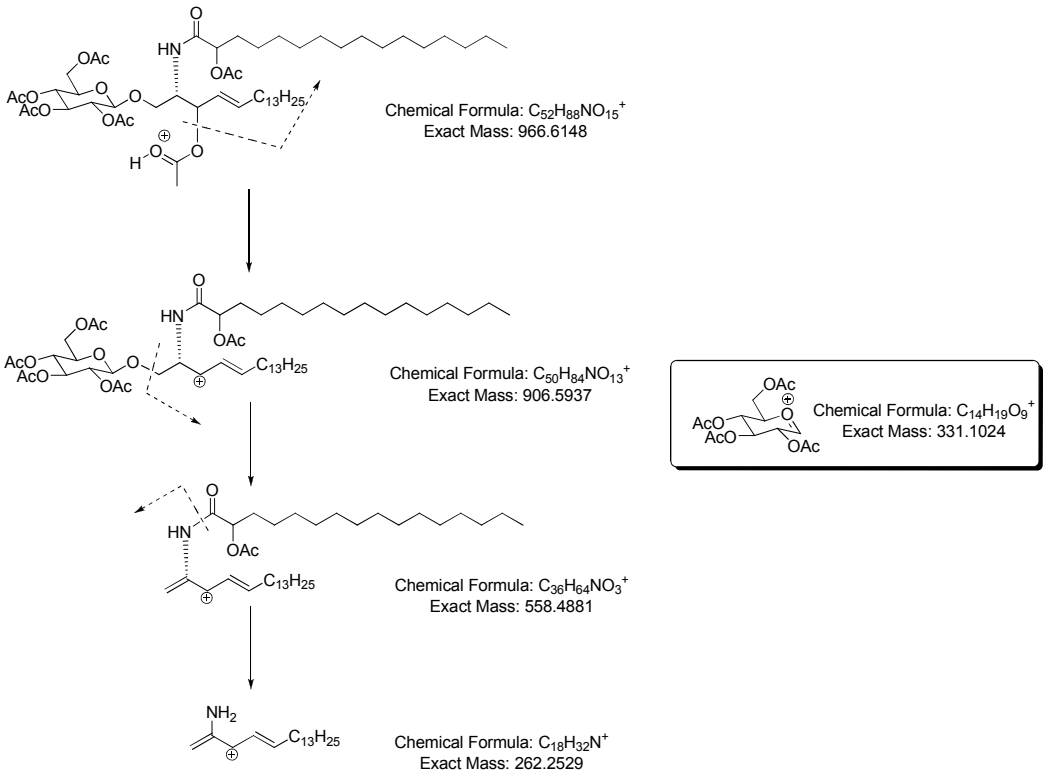

Appendix D: ^{1}H-NMR comparison of acetylated fraction C (Ac.Fr.C) and acetylated commercially available β-glycosylceramides (soya glucocerebroside) – named Ac.Soya GlcCer.

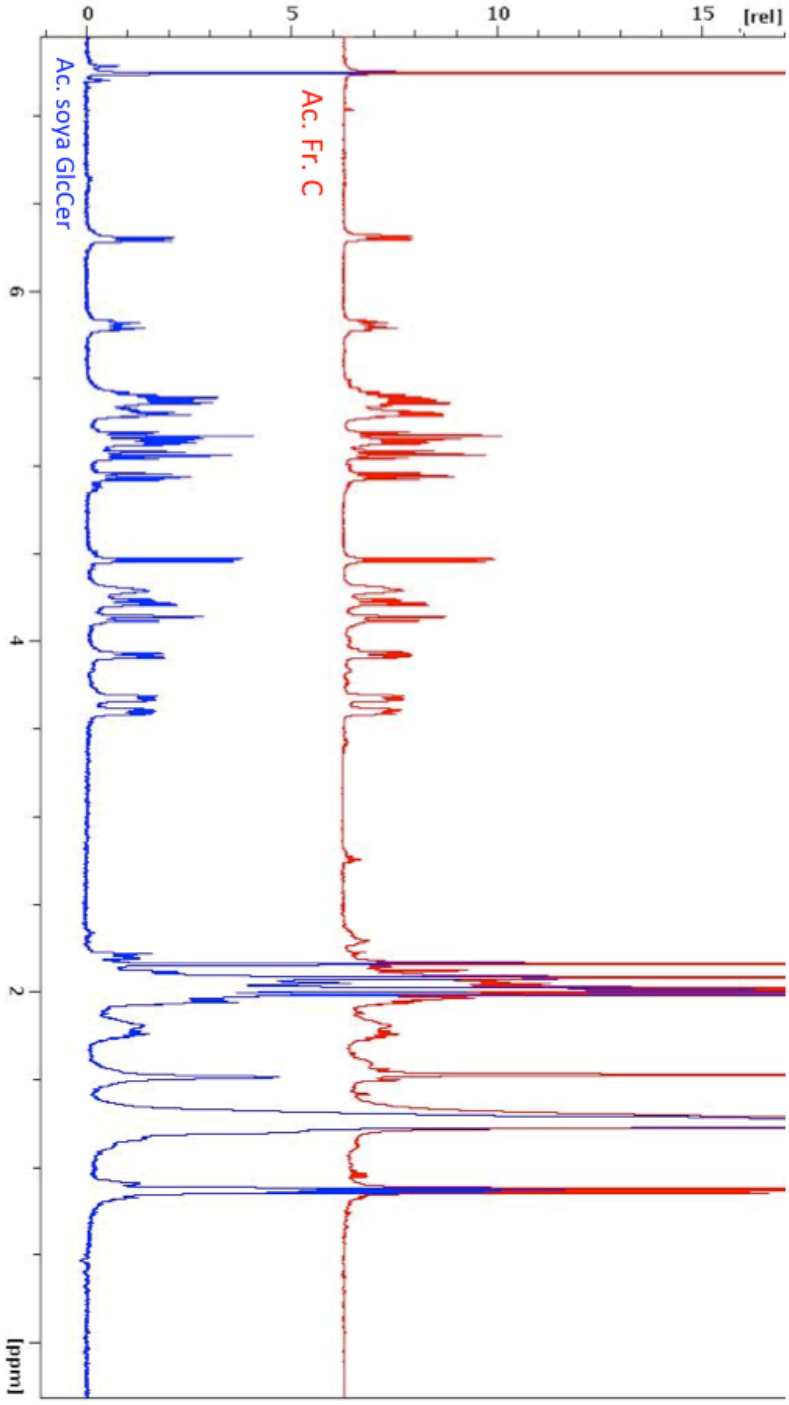

Appendix E: ^{13}C-NMR comparison of acetylated fraction C (Ac.Fr.C) and acetylated commercially available β-glycosylceramides (soya glucocerebroside) – named Ac.Soya GlcCer.

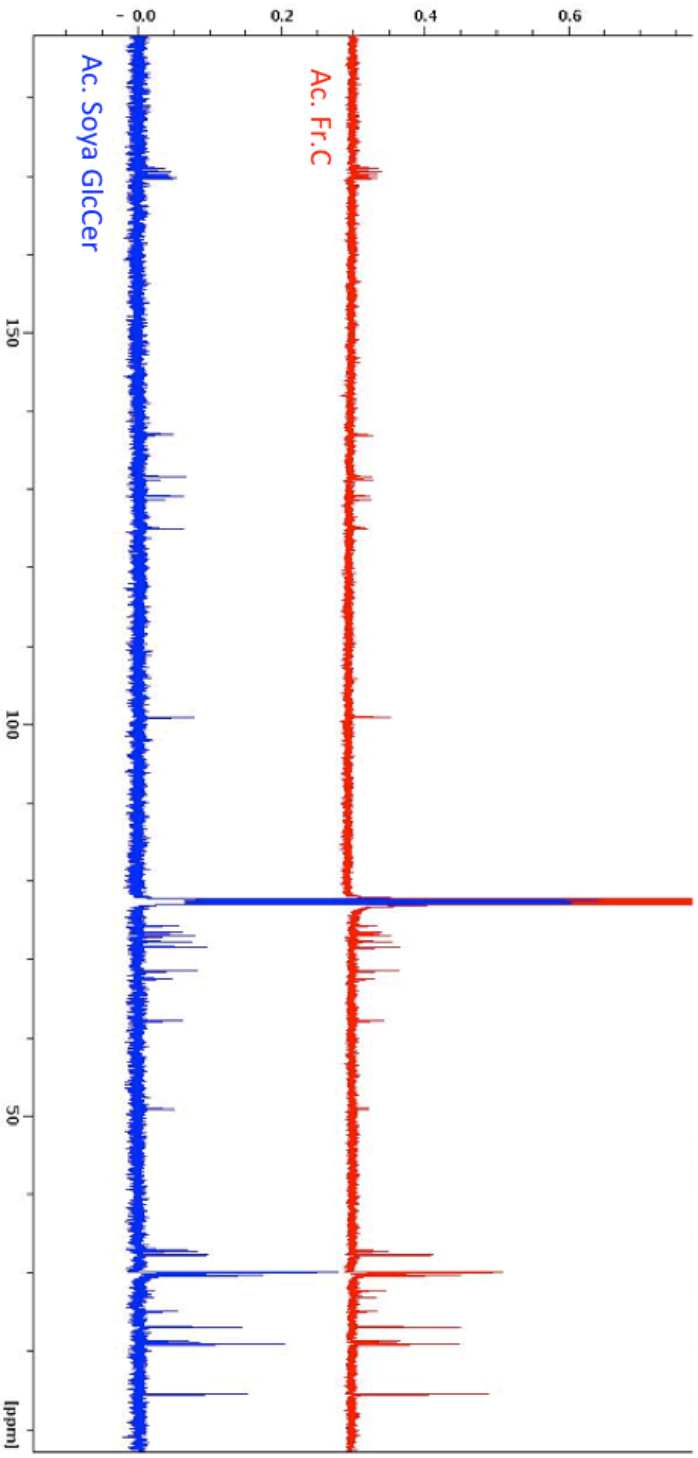

Appendix F: ^{1}H-NMR of synthesized BSSG.

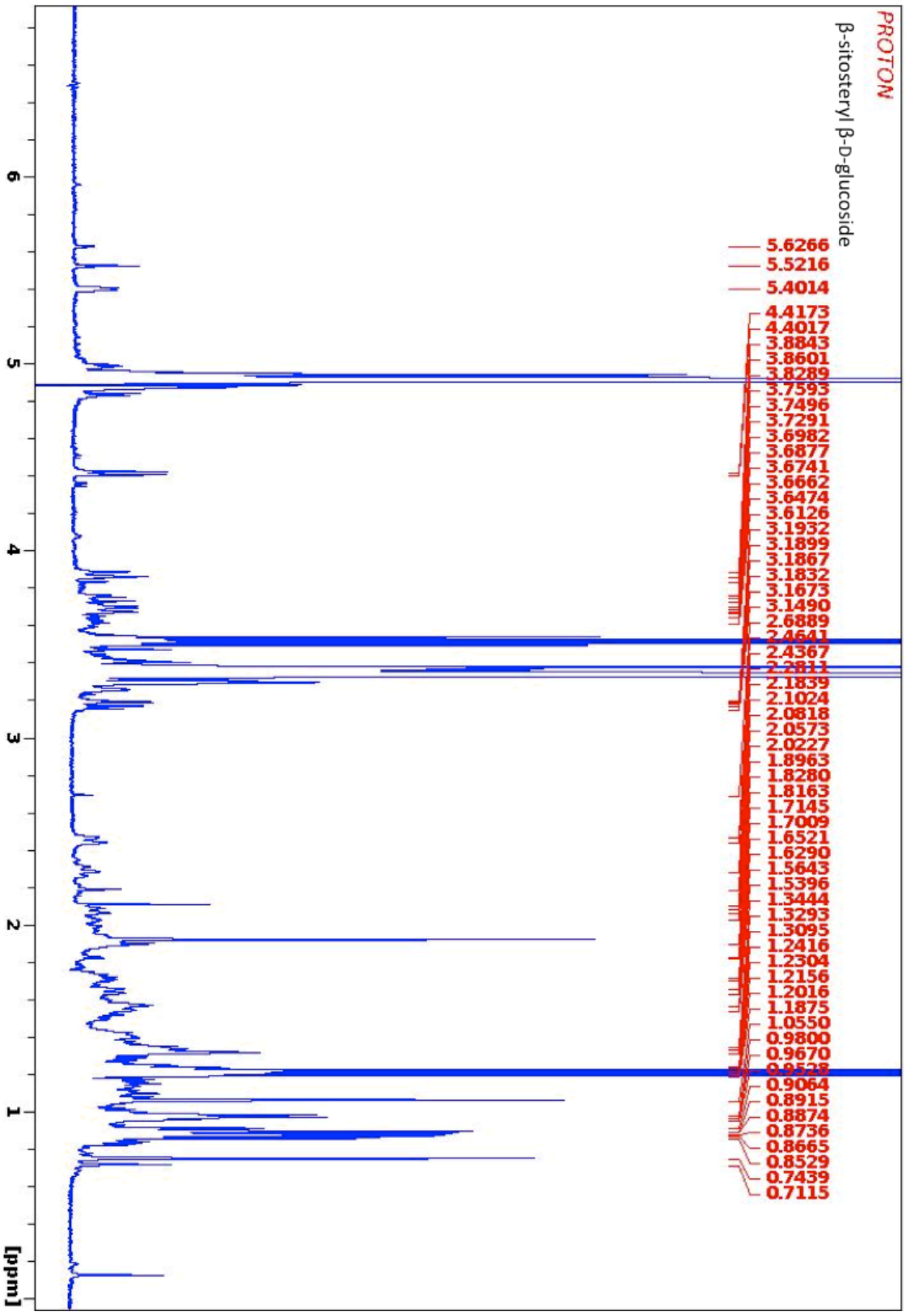

Appendix G: ^{1}H-NMR of synthesized stigmasteryl β-D-glucoside.

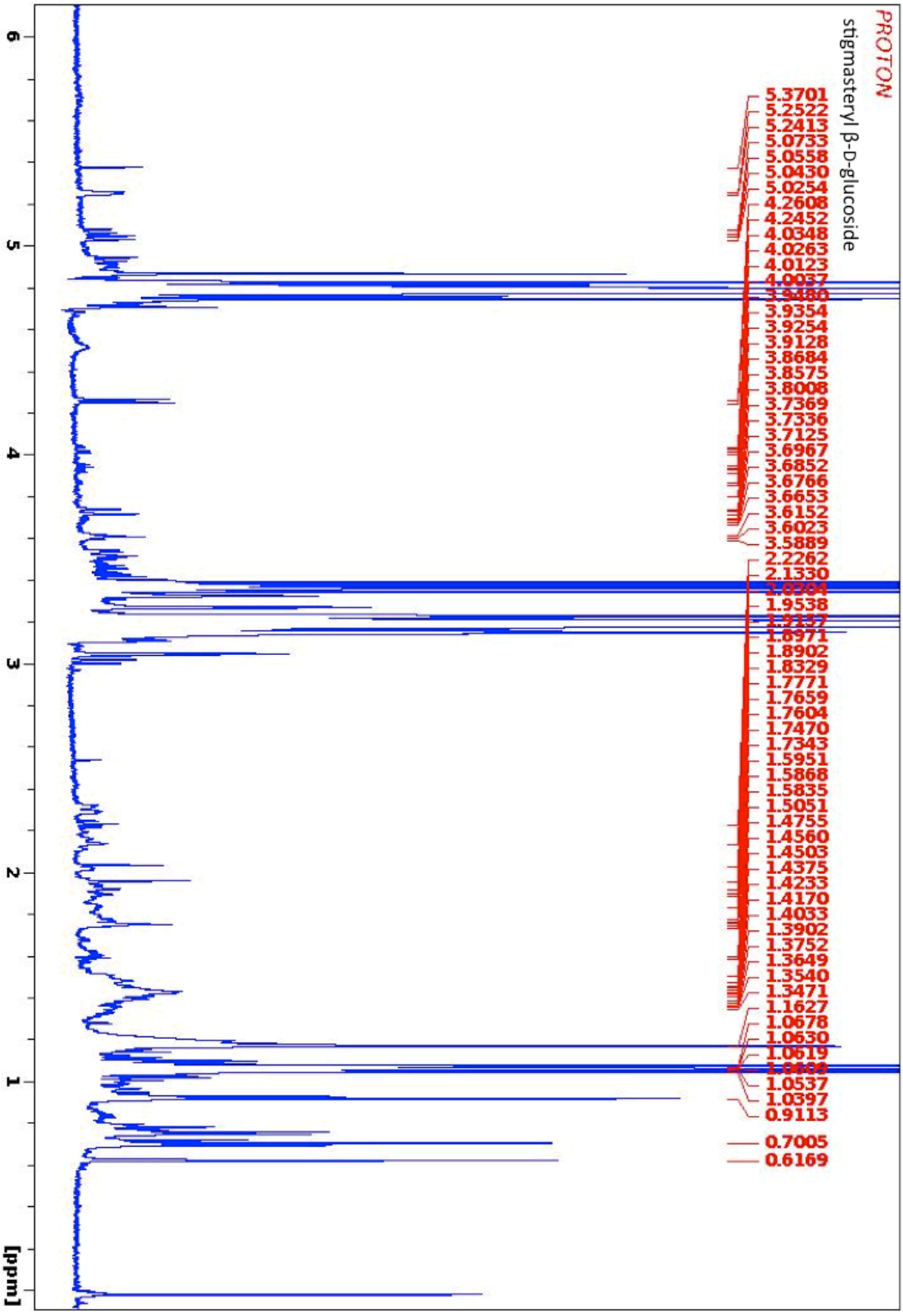

Appendix H: ^{13}C-NMR of synthesized stigmasteryl β-D-glucoside.

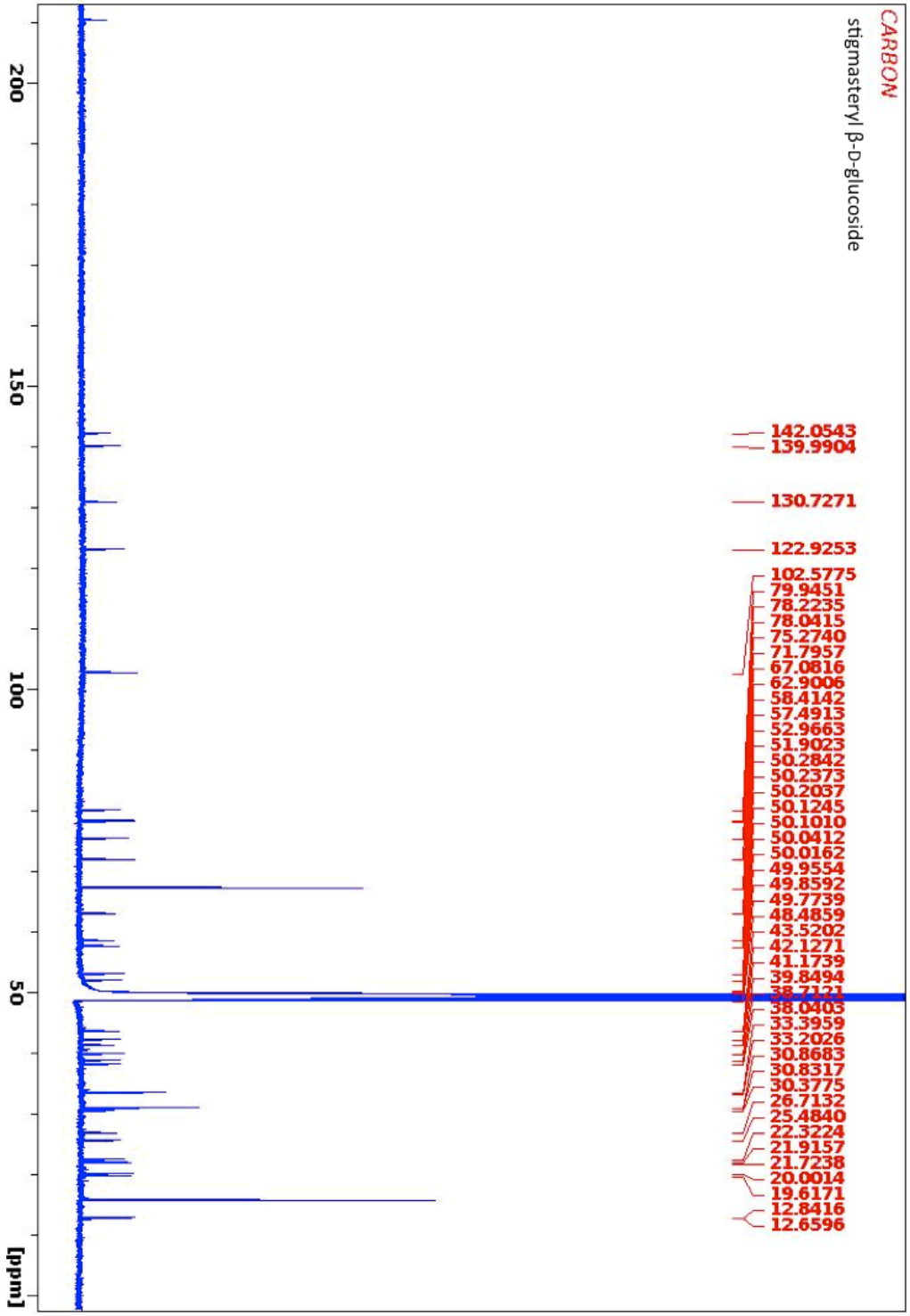

Appendix I: ICP-MS analysis of active fraction C from JTT batch 1.

Analyte	Blank	Fr. C
H	***	***
He	11	4
Li	0	0.015
Be	0	0.013
B	0	0
C	1955	2314
N	0	0
O	0	0
F	0	0
Ne	0	0
Na	***	***
Mg	0	0
Al	7.2	11.2
Si	28.9	25.8
P	0.13	2.23
S	0	0
Cl	0	0
Ar	0	0
K	0	0
Ca	0	0
Sc	0	0
Ti	0	0
V	0	0
Cr	0	0
Mn	0	0
Fe	94	91
Co	0.035	0
Ni	0	0
Cu	0	0
Zn	0	2.099
Ga	0	0
Ge	0	0

Analyte	Blank	Fr. C
As	0	0
Se	0	0
Br	0.112	0
Kr	0	0
Rb	0	0
Sr	0	0
Y	0	0
Zr	0	0
Nb	0	0
Mo	0	0
Ru	0	0
Rh	0.002	0
Pd	0	0
Ag	0	0
Cd	0	0
In	0.006	0
Sn	0.068	0.023
Sb	0.003	0.002
Te	0	0
I	0.02	0
Xe	0	0
Cs	0	0
Ba	0	0
La	0	0
Ce	0	0
Pr	0	0
Nd	0	0
Sm	0	0
Eu	0	0
Gd	0	0
Tb	0	0
Dy	0	0

Analyte	Blank	Fr. C
Ho	0	0
Er	0	0
Tm	0	0
Yb	0	0
Lu	0	0
Hf	0	0.001
Ta	0	0
W	0	0
Re	0	0
Os	0	0
Ir	0	0
Pt	0	0
Au	0	0
Hg	0.019	0.008
Tl	0	0
Pb	0	0
Bi	0.002	0.001
Th	***	***
U	***	***

*** : Not measured

References

Chapter I

1. Sumner, J. *The Natural History of Medicinal Plants*. (Timber Press: 2000).

2. Yamada, H. & Saiki, I. *Juzen-taiho-to (Shi-Quan-Da-Bu-Tang): Scientific Evaluation and Clinical Applications*. (CRC Press: 2005).

3. Kawamura, A. Uncovering the therapeutic potential of natural products with biomarker-guided screening. *IDrugs* **13**, 321–324 (2010).

4. Kawamura, A., Brekman, A., Grigoryev, Y., Hasson, T. H., Takaoka, A., Wolfe, S. & Soll, C. E. Rediscovery of natural products using genomic tools. *Bioorg. Med. Chem. Lett* **16**, 2846–2849 (2006).

5. Kawamura, A., Iacovidou, M., Takaoka, A., Soll, C. E. & Blumenstein, M. A polyacetylene compound from herbal medicine regulates genes associated with thrombosis in endothelial cells. *Bioorg. Med. Chem. Lett.* **17**, 6879–6882 (2007).

6. Brown, P. O. & Botstein, D. Exploring the new world of the genome with DNA microarrays. *Nat. Genet.* **21**, 33–37 (1999).

7. Cousins, R. J., Blanchard, R. K., Popp, M. P., Liu, L., Cao, J., Moore, J. B. & Green, C. L. A global view of the selectivity of zinc deprivation and excess on genes expressed in human THP-1 mononuclear cells. *Proc. Natl. Acad. Sci. USA* **100**, 6952–6957 (2003).

8. Lipshutz, R. J., Fodor, S. P., Gingeras, T. R. & Lockhart, D. J. High density synthetic oligonucleotide arrays. *Nat. Genet.* **21**, 20–24 (1999).

9. Goto, H., Shimada, Y., Sekiya, N., Yang, Q., Kogure, T., Mntani, N., Hikiami, H., Shibahara, N. & Terasawa, K. Effects of Keishi-bukuryo-gan on vascular function and hemorheological factors in spontaneously diabetic (WBN/kob) rats. *Phytomedicine* **11**, 188–195 (2004).

10. Fujita, T., Toda, K., Karimova, A., Yan, S. F., Naka, Y., Yet, S. F. & Pinsky, D. J. Paradoxical rescue from ischemic lung injury by inhaled carbon monoxide driven by derepression of fibrinolysis. *Nat. Med.* **7**, 598–604 (2001).

11. Yachie, A., Niida, Y., Wada, T., Igarashi, N., Kaneda, H., Toma, T., Ohta, K., Kasahara, Y. & Koizumi, S. Oxidative stress causes enhanced endothelial cell injury in human heme oxygenase-1 deficiency. *J. Clin. Invest.* **103**, 129–135 (1999).

12. Medcalf, R. L. & Stasinopoulos, S. J. The undecided serpin. The ins and outs of plasminogen activator inhibitor type 2. *FEBS J.* **272**, 4858–4867 (2005).

13. Yu, Y., Ricciotti, E., Scalia, R., Tang, S.Y., Grant, G., Yu, E., Landesberg, G., Crichton, I., Wu, W., Pure, E., Funk, C.D. & FitzGerald, G.A. Vascular COX-2 modulates blood pressure and thrombosis in mice. *Sci. Transl. Med.* **4**, 132-54 (2012).

14. Saiki, I. A Kampo medicine 'Juzen-taiho-to'--prevention of malignant progression and metastasis of tumor cells and the mechanism of action. *Biol. Pharm. Bull* **23**, 677–688 (2000).

15. Ohnishi, Y., Fujii, H., Hayakawa, Y., Sakukawa, R., Yamaura, T., Sakamoto, T., Tsukuda, K., Fujimaki, M., Nunome, S., Komatsu, Y. & Saiki, I. Oral Administration of a Kampo (Japanese Herbal) Medicine Juzen-taiho-to inhibits liver metastasis of colon 26-L5 carcinoma cells. *Cancer Science* **89**, 206–213 (1998).

16. Hasson, T. H. *Isolation and Characterization of Immunomodulatory Compounds from Juzen-Taiho-To: Novel Understanding of Phytosteryl Glucosides Nano-Aggregates and Synergism.* (The Graduate Center of CUNY: New York, 2009).

17. Iacovidou, M. *Uncovering hidden potential of natural products*. (The Graduate Center of CUNY: New York, 2010).

18. Kunsch, C. & Rosen, C. A. NF-kappa B subunit-specific regulation of the interleukin-8 promoter. *Mol. Cell. Biol* **13**, 6137–6146 (1993).

19. Pahl, H. L. Activators and target genes of Rel/NF-kappaB transcription factors. *Oncogene* **18**, 6853–6866 (1999).

20. Van De Stolpe, A., Caldenhovenm E., Stade, B. G., Koenderman, L., Raaijmakers, J. A., Johnson, J. P. & Van Der Saag, P. T. 12-O-Tetradecanoylphorbol-13-acetate- and tumor necrosis factor alpha-mediated induction of intercellular adhesion molecule-1 is inhibited by dexamethasone. Functional analysis of the human intercellular adhesion molecular-1 promoter. *J. Biol. Chem.* **269**, 6185–6192 (1994).

21. Shakhov, A. N., Collart, M. A., Vassalli, P., Nedospasov, S. A. & Jongeneel, C. V. Kappa B-type enhancers are involved in lipopolysaccharide-mediated transcriptional activation of the tumor necrosis factor alpha gene in primary macrophages. *J. Exp. Med.* **171**, 35 –47 (1990).

Chapter II

1. Sumner, J. *The Natural History of Medicinal Plants*. (Timber Press: 2000).

2. Newman, D. J. & Cragg, G. M. Natural products as sources of new drugs over the last 25 years. *J. Nat. Prod.* **70**, 461–477 (2007).

3. Ginsburg, H. & Deharo, E. A call for using natural compounds in the development of new antimalarial treatments - an introduction. *Malar. J.* **10 Suppl 1**, S1 (2011).

4. Harvey, A. L. Natural products in drug discovery. *Drug Discov. Today* **13**, 894–901 (2008).

5. Shu, Y. Z. Recent natural products based drug development: a pharmaceutical industry perspective. *J. Nat. Prod.* **61**, 1053–1071 (1998).

6. Kawamura, A., Brekman, A., Grigoryev, Y., Hasson, T.H., Takaoka, A., Wolfe, S. & Soll, C.E. Rediscovery of natural products using genomic tools. *Bioorg. Med. Chem. Lett.* **16**, 2846–2849 (2006).

7. Kawamura, A., Iacovidou, M., Takaoka, A., Soll, C. E. & Blumenstein, M. A polyacetylene compound from herbal medicine regulates genes associated with thrombosis in endothelial cells. *Bioorg. Med. Chem. Lett.* **17**, 6879–6882 (2007).

8. Kensil, C. R., Patel, U., Lennick, M. & Marciani, D. Separation and characterization of saponins with adjuvant activity from Quillaja saponaria Molina cortex. *J. Immunol.* **146**, 431–437 (1991).

9. Wang, G.-X., Li, F.-Y., Cui, J., Wang, Y., Liu, Y.-T., Han, J. & Lei, Y. Immunostimulatory Activities of a Decapeptide Derived from Alcaligenes faecalis FY-3 to Crucian Carp. *Scand. J. Immunol.* **74**, 14–22 (2011).

10. Jacobsen, N. E. Fairbrother, W.J., Kensil, C.R., Lim, A., Wheeler, D.A. & Powell, M.F. Structure of the saponin adjuvant QS-21 and its base-catalyzed isomerization product by 1H and natural abundance 13C NMR spectroscopy. *Carbohyd. Res.* **280**, 1–14 (1996).

11. Natori, T., Morita, M., Akimoto, K. & Koezuka, Y. Agelasphins, novel antitumor and immunostimulatory cerebrosides from the marine sponge Agelas mauritianus. *Tetrahedron* **50**, 2771–2784 (1994).

12. Motoki, K., Morita, M., Kobayashi, E., Uchida, T., Akimoto, K., Fukushima, H. & Koezuka, Y. Immunostimulatory and antitumor activities of monoglycosylceramides having various sugar moieties. *Biol. Pharm. Bull.* **18**, 1487–1491 (1995).

13. Tsuji, M. Glycolipids and phospholipids as natural CD1d-binding NKT cell ligands. *Cell. Mol. Life Sci.* **63**, 1889–1898 (2006).

14. Kobayashi, E., Motoki, K., Uchida, T., Fukushima, H. & Koezuka, Y. KRN7000, a novel immunomodulator, and its antitumor activities. *Oncol. Res.* **7**, 529–534 (1995).

15. Taylor, P. R., Martinez-Pomares, L., Stacey, M., Lin, H.-H. Brown, G. D. & Gordon, S. Macrophage receptors and immune recognition. *Annu. Rev. Immunol.* **23**, 901–944 (2005).

16. Kaufmann, S. H. E., Medzhitov, R. & Gordon, S. *The Innate Immune Response to Infection*. (ASM Press: 2004).

17. Paul, W. E. *Fundamental Immunology*. (Lippincott Williams & Wilkins: 2008).

18. Beutler, B. & Rietschel, E. T. Innate immune sensing and its roots: the story of endotoxin. *Nat. Rev. Immunol.* **3**, 169–176 (2003).

19. Waller, E. K. The Role of sargramostim (rhGM-CSF) as immunotherapy. *The Oncologist* **12**, 22–26 (2007).

20. Haworth, C., Brennan, F.M., Chantry, D., Turner, M., Maini, R.N. & Feldmann, M. Expression of granulocyte-macrophage colony-stimulating factor in rheumatoid arthritis: Regulation by tumor necrosis factor-α. *Eur. J. Immunol.* **21**, 2575–2579 (1991).

21. Takeuchi, O., Sato, S., Horiuchi, T., Hoshino, K., Takeda, K., Dong, Z., Modlin, R.L. & Shizuo, A. Cutting edge: role of toll-like receptor 1 in mediating immune response to microbial lipoproteins. *J. Immunol.* **169**, 10–14 (2002).

22. da Silva Correia, J., Soldau, K., Christen, U., Tobias, P. S. & Ulevitch, R. J. Lipopolysaccharide is in close proximity to each of the proteins in its membrane receptor complex. transfer from CD14 to TLR4 and MD-2. *J. Biol. Chem.* **276**, 21129–21135 (2001).

23. Ulevitch, R. J. & Tobias, P. S. Receptor-dependent mechanisms of cell stimulation by bacterial endotoxin. *Annu. Rev. Immunol.* **13**, 437–457 (1995).

24. Greenberg, J. W., Fischer, W. & Joiner, K. A. Influence of lipoteichoic acid structure on recognition by the macrophage scavenger receptor. *Infect. Immun.* **64**, 3318–3325 (1996).

25. Liu, W., Yin, L., Chen, C. & Dai, Y. Function modification of SR-PSOX by point mutations of basic amino acids. *Lipids in Health and Disease* **10**, 59 (2011).

26. Heine, H., El-Samalouti, V.T., Notzel, C., Pfeiffer, A., Lentschat, A., Kusumoto, S., Schmitz, G., Hamann, L. & Ulmer, A.J. CD55/decay accelerating factor is part of the lipopolysaccharide-induced receptor complex. *Eur. J. Immunol.* **33**, 1399–1408 (2003).

27. Sankala, M., Brannstrom, A., Schulthess, T., Bergmann, U., Morgunova, E., Engle, J., Tryggvason, K. & Pikkarainen, T. Characterization of recombinant soluble macrophage scavenger receptor MARCO. *J. Biol. Chem.* **277**, 33378–33385 (2002).

28. Nielsen, M. J., Madsen, M., Møller, H. J. & Moestrup, S. K. The macrophage scavenger receptor CD163: endocytic properties of cytoplasmic tail variants. *J. Leukoc. Biol.* **79**, 837–845 (2006).

29. Daws, M. R., Sullam, P.M., Niemi, E.C., Chen, T.T., Tchao, N.K. & Seaman, W.E. Pattern recognition by TREM-2: binding of anionic ligands. *J. Immunol.* **171**, 594–599 (2003).

30. Saiki, I. A Kampo medicine 'Juzen-taiho-to'--prevention of malignant progression and metastasis of tumor cells and the mechanism of action. *Biol. Pharm. Bull* **23**, 677–688 (2000).

31. Ohnishi, Y., Fujii, H., Hayakawa, Y., Sakukawa, R., Yamaura, T., Sakamoto, T., Tsukada, K., Fujimaki, M., Nunome, S., Komatsu, Y. & Saiki, I. Oral administration of a Kampo (Japanese herbal) medicine Juzen-taiho-to inhibits liver metastasis of colon 26-L5 carcinoma cells. *Cancer Science* **89**, 206–213 (1998).

32. Tagami, K., Niwa, K., Lian, Z., Gao, J., Mori, H. & Tamaya, T. Preventive effect of Juzen-taiho-to on endometrial carcinogenesis in mice is based on Shimotsu-to constituent. *Biol. Pharm. Bull.* **27**, 156–161 (2004).

33. Lian, Z., Niwa, K., Onogi, K., Mori, H., Harrigan, R.C. & Tamaya, T. Anti-tumor effects of herbal medicines on endometrial carcinomas via estrogen receptor-alpha-related mechanism. *Oncol. Rep* **15**, 1133–1136 (2006).

34. Kiyohara, H., Matsumoto, T. & Yamada, H. Combination effects of herbs in a multi-herbal formula: expression of Juzen-taiho-to's immuno-modulatory activity on the intestinal immune system. *Evid. Based Complement Alternat. Med.* **1**, 83–91 (2004).

35. Yamada, H. & Saiki, I. *Juzen-taiho-to (Shi-Quan-Da-Bu-Tang): Scientific Evaluation and Clinical Applications*. (CRC Press: 2005).

36. Gertsch, J., Viveros-Paredes, J. M. & Taylor, P. Plant immunostimulants—Scientific paradigm or myth? *J. Ethnopharmacol.* **136**, 385–391 (2011).

37. Capasso, R., Izzo, A.A., Pinto, L., Bifulco, T., Vitobello, C. & Mascolo, N. Phytotherapy and quality of herbal medicines. *Fitoterapia* **71, Supplement 1**, S58–S65 (2000).

38. Hasson, T. H. *Isolation and Characterization of Immunomodulatory Compounds from Juzen-Taiho-To: Novel Understanding of Phytosteryl Glucosides Nano-Aggregates and Synergism.* (The Graduate Center of CUNY: New York, 2009).

39. Iacovidou, M. *Uncovering hidden potential of natural products*. (The Graduate Center of CUNY: New York, 2010).

40. Van De Stolpe, A., Caldenhoven, E., Stade, B.G., Koenderman, L., Raaijmakers, J.A., Johnson, J.P. & Van Der Saag, P.T. 12-O-Tetradecanoylphorbol-13-acetate- and tumor necrosis factor alpha-mediated induction of intercellular adhesion molecule-1 is inhibited by dexamethasone. Functional analysis of the human intercellular adhesion molecular-1 promoter. *J. Biol. Chem.* **269**, 6185–6192 (1994).

41. Folch, J., Lees, M. & Sloane Stanley, G. H. A simple method for the isolation and purification of total lipides from animal tissues. *J. Biol. Chem.* **226**, 497–509 (1957).

42. Lucena, R., Cárdenas, S. & Valcárcel, M. Evaporative light scattering detection: trends in its analytical uses. *Anal. Bioanal. Chem.* **388**, 1663–1672 (2007).

43. Wei, Y.-J., Qi, L.-W., Li, P., Luo, H.-W., Yi, L. & Sheng, L.-H. Improved quality control method for Fufang Danshen preparations through simultaneous determination of phenolic acids, saponins and diterpenoid quinones by HPLC coupled with diode array and evaporative light scattering detectors. *J. Pharm. Biomed. Anal.* **45**, 775–784 (2007).

44. Niiho, Y., Nakajima, Y., Yamazaki, T., Okamoto, M., Tsuchihashi, R., Kodera, M., Kinjo, J. & Nohara, T. Simultaneous analysis of isoflavones and saponins in *Pueraria* flowers using HPLC coupled to an evaporative light scattering detector and isolation of a new isoflavone diglucoside. *J. Nat. Med.* **64**, 313–320 (2010).

45. Almeling, S. & Holzgrabe, U. Use of evaporative light scattering detection for the quality control of drug substances: influence of different liquid chromatographic and evaporative light scattering detector parameters on the appearance of spike peaks. *J. Chromatogr. A* **1217**, 2163–2170 (2010).

46. Fuzzati, N. Analysis methods of ginsenosides. *J. Chromatogr. B Analyt. Technol. Biomed. Life Sci.* **812**, 119–133 (2004).

47. Dustin, M. L., Rothlein, R., Bhan, A. K., Dinarello, C. A. & Springer, T. A. Induction by IL 1 and interferon-gamma: tissue distribution, biochemistry, and function of a natural adherence molecule (ICAM-1). *J. Immunol.* **137**, 245–254 (1986).

48. Mattson, F. H. & Volpenhein, R. A. Synthesis and properties of glycerides. *J. Lipid Res.* **3**, 281 –296 (1962).

49. Haften, J. L. Fat-based food emulsifiers. *J Am Oil Chem Soc* **56**, 831A–835A (1979).

50. Jia, J. X. & Wasan, K. M. Effects of monoglycerides on rhodamine 123 accumulation, estradiol 17 beta-D-glucuronide bidirectional transport and MRP2 protein expression within Caco-2 cells. *J. Pharm. Pharm. Sci.* **11**, 45–62 (2008).

51. Porter, C. J. H., Trevaskis, N. L. & Charman, W. N. Lipids and lipid-based formulations: optimizing the oral delivery of lipophilic drugs. *Nat. Rev. Drug Discov.* **6**, 231–248 (2007).

52. Håversen, L., Danielsson, K. N., Fogelstrand, L. & Wiklund, O. Induction of proinflammatory cytokines by long-chain saturated fatty acids in human macrophages. *Atherosclerosis* **202**, 382–393 (2009).

53. Han, C. Y., Kargi, A.Y., Omer, M., Chan, C.K., Webitsch, M., O'Brien, K.D., Wight, T.N. & Chait, A. Differential effect of saturated and unsaturated free fatty acids on the generation of monocyte adhesion and chemotactic factors by adipocytes: dissociation of adipocyte hypertrophy from inflammation. *Diabetes* (2009).doi:10.2337/db09-0925

54. Weisberg, S. P., McCann, D., Desai, M., Rosenbaum, M., Leibel, R.L. & Ferrante, A.W. Obesity is associated with macrophage accumulation in adipose tissue. *J. Clin. Invest.* **112**, 1796–1808 (2003).

55. Natori, T., Koezuka, Y. & Higa, T. Agelasphins, novel α-galactosylceramides from the marine sponge Agelas mauritianus. *Tetrahedron Letters* **34**, 5591–5592 (1993).

56. Margalit, M., Abu Gazala, S., Alper, R., Elinav, E., Klein, A., Doviner, V., Sherman, Y., Thalenfeld, B., Engelhardt, D., Rabbani, E. & Ilan, Y. Glucocerebroside treatment ameliorates ConA hepatitis by inhibition of NKT lymphocytes. *Am. J. Physiol. Gastrointest. Liver Physiol.* **289**, G917–925 (2005).

57. Parekh, V. V., Singh, A.K., Wilson, M.T., Olivares-Villagomez, D., Bezbradica, J.S., Inazawa, H., Ehara, H., Sakai, T., Serizawa, I., Wu, L., Wang, C.-R., Joyce, S. & Van Kaer, L. Quantitative and qualitative differences in the in vivo response of NKT cells to distinct alpha- and beta-anomeric glycolipids. *J. Immunol.* **173**, 3693–3706 (2004).

58. Shibuya, H., Kawashima, K., Sakagami, M., Kawashima, H., Shimomura, M., Ohashi, K. & Kitagawa, I. Sphingolipids and glycerolipids. I. Chemical structures and ionophoretic activities of soya-cerebrosides I and II from soybean. *Chem. Pharm. Bull.* **38**, 2933–2938 (1990).

59. Inagaki, M., Harada, Y., Yamada, K., Isobe, R., Higuchi, R., Matsuura, H. & Itakura, Y. Isolation and structure determination of cerebrosides from Garlic, the bulbs of Allium sativum L. *Chem. Pharm. Bull.* **46**, 1153–1156

60. Ilan, Y., Elstein, D. & Zimran, A. Glucocerebroside: an evolutionary advantage for patients with Gaucher disease and a new immunomodulatory agent. *Immunol. Cell Biol.* **87**, 514–524 (2009).

61. Bertram, H. C., Eldibany, M., Padgett, J. & Dragon, L. H. Splenic lymphoma arising in a patient with Gaucher disease. A case report and review of the literature. *Arch. Pathol. Lab. Med.* **127**, e242–245 (2003).

62. Lo, S. M., Stein, P., Mullaly, S., Bar, M., Jain, D, Pastores, G.M. & Mistry, P.K. Expanding spectrum of the association between Type 1 Gaucher disease and cancers: a series of patients with up to 3 sequential cancers of multiple types--correlation with genotype and phenotype. *Am. J. Hematol.* **85**, 340–345 (2010).

63. Brady, R. O., Kanfer, J. N. & Shapiro, D. Metabolism of glucocerebrosides. II. Evidence of an enzymatic deficiency in gaucher's disease. *Biochem. Biophys. Res. Commun.* **18**, 221–225 (1965).

64. Vanderjagt, D. J., Fry, D. E. & Glew, R. H. Human glucocerebrosidase catalyses transglucosylation between glucocerebroside and retinol. *Biochem. J.* **300 (Pt 2)**, 309–315 (1994).

65. Hannun, Y. A. & Obeid, L. M. The Ceramide-centric universe of lipid-mediated cell regulation: stress encounters of the lipid kind. *J. Biol. Chem.* **277**, 25847–25850 (2002).

66. Demarchi, F., Bertoli, C., Greer, P. A. & Schneider, C. Ceramide triggers an NF-|[kappa]|B-dependent survival pathway through calpain. *Cell Death Differ.* **12**, 512–522 (2005).

67. Ruvolo, P. P. Intracellular signal transduction pathways activated by ceramide and its metabolites. *Pharmacological Research* **47**, 383–392 (2003).

68. Hannun, Y. A. Functions of ceramide in coordinating cellular responses to stress. *Science* **274**, 1855+ (1996).

69. Ruvolo, P. P. Ceramide regulates cellular homeostasis via diverse stress signaling pathways. *Leukemia* **15**, 1153–1160 (2001).

70. Smyth, M. J., Obeid, L. M. & Hannun, Y. A. Ceramide: a novel lipid mediator of apoptosis. *Adv. Pharmacol.* **41**, 133–154 (1997).

71. Ruiz-Argüello, M. B., Basáñez, G., Goñi, F. M. & Alonso, A. Different Effects of Enzyme-generated Ceramides and Diacylglycerols in Phospholipid Membrane Fusion and Leakage. *J. Biol. Chem.* **271**, 26616–26621 (1996).

72. Tapiero, H., Townsend, D. M. & Tew, K. D. Phytosterols in the prevention of human pathologies. *Biomed. Pharmacother.* **57**, 321–325 (2003).

73. Bouic, P. J. & Lamprecht, J. H. Plant sterols and sterolins: a review of their immune-modulating properties. *Altern Med Rev* **4**, 170–177 (1999).

74. Bradford, P. G. & Awad, A. B. Phytosterols as anticancer compounds. *Mol Nutr Food Res* **51**, 161–170 (2007).

75. Awad, A. B. & Fink, C. S. Phytosterols as Anticancer Dietary Components: Evidence and Mechanism of Action. *J. Nutr.* **130**, 2127–2130 (2000).

76. Ling, W. H. & Jones, P. J. Dietary phytosterols: a review of metabolism, benefits and side effects. *Life Sci.* **57**, 195–206 (1995).

77. Bouic, P. J., Etsebeth, S., Liebenberg, R.W., Albrecht, C.F., Pegel, K. & Ven Jaarsveld, P.P. beta-Sitosterol and beta-sitosterol glucoside stimulate human peripheral blood lymphocyte proliferation: implications for their use as an immunomodulatory vitamin combination. *Int. J. Immunopharmacol.* **18**, 693–700 (1996).

78. Bouic, P. J. D. Sterols and sterolins: new drugs for the immune system? *Drug Discov. Today* **7**, 775–778 (2002).

79. Bouic, P. J. The role of phytosterols and phytosterolins in immune modulation: a review of the past 10 years. *Curr Opin Clin Nutr Metab Care* **4**, 471–475 (2001).

80. Malich, G., Markovic, B. & Winder, C. The sensitivity and specificity of the MTS tetrazolium assay for detecting the in vitro cytotoxicity of 20 chemicals using human cell lines. *Toxicology* **124**, 179–192 (1997).

Chapter III

1. Lee, J. Y., Sohn, K. H., Rhee, S. H. & Hwang, D. Saturated Fatty Acids, but Not Unsaturated Fatty Acids, Induce the Expression of Cyclooxygenase-2 Mediated through Toll-like Receptor 4. *J. Biol. Chem.* **276**, 16683–16689 (2001).

2. Choi, S.-E. Kim, T.H., Yi, S.-A., Hwang, Y.C., Hwang, W.S., Choe, S.J., Han, S.J., Kim, H.J., Kim, D.J., Kang, Y. & Lee, K.-W. Capsaicin attenuates palmitate-induced expression of macrophage inflammatory protein 1 and interleukin 8 by increasing palmitate oxidation and reducing c-Jun activation in THP-1 (human acute monocytic leukemia cell) cells. *Nutr. Res.* **31**, 468–478 (2011).

3. Håversen, L., Danielsson, K. N., Fogelstrand, L. & Wiklund, O. Induction of proinflammatory cytokines by long-chain saturated fatty acids in human macrophages. *Atherosclerosis* **202**, 382–393 (2009).

4. Bouic, P. J., Etsebeth, S., Liebenberg, R.W., Albrecht, C.F. & Van Jaarsveld, P.P. beta-Sitosterol and beta-sitosterol glucoside stimulate human peripheral blood lymphocyte proliferation: implications for their use as an immunomodulatory vitamin combination. *Int. J. Immunopharmacol.* **18**, 693–700 (1996).

5. Bouic, P. J. The role of phytosterols and phytosterolins in immune modulation: a review of the past 10 years. *Curr Opin Clin Nutr Metab Care* **4**, 471–475 (2001).

6. Listenberger, L. L., Ory, D. S. & Schaffer, J. E. Palmitate-Induced Apoptosis Can Occur Through a Ceramide-Independent Pathway. *J. Biol. Chem.* **276**, 14890–14895 (2001).

7. Bouic, P. J. D. Sterols and sterolins: new drugs for the immune system? *Drug Discov. Today* **7**, 775–778 (2002).

8. Bouic, P. J. & Lamprecht, J. H. Plant sterols and sterolins: a review of their immune-modulating properties. *Altern Med Rev* **4**, 170–177 (1999).

9. Iacovidou, M. *Uncovering hidden potential of natural products*. (The Graduate Center of CUNY: New York, 2010).

10. Wu, D., Xing, G.-W., Poles, M. A., Horowitz, A., Kinjo, Y., Sullivan, B., Bodmer-Narkevitch, V., Plettenburg, O., Kronenberg, M., Tsuji, M., Ho, D. D. & Wong, C.-H. Bacterial glycolipids and analogs as antigens for CD1d-restricted NKT cells. *Proc. Natl. Acad. Sci. U.S.A.* **102**, 1351–1356 (2005).

11. Schmieg, J., Yang, G., Franck, R. W. & Tsuji, M. Superior protection against malaria and melanoma metastases by a C-glycoside analogue of the natural killer T cell ligand α-galactosylceramide. *J. Exp. Med.* **198**, 1631–1641 (2003).

12. Fujio, M., Wu, D., Garcia-Navarro, R., Ho, D. D., Tsuji, M. & Wong, C.-H. Structure-based discovery of glycolipids for CD1d-mediated NKT cell activation: tuning the adjuvant versus immunosuppression activity. *J. Am. Chem. Soc.* **128**, 9022–9023 (2006).

13. Yu, K. O. A., Im, J. S., Molano, A., Dutronc, Y., Illarionov, P. A., Forestier, C., Fujiwara, N., Arias, I., Miyake, S. & Yamamura, T. Modulation of CD1d-restricted NKT cell responses by using N-acyl variants of alpha-galactosylceramides. *Proc. Natl. Acad. Sci. U.S.A.* **102**, 3383–3388 (2005).

14. Azas, N., Laurencin, N., Delmas, F., Di, G. C., Gasquet, M., Laget, M. & Timon-David, P. Synergistic in vitro antimalarial activity of plant extracts used as traditional herbal remedies in Mali. *Parasitol. Res.* **88**, 165–171 (2002).

15. Hemaiswarya, S., Kruthiventi, A. K. & Doble, M. Synergism between natural products and antibiotics against infectious diseases. *Phytomedicine* **15**, 639–652 (2008).

16. Marchetti, O., Moreillon, P., Glauser, M. P., Bille, J. & Sanglard, D. Potent Synergism of the Combination of Fluconazole and Cyclosporine in Candida Albicans. *Antimicrob. Agents Chemother.* **44**, 2373–2381 (2000).

17. Williamson, E. M. Synergy and other interactions in phytomedicines. *Phytomedicine* **8**, 401–409 (2001).

18. Rasoanaivo, P., Wright, C. W., Willcox, M. L. & Gilbert, B. Whole plant extracts versus single compounds for the treatment of malaria: synergy and positive interactions. *Malaria J.* **10**, S4 (2011).

19. Shibuya, H., Kawashima, K., Sakagami, M., Kawanishi, H., Shimomura, M., Ohashi, K. & Kitagawa, I. Sphingolipids and glycerolipids. I. Chemical structures and ionophoretic activities of soya-cerebrosides I and II from soybean. *Chem. Pharm. Bull.* **38**, 2933–2938 (1990).

20. Goodman, L. Neighboring-Group Participation in Sugars. *Advances in Carbohydrate Chemistry* **Volume 22**, 109–175 (1967).

21. Ascherio, A. & Willett, W. C. Health effects of trans fatty acids. *Am. J. Clin. Nutr.* **66**, 1006S–1010S (1997).

22. Kinsella, J. E., Bruckner, G., Mai, J. & Shimp, J. Metabolism of trans fatty acids with emphasis on the effects of trans, trans-octadecadienoate on lipid composition, essential fatty acid, and prostaglandins: an overview. *Am. J. Clin. Nutr.* **34**, 2307–2318 (1981).

23. Mensink, R. P., Zock, P. L., Katan, M. B. & Hornstra, G. Effect of dietary cis and trans fatty acids on serum lipoprotein[a] levels in humans. *J. Lipid Res.* **33**, 1493–1501 (1992).

24. Hasson, T. H. *Isolation and Characterization of Immunomodulatory Compounds from Juzen-Taiho-To: Novel Understanding of Phytosteryl Glucosides Nano-Aggregates and Synergism.* (The Graduate Center of CUNY: New York, 2009).

25. Kawamura, A., Guo, J., Itagaki, Y., Bell, C., Wang, Y., Haupert, G. T., Magil, S., Gallagher, R. T., Berova, N. & Nakanishi, K. On the structure of endogenous ouabain. *P. Natl. Acad. Sci. U.S.A.* **96**, 6654–6659 (1999).

26. Li, C.-H., liao, P.-L., Shyu, M.-K., Liu, C.-W., Kao, C.-C., Huang, S.-H., Cheng, Y.-W. & Kang, J.-J. Zinc oxide nanoparticles–induced intercellular adhesion molecule 1 expression requires Rac1/Cdc42, mixed lineage kinase 3, and c-Jun N-terminal kinase activation in endothelial cells. *Toxicol. Sci.* **126**, 162–172 (2012).

27. Tsou, T.-C., Chao, H.-R., Yeh, S.-C., Tsai, F.-Y. & Lin, H.-J. Zinc induces chemokine and inflammatory cytokine release from human promonocytes. *J. Hazard. Mater.* **196**, 335–341 (2011).

28. Bertram, H. C., Eldibany, M., Padgett, J. & Dragon, L. H. Splenic lymphoma arising in a patient with Gaucher disease. A case report and review of the literature. *Arch. Pathol. Lab. Med.* **127**, e242–245 (2003).

29. Gery, I., Zigler, J. S., Brady, R. O. & Barranger, J. A. Selective Effects of Glucocerebroside (Gaucher's Storage Material) on Macrophage Cultures. *J. Clin. Invest.* **68**, 1182–1189 (1981).

30. Ilan, Y., Elstein, D. & Zimran, A. Glucocerebroside: an evolutionary advantage for patients with Gaucher disease and a new immunomodulatory agent. *Immunol. Cell Biol.* **87**, 514–524 (2009).

31. Barak, V., Acker, M., Nisman, B., Kalickman, I., Abrahamov, A., Zimran, A. & Yatziv, S. Cytokines in Gaucher's disease. *Eur. Cytokine Netw.* **10**, 205–210 (1999).

32. Hollak, C. E. M., Evers, L., Aerts, J. M. F. G. & van Oers, M. H. J. Elevated Levels of M-CSF, sCD14 and IL8 in Type 1 Gaucher Disease. *Blood Cells Mol. Dis.* **23**, 201–212 (1997).

33. Allen, M. J., Myer, B. J., Khokher, A. M., Rushton, N. & Cox, T. M. Pro-inflammatory cytokines and the pathogenesis of Gaucher's disease: increased release of interleukin-6 and interleukin-10. *QJM* **90**, 19–25 (1997).

34. Pandey, M. K., Rani, R., Zhang, W., Setchell, K. & Grabowski, G. A. Immunological cell type characterization and Th1–Th17 cytokine production in a mouse model of Gaucher disease. *Molecular Genetics and Metabolism* **106**, 310–322 (2012).

35. Hein, L. K., Meikle, P. J., Hopwood, J. J. & Fuller, M. Secondary sphingolipid accumulation in a macrophage model of Gaucher disease. *Mol. Genet. Metab.* **92**, 336–345 (2007).

36. Whitmore, M. M., Deveer, M. J., Edling, A., Oates, R. K., Simons, B., Lindner, D. & Williams, B. R. G. Synergistic activation of innate immunity by double-stranded RNA and CpG DNA promotes enhanced antitumor activity. *Cancer Res.* **64**, 5850–5860 (2004).

37. Wiesner, P., Choi, S.-H., Almazan, F., Benner, C., Huang, W., Diehl, C. J., Gonen, A., Butler, S., Witztum, J. L., Glass, C. K. & Miller, Y. I. Low doses of lipopolysaccharide and minimally oxidized low-density lipoprotein cooperatively activate macrophages via nuclear factor κb and activator protein-1 possible mechanism

for acceleration of atherosclerosis by subclinical endotoxemia. *Circ. Res.* **107**, 56–65 (2010).

38. Traub, S., Kubasch, N., Morath, S., Kresse, M., Hartung, T., Schmidt, R. R. & Hermann, C. Structural requirements of synthetic muropeptides to synergize with lipopolysaccharide in cytokine induction. *J. Biol. Chem.* **279**, 8694–8700 (2004).

39. Into, T., Fujita, M., Okusawa, T., Hasebe, A., Morita, M. & Shibata, K. Synergic effects of mycoplasmal lipopeptides and extracellular ATP on activation of macrophages. *Infect. Immun.* **70**, 3586–3591 (2002).

40. Watson, D. S., Endsley, A. N. & Huang, L. Design considerations for liposomal vaccines: Influence of formulation parameters on antibody and cell-mediated immune responses to liposome associated antigens. *Vaccine* **30**, 2256–2272 (2012).

41. Reed, S. G., Bertholet, S., Coler, R. N. & Friede, M. New horizons in adjuvants for vaccine development. *Trends Immunol.* **30**, 23–32 (2009).

Chapter IV

1. Ginsburg, H. & Deharo, E. A call for using natural compounds in the development of new antimalarial treatments - an introduction. *Malar. J.* **10 Suppl 1**, S1 (2011).

2. Rasoanaivo, P., Wright, C. W., Willcox, M. L. & Gilbert, B. Whole plant extracts versus single compounds for the treatment of malaria: synergy and positive interactions. *Malar. J.* **10**, S4 (2011).

3. Ascierto, P. A. & Marincola, F. M. Combination therapy: the next opportunity and challenge of medicine. *J. Transl. Med.* **9**, 115 (2011).

4. Soliman, M. M., Ashcroft, D. M., Watson, K. D., Lunt, M., Symmons, D. P. M. & Hyrich, K. L. Impact of concomitant use of DMARDs on the persistence with anti-TNF therapies in patients with rheumatoid arthritis: results from the British Society for Rheumatology Biologics Register. *Ann. Rheum. Dis.* **70**, 583–589 (2011).

5. Johnston, A., Gudjonsson, J. E., Sigmundsdottir, H., Runar Ludviksson, B. & Valdimarsson, H. The anti-inflammatory action of methotrexate is not mediated by lymphocyte apoptosis, but by the suppression of activation and adhesion molecules. *Clin. Immunol.* **114**, 154–163 (2005).

6. Dionne, R. A., Campbell, R. A., Cooper, S. A., Hall, D. L. & Buckingham, B. Suppression of postoperative pain by preoperative administration of ibuprofen in comparison to placebo, acetaminophen, and acetaminophen plus codeine. *J. Clin. Pharmacol.* **23**, 37–43 (1983).

7. Raffa, R. B. Pharmacology of oral combination analgesics: rational therapy for pain. *J. Clin. Pharm. Ther.* **26**, 257–264 (2001).

8. Reddy, R. C., Vatsala, P. G., Keshamouni, V. G., Padmanaban, G. & Rangarajan, P. N. Curcumin for malaria therapy. *Biochem. Biophys. Res. Commun.* **326**, 472–474 (2005).

9. Cui, L., Miao, J. & Cui, L. Cytotoxic Effect of Curcumin on Malaria Parasite Plasmodium falciparum: Inhibition of Histone Acetylation and Generation of Reactive Oxygen Species. *Antimicrob. Agents Chemother.* **51**, 488–494 (2007).

10. Shoba, G., Joy, D., Joseph, T., Majeed, M., Rajendran, R. & Srinivas, P. S. Influence of piperine on the pharmacokinetics of curcumin in animals and human volunteers. *Planta Med.* **64**, 353–356 (1998).

11. Srinivasan, K. & Suresh, D. Influence of curcumin, capsaicin, and piperine on the rat liver drug-metabolizing enzyme system in vivo and in vitro. *Can. J. Physiol. Pharm.* **84**, 1259–1265 (2006).

12. Anand, P., Kunnumakkara, A. B., Newman, R. A. & Aggarwal, B. B. Bioavailability of Curcumin: Problems and Promises. *Mol. Pharmaceutics* **4**, 807–818 (2007).

13. Lambert, J. D., Hong, J., Kim, D. H., Mishin, V. M. & Yang, C. S. Piperine enhances the bioavailability of the tea polyphenol (-)-epigallocatechin-3-gallate in mice. *J. Nutr.* **134**, 1948–1952 (2004).

14. Hasson, T. H. *Isolation and Characterization of Immunomodulatory Compounds from Juzen-Taiho-To: Novel Understanding of Phytosteryl Glucosides Nano-Aggregates and Synergism.* (The Graduate Center of CUNY: New York, 2009).

15. Kozikowski, B. A., Burt, T. M., Tirey, D. A., Williams, L. E., Kuzmak, B. R., Stanton, D. T., Morand, K. L. & Nelson, S. L. The Effect of Room-Temperature Storage on the Stability of Compounds in DMSO. *J. Biomol. Screen* **8**, 205–209 (2003).

16. Berne, B. J. & Pecora, R. *Dynamic Light Scattering: With Applications to Chemistry, Biology, and Physics*. (Courier Dover Publications: 2000).

17. Letchford, K. & Burt, H. A review of the formation and classification of amphiphilic block copolymer nanoparticulate structures: micelles, nanospheres, nanocapsules and polymersomes. *Eur. J. Pharm. Biopharm.* **65**, 259–269 (2007).

18. Li, S.-D. & Huang, L. Pharmacokinetics and biodistribution of nanoparticles. *Mol. Pharmaceutics* **5**, 496–504 (2008).

19. Champion, J., Walker, A. & Mitragotri, S. Role of particle size in phagocytosis of polymeric microspheres. *Pharm. Res.* **25**, 1815–1821 (2008).

20. Singh, R. & Lillard Jr., J. W. Nanoparticle-based targeted drug delivery. *Exp. Mol. Pathol.* **86**, 215–223 (2009).

21. Dobrovolskaia, M. A. & McNeil, S. E. Immunological properties of engineered nanomaterials. *Nat. Nanotechnol.* **2**, 469–478 (2007).

22. van Zijverden, M. & Granum, B. Adjuvant activity of particulate pollutants in different mouse models. *Toxicology* **152**, 69–77 (2000).

23. Chong, C. S. W., Cao, M., Wong, W. W., Fischer, K. P., Addison, W. P., Kwon, G. S., Tyrrell, D. L. & Samuel, J. Enhancement of T helper type 1 immune responses against hepatitis B virus core antigen by PLGA nanoparticle vaccine delivery. *J. Control Release* **102**, 85–99 (2005).

24. Cui, Z. & Mumper, R. J. Coating of cationized protein on engineered nanoparticles results in enhanced immune responses. *Int. J. Pharm.* **238**, 229–239 (2002).

25. Conner, S. D. & Schmid, S. L. Regulated portals of entry into the cell. *Nature* **422**, 37–44 (2003).

26. Aderem, A. & Underhill, D. M. Mechanisms of phagocytosis in macrophages. *Annu. Rev. Immunol.* **17**, 593–623 (1999).

27. Cuña, M., Alonso-Sandel, M., Remunan-Lopez, C., Pivel, J. P., Alonso-Lebrero, J. L. & Alonso, M. J. Development of phosphorylated glucomannan-coated chitosan nanoparticles as nanocarriers for protein delivery. *J. Nanosci. Nanotechnol.* **6**, 2887–2895 (2006).

28. Vonarbourg, A., Passirani, C., Saulnier, P., Simard, P., Leroux, J. C. & Benoit, J. P. Evaluation of pegylated lipid nanocapsules versus complement system activation and macrophage uptake. *J. Biomed. Mater. Res. A.* **78**, 620–628 (2006).

29. von zur Muhlen, C., von Elverfeldt, D., Bassler, N., Neudorfer, I., Steitz, B., Petri-Fink, A., Hofmann, H., Bode, C. & Peter, K. Superparamagnetic iron oxide binding and uptake as imaged by magnetic resonance is mediated by the integrin receptor Mac-1 (CD11b/CD18): Implications on imaging of atherosclerotic plaques. *Atherosclerosis* **193**, 102–111 (2007).

30. Shukla, R., Bensal, V., Chaudhary, M., Basu, A., Bhonde, R. R. & Sastry, M. Biocompatibility of gold nanoparticles and their endocytotic fate inside the cellular compartment: a microscopic overview. *Langmuir.* **21**, 10644–10654 (2005).

31. Ilan, Y., Elstein, D. & Zimran, A. Glucocerebroside: an evolutionary advantage for patients with Gaucher disease and a new immunomodulatory agent. *Immunol. Cell Biol.* **87**, 514–524 (2009).

32. Demarchi, F., Bertoli, C., Greer, P. A. & Schneider, C. Ceramide triggers an NF-|[kappa]|B-dependent survival pathway through calpain. *Cell Death Differ.* **12**, 512–522 (2005).

33. Cui, Z. & Mumper, R. J. Microparticles and nanoparticles as delivery systems for DNA vaccines. *Crit. Rev. Ther. Drug Carrier Syst.* **20**, 103–137 (2003).

34. Peek, L. J., Middaugh, C. R. & Berkland, C. Nanotechnology in vaccine delivery. *Adv. Drug Deliv. Rev.* **60**, 915–928 (2008).

35. Kataoka, K., Harada, A. & Nagasaki, Y. Block copolymer micelles for drug delivery: design, characterization and biological significance. *Adv. Drug Deliv. Rev.* **47**, 113–131 (2001).

36. Torchilin, V. P. Micellar nanocarriers: pharmaceutical perspectives. *Pharm. Res.* **24**, 1–16 (2007).

37. Chen, M., Wang, S., Tan, M. & Wang, Y. Applications of nanoparticles in herbal medicine: zedoary turmeric oil and its active compound β-elemene. *Am. J. Chin. Med.* **39**, 1093–1102 (2011).

38. Tiyaboonchai, W., Tungpradit, W. & Plianbangchang, P. Formulation and characterization of curcuminoids loaded solid lipid nanoparticles. *Int. J. Pharm.* **337**, 299–306 (2007).

39. Su, Y. L., Fu, Z. Y., Zhang, J. Y., Wang, W. M., Wang, H., Wang, Y. C. & Zhang, Q. J. Microencapsulation of Radix salvia miltiorrhiza nanoparticles by spray-drying. *Powder Technol.* **184**, 114–121 (2008).

40. Yen, F.-L., Wu, T.-H., Lin, L.-T., Cham, T.-M. & Lin, C.-C. Nanoparticles formulation of Cuscuta chinensis prevents acetaminophen-induced hepatotoxicity in rats. *Food Chem. Toxicol.* **46**, 1771–1777 (2008).